2013

Optimization of Feline Adipose-derived Multipotent Stromal Cell Isolation and Canine Cranial Cruciate Ligament Regeneration with Intra-articular Adipose-derived Multipotent Stromal Cells

Nan Zhang
Louisiana State University and Agricultural and Mechanical College, nzhang7@tigers.lsu.edu

OPTIMIZATION OF FELINE ADIPOSE-DERIVED MULTIPOTENT STROMAL CELL ISOLATION AND CANINE CRANIAL CRUCIATE LIGAMENT REGENERATION WITH INTRA-ARTICULAR ADIPOSE-DERIVED MULTIPOTENT STROMAL CELLS

A Dissertation

Submitted to the Graduate Faculty of the
Louisiana State University and
Agricultural and Mechanical College
in partial fulfillment of the
requirements for the degree of
Doctor of Philosophy

in

The Interdepartmental Program in
Veterinary Medical Sciences
through the
Department of Veterinary Clinical Sciences

by
Nan Zhang
B.S., Tianjin Medical University, 2007
August 2013

This dissertation is dedicated to my family for all their love and support. I am particularly grateful for my parents, for their unconditional love, care and support. They have provided me with all a daughter could ever ask for, inspired me in all aspects, supported my interests, and urged me on every step of the way. I would like to thank my grandparents, uncles and aunts for being my models in life and work. To my brothers, for loving, inspiring and taking care of me always. Thank you for all the love, education and company for all these years for encouraging and facilitating my pursuit of a Ph.D. in the U.S.

ACKNOWLEDGEMENTS

This dissertation would not have been possible without the help from all my colleagues in the Laboratory of Equine and Comparative Orthopedic Research. I would like to express my deepest appreciation to my major professor, Dr. Mandi J. Lopez, for all her support, knowledge and advice. She has instilled in me so many qualities of being a professional scientist. She provided me with a wonderful environment to work in with excellent management, resources, personnel and teamwork. Dr. Lopez continually provides me with opportunities to communicate and collaborate with people from diverse backgrounds.

I would like to express my appreciation to all of my committee members. Dr. Frank M. Andrews has always supported me and has never hesitated to provide me with wonderful chances to further my education. I would like to thank Dr. Jeffrey M. Gimble for his valuable vision and pioneering work with stem cells. I would like to thank Dr. Daniel Hayes for his advice and expertise in scaffolds, and for his inspiration and encouragement. Last but not least, I would like to thank Dr. Shaomian Yao for his help and support.

I would like to acknowledge and extend my gratitude to my co-workers in the laboratory: Dr. Masudul Haque, Dr. Dejiang Feng, Dr. Lin Xie, Dr. Prakash Bommala, Carmel Fargason, Vanessa Marigo, Laura Kelly, Patrick Daigle, Holly Attuso, Victoria Roper, Corrine Plough, Javier Jarazo and Wei Duan. I could not have accomplished my work without their endless help. I have been very blessed to work in an environment with such a supportive team. I would like to show my appreciation to Marilyn Dietrich, Dr. Xiaochu Wu, Dr. Gregory McCormick, Dr. Julia Sokolova and Tom McClure for their expertise. I would also thank Dr. Dale L. Paccamonti, Sam Frazier, Jackie Bourgeois and everyone in the Department of Veterinary Clinical

Sciences and the Equine Health Studies Program for their kind help. I also thank Megan Barnum, Lauren Hoft and Sarah Dwyer for scaffold and bioreactor design. I am also grateful for all the help and advice of Dr. Boyu Zhang and all my friends.

TABLE OF CONTENTS

LIST OF TABLES

LIST OF FIGURES

ABSTRACT

Adult multipotent stromal cells (MSCs) have become popular within veterinary sciences for direct administration and tissue regeneration due to their differentiation, trophic and immunosuppressive properties. However, current isolation and expansion techniques provide a heterogeneous population with other types of cells, which may affect the efficiency and efficacy of treatments. The progenitor properties and function need to be further evaluated *in vitro* prior to *in vivo* application. The first part of this dissertation was to identify the optimal MSC source for general canine orthopedic applications such as intra-articular injection and joint tissue regeneration. Based on side-by-side comparisons of cell doublings, colony forming unit frequencies, target gene expression and immunophenotype, the infrapatellar fat pad (IFP) had MSCs with higher yield, expansion, multipotentiality and progenitor immunophenotypes than joint capsular and cranial cruciate ligament (CrCL) synovium. The second part of this dissertation was designed for optimization of isolation and *in vitro* expansion techniques for feline adipose-derived MSCs (ASCs). A new method was designed with which a therapeutic dose of ASCs (7×10^6 cells/kg) was available within 3 cell passages from epididymal adipose excised during castration. The isolated ASCs maintained their progenitor properties after cryopreservation. Feline-specific culture medium to induce adipogenesis, osteogenesis and chondrogenesis was also developed in the study for later application in feline tissue regeneration studies. The third part of this dissertation to apply canine IFP ASCs for CrCL regeneration. A custom perfusion bioreactor was designed and built to accommodate canine CrCL templates on which to grow viable grafts with IFP ASCs. Culture medium and template composition and design were optimized to induce the ASCs into fibroblasts to form a collagenous ligament. Compared to ASC

templates cultured in stromal (basal) medium those cultured in induction medium had enhanced collagen deposition, procollagen synthesis and ligament specific gene mRNA levels. The results from this investigation confirm the feasibility of growing new canine CrCLs from ASCs in the laboratory for implantation to treat dogs with CrCL disruption. Overall, the investigations in this dissertation provide vital translational information for canine and feline MSC therapies, and may contribute to better efficiency and efficacy of *in vivo* treatment and tissue regeneration.

CHAPTER 1. STROMAL CELL RESEARCH

1.1 Stromal Cell Introduction

1.1.1 Multipotent Stromal Cell Nomenclature

Stromal (Stem) cells are functional units that are capable of self-renewal through mitotic cell division and have the potential to differentiate into different cell lineages. The term stromal was first proposed by Edmund Beecher Wilson in 1896 [1]. Over 70 years later, Canadian scientists Ernest A. McCulloch and James E. Till confirmed the existence of self-renewing cells from mouse bone marrow [2, 3]. Friedenstein and his colleagues then discovered that bone marrow-derived cells were able to differentiate towards osteogenesis [4]. The initial adherent cells expanded *in vitro* into round-shaped colonies of fibroblastoid cells or colony forming unit-fibroblasts (CFU-f). During that same time period, several groups found that bone or bone extracts formed cartilage or bone after subcutaneous or intramuscular implantation [5-7]. In the 1970s, bone marrow-derived cells were shown to have proliferative abilities, specific phenotypic characteristics and to differentiate into adipocytes, chondrocytes and even myoblasts *in vitro* [8-11]. Additionally, they were capable of differentiating into non-mesenchymal lineages such as neurons. Though differentiated cells did not generate action potentials, this confirmed the plasticity of MSCs [12-14]. Caplan proposed the name mesenchymal stem cells (MSCs) for the cells isolated from stroma based on their ability to differentiate into cells within mesenchymal lineages[15]. However, there is intense debate over whether or not the cells should be considered true stem cells. As a result, the term “multipotent mesenchymal stromal cells” has been proposed to replace “mesenchymal stem cells” [16, 17].

1.1.2 Multipotent Stromal Cell Definition and Identification

The term MSC refers to a heterogeneous cell population. The International Society for Cell Therapy defines an MSC as a cell with the following properties: adherence to plastic under standard culture conditions; CD73+, CD90+, CD105+, CD34-, CD45-, HLA-DR-, CD14- or CD11b-, CD79a- or CD19-; and *in vitro* osteogenesis, adipogenesis and chondrogenesis (demonstrated by staining) [18, 19]. However, these criteria are not applied uniformly across species [20].

So far, MSCs have been isolated from numerous species including humans, dogs and cats, and from many tissues including bone marrow, adipose, cartilage and synovium [21-25]. Cells derived from different sources show different *in vitro* phenotypic characteristics and proliferation, but they share the ability to differentiate into mesenchymal lineages and surface marker expression [26-28]. Variability in cell characterization influences the ability to translate uniform MSC-based products into clinical practice. Uniform definitions and quality control standards are needed to predict *in vivo* behavior of implanted cells [29].

1.2 Multipotent Stromal Cell Characteristics

1.2.1 Multipotent Stromal Cell Niche

The stromal cell niche is the complex, three-dimensional (3D) microenvironment where adult stromal cells reside [30, 31]. The interactions between stromal cells with the other cells and extra-cellular matrix (ECM) within the niche are complex. Paracrine interactions occur though growth factors, chemokines and cytokines, among other factors [31]. Cell-cell interactions occur through cell associated proteins like cadherins and notch ligands. Interactions with the ECM are possible with proteins like fibronectin, laminin, collagen and proteoglycan. Other things that contribute to MSC regulation in the niche include ions, hormones and substrate biomechanical

properties and architecture. A combination of genetic expression and environmental signals are required for MSCs give up their 'stemness' and go through lineage-specific progenitor division toward terminal differentiation into effector cells [32]. Reconstruction of a functional niche is a critical component of regenerative medicine.

1.2.2 Multipotent Stromal Cell and Pericytes

The exact location and specific role of native MSCs within host tissue is not well defined. There are few reports surrounding *in vivo* MSC niches with the exception of the hair follicle, intestine, synovium and bone marrow [33-36]. I*n vitro* conditions do not fully replicate the natural niche, which makes it difficult to study. Under *ex vivo* culture conditions, MSCs are known to undergo phenotypic alterations that may not occur *in vivo* [23]. The perivascular location has recently been suggested as an MSC niche in human [37, 38]. Pericytes, thought to be progenitor cells, are located on the abluminal side of small blood vessels, including arterioles, capillaries, and venules in multiple human organs, including skeletal muscle, pancreas, adipose tissue and placenta [38]. They are closely associated with endothelia cells and appear to function similarly to MSCs [39]. They have a similar cell phenotype and immunophenotype (CD146+, CD34-, CD45- and CD56-) to MSCs and are capable of osteogenesis, adipogenesis and chondrogenesis *in vitro* [38, 40-42]. Distinct similarities have been shown between *in situ* and *in vitro* properties of MSCs and pericytes [43].

The perivascular niche is unlikely to be the only MSC niche [38]. Avascular tissues like cartilage also contain MSCs [44]. Hematopoietic stromal cells (HSCs) are believed to have at least two niches, the endosteal niche on the surface of trabeculae; and the perivascular niche within bone marrow sinusoids [45]. Ways to identify and recreate MSC niches *in vitro* remain a vital part of MSC investigations.

1.3 Therapeutic Effects of Multipotent Stromal Cells

1.3.1 Trophic Effects of Multipotent Stromal Cells

Tissue MSCs are thought to replace cells lost to age, disease or trauma. They are also known to have a paracrine effect, production of local bioactive factors. The MSC production of cytokines and growth factors is reported to be relatively constant among different donors and not influenced by age or health status [46]. However, the bioactive factors produced by MSCs are affected by differentiation and the local environment [46]. Effects of these factors can be direct, inducing intracellular signaling, indirect, stimulating other cells in the vicinity to secret other bioactive factors, or both. The indirect activity is referred as trophic, since the MSCs do not differentiate themselves, but their bioactive factor secretion mediates cell behavior. Some trophic effects include local immune suppression, enhancing angiogenesis, inhibiting apoptosis and fibrosis and inducing differentiation and mitosis of tissue-specific and tissue-intrinsic progenitors [46].

Exogenous MSCs have been shown to contribute to tissue repair by homing to damaged tissue where they secrete paracrine and autocrine signals to influence local cellular dynamics. This effect has been shown in spinal cord injury, myocardial infarction, meniscus, cartilage and bone repair and Crohn's disease [28, 47-49]. Chopp et al showed that rat marrow MSCs promote intrinsic neural progenitor cells to regenerate functional neurological pathways in damaged brain tissue when applied directly or systemically. Notably, the exogenous cells do not differentiate into neurons or neuronal support cells to mediate the effect [47, 50].

1.3.2 Immunomodulatory Effects of Multipotent Stromal Cells

The MSCs play multiple roles in immunomodulation. The immunosuppressive effect of MSCs allows them to be used for allogeneic

transplantation [51]. By definition, major histocompatibility complex (MHC) class I proteins are expressed by MSCs while MHC class II proteins are not [52, 53]. However, this characteristic is influenced by the microenvironment. The MHC II expression can be either upregulated or downregulated by IFN-γ [54-57]. Therefore, the immunosuppressive effect of MSCs is independent of MHC-I and II expression. The MSCs modulate the functions of the major immune cells including T, B cells, natural killer (NK) cells, monocytes and dendritic cells (DC). They suppress T-cell proliferation, cytotoxic T lymphocyte formation and IFN-γ production, thus inducing the expansion of T_{reg} cells [58-61]. MSCs also inhibit B cell proliferation, differentiation, chemotactic functions and IgG secretion [62-64]. Additionally, they inhibit NK cell proliferation, NK cell-mediated cytolysis and NK cell production of IFN-γ [65]. They also inhibit both DC maturation and activation, and differentiation of monocytes to DCs, thus increasing T cell anergy [66]. Thus, MSCs are currently being used to reduce immunological rejection [51].

The MSC immunosuppressive function is mediated by soluble factors, since cellular communication is not contact-dependent [51, 67]. Several factors have been found in co-culture systems of immune cells and MSCs (human and murine BMSCs, placenta and dental pulp MSCs), such as stem cell factor, interleukin (IL)-1β, IL-6, IL-8, IL-10, IL-12, IFN-γ, transforming growth factor-β1, vascular endothelial growth factor (VEGF), prostaglandin E2, macrophage colony-stimulating factor, hepatocyte growth factor and indoleamine 2,3-dioxygenase [65, 68-71]. However, mechanisms of how MSCs interact with immune cells are still unclear. Research of this issue is crucial for safe and effective use of MSCs.

1.3.3 Multipotent Stromal Cell Homing

MSCs have been found localized in inflamed tissue. Up to 100 times more MSCs are found in the synovial fluid patients with ligament injury compared to healthy donors [72]. Additionally, compared to non-injured mice, an increased amount of circulating BMSCs are observed in peripheral blood from mice with intimal hyperplasia [73]. The arrest of MSCs within the vascular system of a tissue followed by transmigration across the endothelium is called homing [74]. It is a prerequisite for MSCs to function, particularly when MSCs are administered by systemic infusion. Homing requires a multistep process with adhesive and signaling events, including adhesion to the endothelium, transendothelial migration, chemotaxis, matrix degradation and invasion and *in situ* differentiation [74, 75]. The mechanisms of MSC homing are not fully understood, but preliminary studies show that MSCs share at least some features with homing of leukocytes to sites of inflammation [76]. Initially, cells are rolled on the endothelium by selectins, which are expressed in inflamed venules [77]. This process allows cytokines to activate MSCs and stimulates the cells toexpress high affinity integrins to help them adhere to the vascular endothelium of the target site [78]. Then, cells migrate transendothelially and invade into ECM by integrin-ECM molecules interactions and matrix degradation [79, 80].

Numerous chemokines are reportedly involved in the recruitment of MSCs to the target tissue. For example, the upregulation of stromal cell derived factor-1 enhances murine BMSC and endothelial progenitor cell homing and incorporation into ischemic tissues [76, 80]. Interleukin 8 and its cellular receptors also contribute to homing of intravenous infused human CD34+ progenitor cells to ischemic myocardium in rats [81]. Vascular endothelial growth factor induces bone marrow-derived circulating cell recruitment in mice [82]. Integrins such as integrin-β1,

integrin α4β1, E- and P-selectin are also involved in recruiting BMSCs, endothelial progenitor cells in target tissues like tumor, hind limb ischemia and myocardial infraction [83-88]. These factors may be further used to attract MSCs to specific locations in further studies.

Culture conditions have a significant impact on MSC homing. Freshly isolated mouse MSCs have higher homing capacity compared to culture-expanded populations [89]. Homing receptors like CXC chemokine receptor type 4 are expressed in stromal vascular fraction cells but not in cultured MSCs [28]. Transendothelial MSC migration is reduced with *in vitro* passage, potentially due to production of tissue inhibitor of metalloproteinases-3, a natural MMP inhibitor [90]. Another reason may be loss of surface markers during *in vitro* culture. Interestingly, simulation of ischemic environments *in vitro* or hypoxic preconditioning, seems to enhance MSC transendothelial migration by upregulation of MSC MMP production [91, 92]. All of these factors need to be considered to enhance MSC therapy.

1.3.4 Multipotent Stromal Cell Heterogeneity

Differences in MSCs among donors may contribute to differences in clinical trial outcomes [93]. Different patient donors have different MSC *in vitro* expansion rates and differentiation potentials [94]. Results are also influenced by factors such as donor age and health status, harvest technique, culture methods and plating density. Plastic adherence selects for a heterogenous MSC population. MSC heterogeneity seems to be reduced by consistency among isolation and culture procedures and selection of MSCs based on surface marker expression. There is no single marker unique to MSCs with which to yield a pure population. So, panels of markers like CD29, CD44, CD71, CD73, CD90, CD105, CD106, CD120a, CD124, CD146, CD271, nestin, SSEA1, and SSEA4 are often used to identify and/or isolate MSCs

[95]. Additionally, genomic transcripts and proteins have been used to identify MSC amongst hematopoietic, endothelial and periosteal cells and synovial fibroblasts [96].

Use of such techniques does not confirm multipotentiality of an MSC isolate. A significant percentage of MSCs that were capable of osteogenesis *in vitro* did not form heterotopic osseous tissue *in vivo* [97]. Additionally, MSCs lose their multipotentiality and change immunophenotype with increasing passage. Subpopulations of MSCs isolated with different sets of surface markers have different properties. For example, human BMSCs that are CD271+, W8B2+ and CD56+ have higher chondrogenic than adipogenic potential [98]. A cellular subset of $CD105+^{low}$ human ASCs was found to be more osteogenic than $CD105+^{high}$ ASCs both *in vitro* and *in vivo* [99]. These results confirm the importance of identifying characteristics of different MSC immunophenotypes.

Heterogeneity also exists among MSCs from different tissue sources. Rat MSCs derived from epididymal adipose had higher multipotentiality than epicardial cells *in vitro*, but their expansion rates were lower [100]. Joint tissue-derived MSCs, including ASCs and SSCs, displayed significantly higher chondrogenic capacity than BMSCs *in vivo* [101]. Additionally, despite similar *in vitro* capacities, human ASCs exhibited significantly higher potential to differentiate into muscle cells than umbilical cord MSCs *in vivo* [102]. Compared to subcutaneous fat, patellar adipose from human patients with knee osteoarthritis (OA) have a lower number of capillary-like structures and higher numbers of stromal and alkaline phosphatase CFUs [103].

Questions remain about how disease affects MSCs. It is not known if inflammation in the local environment affects MSCs or if they are protected within their niche. The BMSCs from iliac crest or tibia/femur in OA patients had significantly lower *in vitro* expansion rates and chondrogenic and adipogenic

capacities than those from patients without OA, but the osteogenic potential was not affected [104]. In contrast, MSCs isolated from mice with vascular injuries retained *in vitro* trilineage differentiation potential up to 10 passages while those from normal mice MSCs retained the trilineage differentiation property only to passage 1 [73]. There are many possible reasons for variable results from MSCs harvested from normal versus diseased or injured tissues including type and level of disease, harvest location, cell types, individual variation, species differences and MSC isolation and expansion methods. Therefore, in order to identify factors that contribute to different MSC behavior, variables should be limited as much as possible.

1.3.4 Adipose Derived Multipotent Stromal Cells (ASCs) versus Preadipocytes

ASCs are important to innate immunity and angiogenesis, two properties that are vital to development of viable tissues derived from them. It is proposed that there are two types of precursor cells in adipose tissue, preadipocytes with limited differentiation capacities and ASCs [105]. Compared to ASCs, preadipocytes have a shorter lifespan and cannot be maintained *in vitro* for prolonged periods of time [105]. Additionally, preadipocytes are reported to be CD34+ in contrast to ASCs, the majority of which are CD34- [18, 19]. Preadipocytes secrete numerous inflammatory cytokines such as TNF-α and are sensitive to lipopolysaccharide activation [106]. They also have many proteins in common with monocyte/ macrophages, such as adipocyte protein 2, peroxisome proliferator-activated receptors-gamma (PPAR-γ), and nicotinamide adenine dinucleotide phosphate-oxidase [107, 108]. Preadipocytes can also display phagocytic activity [109, 110]. Macrophage-like properties decline after commitment of preadipocytes into adipocytes, so they may be limited to adipocyte progenitors [109].

Preadipocytes are also have properties of endothelial-like progenitors [111]. Development of a capillary network is required to support optimal tissue function and remodeling. Human CD34+/CD31- ASCs have been shown to differentiate into an endothelial phenotype *in vitro* and *in vivo* [53]. Additionally, adipogenic lineage proteins induce potent proangiogenic factors, including monobutyrin, VEGF and leptin [112-115]. Thus, ASCs may be beneficial in vascular reconstruction during tissue regeneration.

1.4 Multipotent Stromal Cells in Tissue Engineering

MSCs in combination with scaffolds are often used for tissue engineering. Cell-scaffold constructs have the potential to provide a spatial and temporal microenvironment that mimics the stromal cell niche to support cell proliferation, regulate cell function and promote tissue regeneration [116].

1.4.1 Cell Sources

Potential MSC sources include fully differentiated, adult cells, adult MSCs, embryonic stem cells (ESCs) and induced-pluripotent stem cells [117]. Fully differentiated adult cells have limited proliferation capacity and lifespan both *in vitro* and *in vivo* [118]. Compared to MSCs, ESCs have higher differentiation potential. However, their application is limited due to ethical issues, potential risk of tumor formation and immune rejection. Therefore, adult MSCs have become a popular source in tissue engineering. There are over 20 tissue sources of adult MSCs. Historically, the tissue forming capacity of MSCs was thought to be limited to the mesoderm. However, recent evidence shows that MSCs have greater plasticity (the capacity to differentiate into cell types from different germ layers) than previously thought [13]. In fact, under appropriate culture conditions, MSCs are capable of differentiating into all three germ layers [119, 120]. Though the mechanism of

transdifferentiation or plasticity is not fully understood, this MSC characteristic has distinct advantages for tissue engineering.

Cell sources can also be categorized as autologous, allogeneic and xenogeneic cells. Autologous cells are least likely to undergo immune rejection, since they are from the same individual body. However, they are not always available, and may not be viable or expandable *in vitro*. Harvest of autologous cells may cause donor site morbidity [121]. In addition, cells may be influenced by diseased conditions. Allogeneic cells from individuals of the same species and xenogeneic cells from individuals of different species offer alternatives to this situation [122]. Concerns surrounding allo- and xenogeneic sources also include disease transmission, infection and immune rejection [123, 124].

1.4.2 Scaffold Carriers

Extra-cellular matrix varies among tissues [125]. The ECM has five major functions [126]. It provides structural support and a physical environment so that cells are able to attach, proliferate, migrate, differentiate and function. It also confers mechanical properties to the tissue. The ECM provides bioactive cues for regulating the activities of residing cells. Finally, the ECM provides a dynamic environment for vascularization and new tissue formation. The goal of scaffold synthesis is to replicate the ECM of the target tissue to give the best chance to recreate it. Scaffolds should be composed of materials to give it similar physical and mechanical properties as the native tissue as well as degradation that occurs at the same rate as tissue generation. Porosity should be sufficient for nutrient transfer and cell adhesion without compromising mechanical strength.

Four wide categories of scaffolds designed to carry MSCs include porous structures, decellularized ECM, confluent cells with ECM, and cells encapsulated in

hydrogel [126]. Porous structures composed of natural or synthetic biodegradable and biocompatible materials are one of the most popular approaches to scaffold carriers. Scaffolds can be designed to mimic hard and soft tissue ECM. The ideal pore diameter is around 150 μm for hard tissue formation and 200 – 250 μm for soft tissue formation [124]. Natural ECM that is decellularized has similar composition and mechanical properties as native tissue ECM. However, complete decellularization is required to minimize immunogenicity, and tissue properties may be altered by harvest, decellularization and deproteinization [127, 128]. Layers of sheets of confluent cells within the ECM they produce are typically used to reconstruct highly cellular tissues like epithelium and endothelium. Injectable hydrogel has been applied for cartilage and soft tissue generation with MSCs [129, 130]. Hydrogel formulations can be made with both natural and synthetic materials by physical and chemical crosslinking [131, 132]. Scaffolds are customized to the intended *in vivo* application. Tissue-specific properties and the amount of tissue to be regenerated are considerations when identifying scaffold carriers.

There are general approaches to prepare MSC-scaffold constructs for implantation. One is to inject MSCs into scaffolds during surgery [133]. Another approach is to culture MSC-scaffold constructs in differentiation medium for a period of time (7-21 days) to induce cell differentiation and tissue specific ECM production and then implant them orthotopically [134]. Pre-seeding of human BMSCs on the poly-L lactic acid (PLLA) mesh has higher osteogenic potential in rats compared to injecting MSCs into the scaffold during surgery [135]. Another approach is to encapsulate MSC-scaffold constructs within protective coatings and allow cells to mature *in vitro* in an orthotopic implantation site. Oligo(poly(ethylene glycol) fumarate) hydrogel composites loaded with rabbit BMSCs and TGF-β1 showed

chondrocyte potential *in vitro* [136]. Co-encapsulation of TGF-β3 in hyaluronic acid hydrogels with human BMSCs supports neo-cartilage formation when implanted subcutaneously in mice [137]. So far, there is no clear agreement about which approach is better. Specific circumstances should be considered to identify MSC-scaffold pre-implantation conditions, including material types of the scaffold, cell types and types of tissue forming.

1.4.3 Bioreactors for 3-Dimensional Culture

Monolayer culture does not mimic the mechanics and cell-cell or cell-ECM orientation. Problems associated with 3-D scaffolds include difficulties with gas exchange and nutrient delivery. Additionally, cell seeding is more difficult in 3-D scaffolds, and non-homogenous cell distribution can result in non-uniform tissue formation. A 3-D cell culture system is a natural step between 2D in vitro culture and *in vivo* conditions.

Bioreactors are dynamic systems used to load and culture cells on scaffolds [138]. There are a number of different types of bioreactors including rotating wall vessels, direct perfusion systems and spinner flasks [138]. Spinner flasks and rotating wall vessels are normally used to enhance nutrient transport into the porous structure by rotating the medium [139]. A perfusion system is a more complex setup designed to direct fluid through the inside of the construct [140].

Perfusion bioreactors provide a more uniform distribution of the medium within scaffolds compared to spinner flask and rotating vessels, and they provide mechanical stimulation of cells in the scaffold in the form of shear stress [141]. Shear stress is critical for cell differentiation and ECM deposition [142]. Perfusion bioreactors are preferred for orthopedic tissue engineering [143]. The chamber (cartridge) is customized to hold the scaffold. For optimal cell loading, the chamber

should approximate the sides of the scaffold. Fluid is moved through the chamber by a pump. Common flow rates range from 0.3 – 3.0 ml/min [144]. Perfusion bioreactors have been shown to increase production of growth factors that contribute to cell differentiation [145]. Dynamic perfusion culture also helps reduce the concentration of these factors in the local area and promote differentiation of rat BMSCs throughout starch-based fiber scaffolds [145]. Production and distribution of growth factors *in vitro* may be a benefit of perfusion bioreactors for tissue regeneration *in vivo*. However, perfusion bioreactors require optimization for targeted tissue production. Cell seeding is crucial for tissue regeneration and is specific to tissue type. It also ranges widely for a given purpose. For example, human anterior cruciate ligament regeneration in a bioreactor with BMSCs has been reported to require between 10^6 to 10^8 cells/cm^3 [123, 146]. An optimal cell density should be based on both cell (expansion and differentiation) and tissue (type, density, matrix deposition) characteristics. Flow rate is another parameter that varies widely among different scaffold types, cell sources, tissues, and system capacities [123]. Most importantly, more *in vivo* models should be tested before putting the perfusion bioreactors into a clinical setting.

1.5 Veterinary MSC Applications

In general, MSC-applications are at very early stage in veterinary medicine. The mechanism of MSC function *in vivo* is still not fully understood, and efficacy *in vitro* or in preclinical animal studies has not been established. Perhaps the earliest application of MSCs in veterinary medicine has been the use of MSCs to treat equine suspensory ligament desmitis using 20 ~ 60 ml of bone marrow mononuclear cells [147]. Treatment led to an improvement in athletic function rates compared to conventional treatment in many studies. There was no evidence to confirm the

therapeutic effects were from MSCs, since only 1 in 10,000 - 15,000 cells of mononuclear cells of bone marraow aspirate are estimated to be MSCs [148]. MSC-mediated therapies have been also been applied to dogs to treat tendon, ligament and cartilage/joint injuries. So far, different cell sources have been used, including the adipose-derived stromal vascular fraction (SVF) and culture-expanded BMSCs and ASCs. Compared to culture-expanded cells, SVF require a larger tissue harvest volume to achieve therapeutic doses. Also, culture-expanded MSCs need to be fully characterized according to the minimum criteria mentioned above. BMSCs are the most investigated MSCs in veterinary medicine, and have been characterized in horses, dogs, and cats, among other domestic species. They have displayed comparable expansion rates, differentiation potential and surface marker expression as human and rat BMSCs. Adipose tissue is another option for MSC harvest with a 500 fold greater number of SVFs [149]. With a treatment of 4.2 ~ 5 x 10^6 SVF from adipose, the lameness, pain and range of motion have been significantly improved for dogs with chronic OA [150]. Both culture-expanded BMSCs and ASCs have been applied in cats with chronic kidney disease (CKD). In a pilot study, two out of the four cats administered 1 ~ 4 x 10^6 ASCs by unilateral intrarenal injection had a modest increase in glomerular filtration rate along with a mild decrease in serum creatinine concentration, indicating improved kidney function [151]. This and other studies emphasize the need for controlled *in vitro* and *in vivo* studies as well as clinical trials.

This dissertation focuses on the clinical translation of MSC-based therapies. Chapter two is to identify the optimal MSC intra-articular source for general orthopedic therapies. Applications include direct administration into the joint to treat osteoarthritis and tissue regeneration of intra-articular tissues, such as cartilage,

ligaments and tendons. Chapter three discusses a new isolation method of MSCs from excised feline tissue. The purpose of this study is to collect MSCs without the need for additional tissue harvest. Compared to canine and equine, MSCs in feline remain largely unexplored. This study also provides vital information on *in vitro* culture, multipotentiality and cryopreservation. As a continuation of chapter two, chapter four surrounds generation of viable canine cranial cruciate ligament (CrCL) structures using ASCs and biocompatible scaffolds under custom induction and perfusion culture conditions. Results of these studies are intended to contribute tto canine and feline tissue engineering and regenerative medicine.

CHAPTER 2. CANINE INTRA-ARTICULAR MULTIPOTENT STROMAL CELLS (MSC) FROM ADIPOSE HAVE THE HIGHEST IN VITRO EXPANSION RATES, MULTIPOTENTIALITY, AND MSC IMMUNOPHENOTYPES

2.1 Introduction

Rupture of the cranial cruciate ligament (CrCL) is the leading orthopedic disorder of the canine stifle [152, 153]. Concomitant intra- and periarticular damage occurs with 70% of CrCL ruptures, and quality of life is reduced by the progressive pain, dysfunction, and osteoarthritis [154, 155]. Many tissues within the stifle have limited regenerative and reparative capacities, so surgical intervention is often necessary to restore joint function [156]. Current surgical options do not necessarily restore damaged tissues or inhibit joint degeneration [157]. The emerging field of tissue engineering with adult multipotent stromal cells (MSCs) has significant potential for generation of viable, functional, engineered stifle tissues to replace those lost to injury and degeneration [158]. Meanwhile, knee pain is a complaint in as many as 20% of the general adult population in United States, and more than 20 million people seek medical attention for knee pain each year [159]. The canine stifle (knee) is an established large animal model for human knee studies given its similar anatomy structure and joint kinetics [160]. The model is routinely used to develop and test surgical procedures, implants, and mechanisms of CrCL treatment and reconstruction [161, 162]. Additionally, significant preclinical work surrounding isolation, characterization and therapeutic application of adult MSCs has been done with the model [163-165].

Ideal cell candidates for intra-articular tissue regeneration should have high proliferative capacity, produce tissue specific extracellular matrix and survive in the intra-articular environment [166]. Orthotopic adult stromal cells have greater commitment to tissue-specific lineages than those from heterotopic sources [167].

Intra-articular stromal cells have better expansion capacity and potential for stifle joint tissue regeneration than cells from other sources [168]. Infrapatellar (IFP) adipose and synovium are established intra-articular MSC sources, and CrCL cell isolates are reported to have higher expression of ligament specific phenotypic markers than peri-articular ligaments and tendons [169, 170]. For the potential benefits of orthotopic stromal cell tissue regeneration to be realized in clinical stifle therapies, it is critical to identify the optimum intra-articular source of adult MSCs. A direct comparison of cell isolate phenotypes and their *in vitro* expansion capacities and multipotentiality within individuals is key to achieving this goal.

Recently, canine IFP adipose derived multipotent stromal cells (ASCs) were shown to have greater or equal expansion capacity to bone marrow MSCs and comparable multipotentiality following cryopreservation [171]. Based on this information and the stated goal above, we hypothesized that stifle joint MSCs from IFP (ASC) had higher stromal cell tissue density, *in vitro* expansion rates, multipotentiality, and MSC cell immunophenotypes than synovium lining the joint capsule (SSC) and synovium surrounding the CrCL (LSC) up to cell passage (P) 6.

2.2 Materials and Methods

2.2.1 Ethics Statement

All animal experiments were approved by the LSU Institutional Animal Care and Use Committee.

2.2.2 Study Design

Synovium lining the joint capsule, IFP, and CrCL were collected from one normal stifle of six mixed breed female dogs (23.1 ± 0.9 kg, 3.3 ± 0.4 years, mean ± SEM) undergoing stifle surgeries for reasons unrelated to the investigation. Stifles included

in the study had no detectable radiographic changes or visible intra-articular abnormalities. The following assessments were performed on cells from all tissues in each dog: P0-6 cell doublings (CD) and doubling times (DT); P0, 3 and 6 $CD29^+$, $CD44^+$, $CD90^+$, $CD34^+$, and $CD45^+$ cell percentages; P0, 3 and 6 fibroblastic, osteogenic, and adipogenic colony forming unit frequencies; P0 chondrogenic pellet alcian blue (proteoglycan) staining; P0 and 3 stromal (undifferentiated) and differentiated (adipogenic, osteogenic, and chondrogenic) cell MSC and lineage specific target gene mRNA levels. Cell immunophenotypes were also determined in the stromal vascular fraction (SVF) of pooled tissue harvests collected immediately post-mortem from both normal stifles of ten adult, female, mixed-breed dogs euthanized for unrelated reasons. Pooling was necessary for adequate cell numbers, so only one SVF sample for each cell type was evaluated for nucleated cell density and with flow cytometry.

2.2.3 Cell Isolation and Expansion

Adipose tissue and joint capsular synovial cells were isolated sterilely according to a published protocol with minor modifications [171]. Briefly, adipose tissue and synovium were minced into small pieces, and the CrCL surface was vigorously lavaged with PBS to detach the synovial membrane. Tissues were then digested with collagenase solution (DMEM-Ham's F12 [HyClone, Logan, UT], 0.1% type I collagenase [Worthington, Biochemical Corporation, NJ], 1% bovine serum albumin). After 1 hr, the pellet resulting from centrifugation (260 g, 5 min) was resuspended in stromal medium (DMEM-Ham's F12, 10% fetal bovine serum [FBS] [HyClone], 1% antibiotic/antimycotic solution) and filtered (100 μm, BD Falcon, Bedford, MA) following addition of an equal volume of red cell lysis buffer (0.16 mol/L NH_4Cl, 0.01 mol/L $KHCO_3$, 0.01% EDTA). The resulting SVF were seeded in 10 mm dishes

(CellStar, Greiner, NC) at a density of 5 x 10^3 cells/cm^2 in stromal medium and cultured under standard conditions (37°C, 5% CO_2). Medium was refreshed after 4 hours and then every 2-3 days. Subsequent passages were performed at 80% confluence with a cell seeding density of 5 x 10^3 cells/cm^2. For purposes of this study, primary cell isolates were considered the SVF. The first cell passage of the primary cells was P0.

2.2.4 Cell Expansion (P0-6)

Cell doublings (CD) and cell doubling time (DT) were determined with duplicate cultures in 12-well plates at an initial seeding density of 5 x 10^3 cells/cm^2 [172]. Cells were counted after 2, 4, and 6 days of culture. CD and DT were calculated with the formulae: CD= $\ln(N_f / N_i)/\ln(2)$ DT= CT/CD (N_i: initial cell number; N_f: final cell number; CT=culture time) [173].

2.2.5 Multipotentiality (P0, 3, 6)

Limiting-dilution assays to determine fibroblastic (CFU-F), adipogenic (CFU-Ad), and osteogenic (CFU-Ob) colony forming unit frequencies [174]. A total of 5 x 10^3, 2.5 x 10^3, 1.25 x 10^3, 6.25 x 10^2, 3.12 x 10^2, or 1.56 x 10^2 cells were placed in each well of one row (one concentration/row, 8 replicates/concentration) in a 96-well plate. Cells were cultured in stromal medium for 7 days. Fibroblastic (CFU-F) colonies were then fixed with 1% paraformaldehyde and stained with 0.1% toluidine blue. For adipogenesis (CFU-Ad), cells were cultured in stromal medium for 7 days, followed by culture in adipogenic medium (DMEM-Ham's F12, 3% FBS, 1% antibiotic/antimycotic solution, 33 µmol/L biotin, 17 µmol/L pantothenate, 1 µmol/L dexamethasone, 100 µmol/L indomethacin, 1 µmol/L insulin, 0.5 mmol/L isobutylmethylxanthanine [IBMX], and 5 µmol/L rosiglitazone) for 21 days. Wells were then fixed as above and stained with oil red O. Similarly, osteogenesis wells

were cultured in stromal medium for 7 days and then cultured in osteogenic medium (DMEM-Ham's F12, 10% FBS, 1% antibiotic/antimycotic solution, 10 mmol/L β-glycerophosphate, 10 nmol/L dexamethasone, and 50μg/ml sodium 2-phosphate ascorbate) for 21 days. Colonies were fixed in 70% ETOH and stained with 2% alizarin red. Wells were considered positive for MSC, adipogenesis, or osteogenesis when there were ≥10 toluidine blue-stained colonies, ≥10 oil red O-stained colonies, or ≥1 alizarin red-stained colonies, respectively [175]. The ratio of negative to total wells in rows (one for each concentration) containing negative wells were used to estimate the CFU for each concentration using the equation $F=e^{-x}$ (F: ratio of negative to total wells within a row (concentration), e: natural logarithm constant 2.71, x: CFU number per well). Based on a Poisson distribution of a clonal cell lineage, the value of F = 0.37 occurs when the number of total cells plated in a well contains a single CFU.[13,14] The mean value from each plate was used as the CFU for each animal/cell type/differentiation medium. For chondrogenesis, 2.5 x 10^5 cells were centrifuged (200 x g, 5 min) to form a pellet in a 1.5 ml microcentrifuge tube following 7 days of culture in stromal medium. The pellet was cultured in chondrogenic differentiation medium (DMEM-Ham's F12, 3% FBS, 1% antibiotic/antimycotic solution, 50 μg/mL abscorbate phosphate, 100 nmol/L dexamethasone, 40 μg/mL proline, 2 mmol/L sodium pyruvate, 1% ITS, and 10 ng/mL TGF- β3) for 21 days with media changes every 2–3 days. Pellets were formalin-fixed, paraffin-embedded, sectioned (5 μm) and stained with alcian blue.

2.2.6 Expression of marker genes

Total RNA was isolated from cells (RNAqueous Kit, Ambion, Grand Island, NY), DNase-treated, and reverse-transcribed using oligo (dT) primers and Moloney murine leukemia virus reverse transcriptase. For chondrogenesis, pellet total RNA was

extracted by homogenization in TRI Reagent (Sigma Aldrich, St Louis, MO). Target gene mRNA levels were quantified with qRT-PCR using SYBR Green technology (MJ Research Chromo4 Detector, Bio-Rad Laboratories). Canine-specific primers for MSC and adipogenic, osteogenic, and chondrogenic lineages were used (Table 1) [174]. Values were normalized to glyceraldehyde 3-phosphate dehydrogenase (GAPDH). Relative gene expression was quantified according to $2^{-\Delta\Delta Ct}$ [176].

Table 1 Canine-specific primer sequences for adipogenic, osteogenic, chondrogenic, and progenitor genes

	Primer	**Forward Primer**	**Reverse Primer**
Housekeeping	GAPDH	TGGCAAAGTGGATATTGTCG	AGATGGACTTCCCGTTGATG
Adipogenic	PPAR-γ	TTCTCCAGCATTTCCACTCC	AGGCTCCACTTTGATTGCAC
	Leptin	TGTGTTGAAGCTGTGCCAAT	CCCTCTGTTTGGAGGAGACA
Osteogenic	Col1	GGTGGTGGCTATGACTTTGG	CAGTTCTTGGCTGGGATGTT
	OPG	TGTCTATACTGCAGGCCGGTG	TCAGGCAGAACTCAAGCTCCA
Chondrogenic	Aggrecan	TTGCACTCAGGAGAGGAGAC	CCACGCAGGTGGCTCCATTC
	Col2	ACCTCAAGAAGGCCCTGCTC	CCCCACTTACCGGTGTGTTT
MSC	Sox2	CCTGACCTGTTTCGTGACCT	CTATCGCCAGCTCGTACTCC
	Nanog	AATAACCCGAATTGGAGCAG	AGCGATTCCTCTTCACAGTTG

PPAR-γ, peroxisome proliferator-activated receptor gamma; Col1, collagen type I; OPG, osteoprotegerin; Col2, collagen type II; Sox2, sex determining region Y-box 2; Nanog, homeobox protein nanog.

2.2.7 Immunophenotype

Cell aliquots (10^5) were resuspended in 200 ml PBS containing 5 ul antibody. Cells were incubated with antibodies specific for canine antigens or validated for canine cross reactivity against PE-CD34, FITC-CD44, PE-CD45, and PE-CD90 for 30 min at room temperature (Table 2). The cells were then washed with PBS and fixed with 4%

paraformaldehyde. For non-conjugated CD29 staining, the cells were incubated with antibody for 30 min at room temperature. They were then incubated with a secondary antibody, FITC-conjugated goat anti-mouse IgG (Sigma Aldrich) for 30 min, washed with PBS, and fixed as above. For negative autofluorescence control, cells were not incubated with antibodies. Cellular fluorescence was evaluated by flow cytometry using a FACSCalibur flow cytometer and CellQuest Pro software (BD Biosciences, San Jose, CA). Cell percentages expressing each antigen were determined. Due to low SVF cell numbers, flow cytometry was performed on representative samples for each tissue type using pooled cells from unrelated dogs. Pooling was necessary for adequate cell numbers so only one sample was processed for each antibody.

Table 2 Antibodies against canine MSC surface markers

Antibody	**Label**	**Marker Expression**	**Manufacturer**	**Cat No.**	**Target Species**
CD29	N/A	β1 integrin	BD Biosciences	610468	Human
CD34	PE	Hematopoietic progenitor (HSC)	BD Biosciences	559369	Canine
CD44	FITC	Hyaluronic acid receptor	eBiosciences	115440	Canine
CD45	PE	HSC, leukocyte antigen	eBiosciences	125451	Canine
CD90	PE	Thy-1, fibroblasts, MSC, HSC	eBiosciences	125900	Canine
IgG	FITC	Secondary antibody	Sigma-Aldrich	F9006	Mouse

2.2.8 Statistical Analysis

All results are presented as mean ± SEM. ANOVA models (GraphPad Prism, La Jolla, CA) were used to compare CD, DT, CFU frequency, RNA levels, and cell surface marker percentages among passages within cell types and among cell types within passages. Tukey's post hoc tests were applied for multiple group comparisons ($P<0.05$).

2.3 Results

2.3.1 Cell Harvest

Using pooled samples, 3.4 x 10^5 nucleated cells/g were isolated from IFP (2 – 3g/stifle), 3.0 x 10^5 cells/g from synovial membrane (1 – 2g/stifle), and 1.1 x 10^6 cells/g of CrCL (2.2 x 10^5 cells/CrCL).

2.3.2 Cell Expansion

Day 2 and day 4 cell counts were used as the initial number to calculate expansion rates on days 4 and 6, respectively. Differences were not significant between days, so data was collapsed over this variable. The overall (P0-P6 combined) CD for ASC, SSC, and LSC were 1.7 ± 0.1, 1.5 ± 0.1, and 1.2 ± 0.1 CD/day, respectively (Table 3).

Table 3 Canine ASC, SSC, and LSC cell doublings (CD/day) for P0-6 (mean ± SEM)

	P0	**P1**	**P2**	**P3**	**P4**	**P5**	**P6**
ASC	1.9±0.2 $^{A,a/b}$	2.0±0.2 $^{A,a/b}$	2.1±0.2 ^{A,a}	1.6±0.2 $^{A,a/b/c}$	1.8±0.2 $^{A,a/b}$	1.4±0.6 $^{A,b/c}$	0.9±0.1 ^{A,d}
SSC	1.9±0.2 ^{A,a}	1.8±0.2 ^{A,a}	1.7±0.2 ^{A,a}	1.7±0.2 ^{A,a}	1.5±0.2 ^{A,a}	1.3±0.1 ^{A,a}	0.5±0.1 ^{B,b}
LSC	1.5±0.1 $^{A,a/b}$	1.8±0.1 ^{A,a}	1.5±0.2 $^{A,a/b}$	1.4±0.2 $^{A,a/b}$	1.1±0.1 $^{B,b/c}$	0.8±0.1 $^{B,c/d}$	0.4±0.1 ^{B,d}

Columns with different upper-case letters within passages and those with different lower-case letters within cell types are significantly different from each other ($P<0.05$).

The corresponding overall DT (P0-6) were 0.7 ± 0.1, 0.7 ± 0.1, and 0.8 ± 0.1 days/CD (Table 4). Within cell types, P6 ASC had significantly lower CD than P0, 1, 2, and 4, and significantly higher DT than P0-4. The P6 SSC had significantly lower CD and higher DT than all previous passages, and P6 LSC had significantly lower CD and higher DT than P0-4. There were no significant differences in CD among cell types for P0-3. For P4-6, LSC CD was significantly lower than ASC. The P5 SSC CD value was significantly higher than LSC. After P5, SSC and LSC had significantly higher DT than ASC.

Table 4 Canine ASC, SSC, and LSC doubling times (days/CD) for P0-6 (mean ± SEM)

	P0	P1	P2	P3	P4	P5	P6
ASC	$0.6\pm0.1^{A,a}$	$0.6\pm0.1^{A,a}$	$0.5\pm0.0^{A,a}$	$0.8\pm0.1^{A,a}$	$0.6\pm0.1^{A,a}$	$0.8\pm0.1^{A,a/b}$	$1.2\pm0.1^{A,c}$
SSC	$0.6\pm0.1^{A,a}$	$0.7\pm0.1^{A,a}$	$0.7\pm0.1^{A,a}$	$0.7\pm0.1^{A,a}$	$0.8\pm0.1^{A,a}$	$0.9\pm0.9^{A,a}$	$3.0\pm0.6^{B,b}$
LSC	$0.7\pm0.1^{A,a}$	$0.6\pm0.1^{A,a}$	$0.8\pm0.1^{A,a}$	$0.8\pm0.1^{A,a}$	$1.0\pm0.1^{A,a}$	$1.6\pm0.2^{B,b}$	$3.7\pm0.6^{A,c}$

Columns with different upper-case letters within passages and those with different lower-case letters within cell types are significantly different from each other ($P<0.05$).

2.3.3 Multipotentiality

All cell types displayed characteristic adipogenic (See A-C in Figure 1), osteogenic (See D-F in Figure 1), and chondrogenic (See G-H in Figure 1) differentiation. The CFU frequency indicates the minimum number of cells that includes one capable of forming a fibroblastic (CFU-F) colony or differentiating into osteogenic (CFU-Ob) or adipogenic (CFU-Ad) cell lineages. Results were presented as frequencies, so higher numbers indicate more cells required for a cell with the indicated reduced differentiation capacity. Due to limited cell expansion past P4, P6 LSC were not included in CFU assays. Within cell types, the P6 ASC and SSC CFU-F were significantly higher than P0, and the LSC P3 CFU-Ad was significantly higher than P0 (Table 5). Among cell types, P0 and P3 LSC had significantly higher CFU-F, CFU-Ad and CFU-Ob than ASC. The P3 SSC had significantly higher CFU-Ad than ASC, and P6 SSC had significantly higher CFU-Ad and CFU-Ob than P6 ASC.

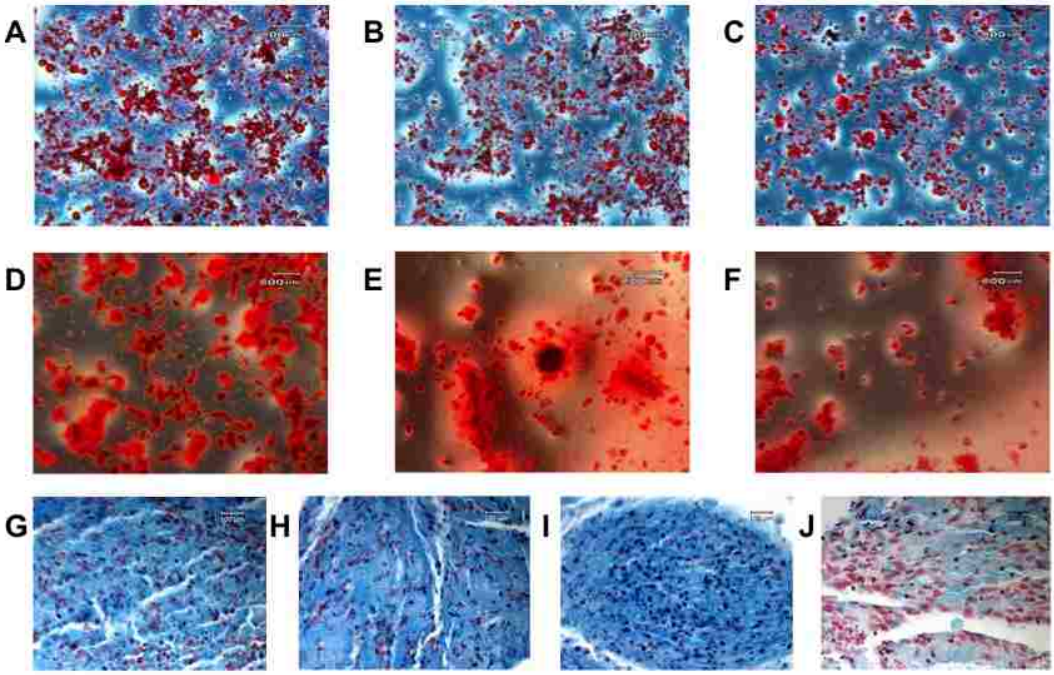

Figure 1 Trilineage differentiation of canine ASCs, SSCs and LSCs

P0 ASC, SSC, and LSC after 21 days culture in adipogenic (A, B and C), osteogenic (D, E and F), and chondrogenic medium (G, H, and I). Lipid droplets stain red with Oil Red O, calcified colonies stain red with Alizarin red, and proteoglycans stain blue with Alcian blue. A stromal cell pellet cultured in stromal medium and stained with Alcian blue (J) is included for comparison. Original magnification: A-F, 10x, G-J, 63x, scale bar = 600 μm.

Table 5 Colony forming unit frequencies for canine ASC, SSC, and LSC following fibroblastic (CFU-F), adipogenic (CFU-Ad), or osteogenic (CFU-Ob) induction

		ASC	**SSC**	**LSC**
CFU-F	P0	212.0±45.6^{A,a}	248.3±42.7^{A,a}	1343.5±170.6^{B,a}
	P3	565.6±104.9^{A,a}	919.7±158.9^{A,b}	4423.4±871.5^{B,b}
	P6	3888.2±747.2^{A,b}	7834.7±1892.4^{B,c}	
CFU-Ad	P0	155.0±58.6^{A,a}	739.1±157.7^{B,a}	1570.4±213.6^{C,a}
	P3	387.5±88.8^{A,a}	1528/7±269.1^{B,b}	4411.4±357.2^{C,b}
	P6	6602.8±979.8^{A,b}	9350.0±65.7^{B,c}	
CFU-Ob	P0	703.6±193.2^{A,a}	820.6±106.4^{A,a}	1734.1±196.4^{B,a}
	P3	1274.8±302.5^{A,a}	1596.6±235.6^{A,b}	3670.8±494.2^{B,b}
	P6	6266.7±945.4^{A,b}	10050.0±1068.9^{B,c}	

Columns with different upper-case letters within passages and those with different lower-case letters within cell types are significantly different from each other ($P<0.05$).

2.3.4 Target Gene Expression

Compared to SSC and LSC at the same passages, induced P0 and P3 ASC had significantly higher mRNA levels of peroxisome proliferator-activated receptor gamma (PPAR-γ) and leptin following adipogenic induction, osteoprotegerin (OPG) and collagen 1 (Col1) following osteogenic induction, and aggrecan following chondrogenic induction (See A-F in Figure 2). Following adipogenic and osteogenic induction, P0 and P3 ASC had significantly lower mRNA levels of homeobox protein nanog (Nanog) than SSC and LSC, and the same was true for sex determining region Y-box 2 (Sox2) expression following adipogenic induction. There were significantly lower mRNA levels of Sox2 in P3 ASC compared to LSC and SSC following osteogenic induction.

2.3.5 Immunophenotype

The majority of P0 and P3 cells were $CD29^+$, $CD44^+$, $CD90^+$, $CD34^-$ and $CD45^-$ (Figure 3), and the SVF of all cell types had lower percentages of $CD44^+$ and $CD90^+$ cells than P0 and 3 (See A-C in Figure 4). The SSC and LSC SVF had higher $CD34^+$ percentages than the ASC SVF (See D in Figure 4). With increasing passages, the percentages of $CD34^+$, $CD29^+$, $CD44^+$, and $CD90^+$ cells tended to decrease in all cell types, while the percentages of $CD45^+$ cells remained relatively constant (See E-H in Figure 4). Among cell types, the P0 ASC $CD29^+$ percentage was significantly higher than the LSC (See A in Figure 4). The P3 ASC and SSC $CD29^+$ percentages were significantly higher than LSC, and P6 ASC percentage significantly higher than SSC (See B in Figure 4). The $CD44^+$ percentage was significantly higher for P3 SSC than ASC, though the P6 ASC percentage was significantly higher than P6 SSC. The P6 ASC $CD90^+$ percentage was significantly higher than P6 SSC (See C in Figure 4). As above, due to limited cell expansion, flow cytometry was not performed on P6 LSC.

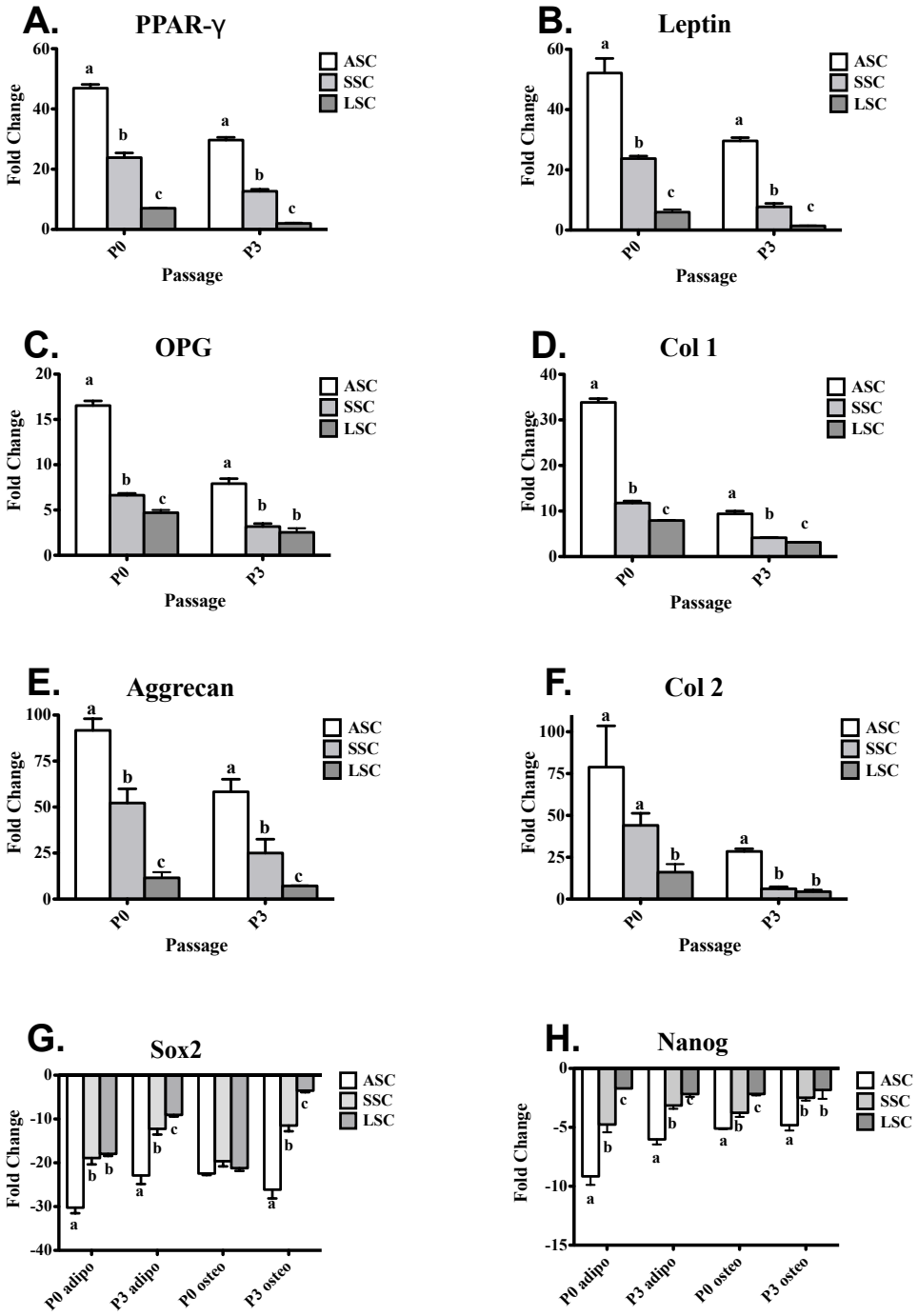

Figure 2 Fold change (mean ± SEM, n=6, 3 replicates) of adipogenic (A, B), osteogenic (C, D), and chondrogenic (E, F) target genes in ASC, SSC and LSC

Values were normalized to GAPDH and relative to cells cultured in stromal medium. The fold change of MSC target genes (G, H) was evaluated for each cell type similarly following adipogenic and osteogenic induction. Columns with different letters within passages are significantly different from each other ($P < 0.05$).

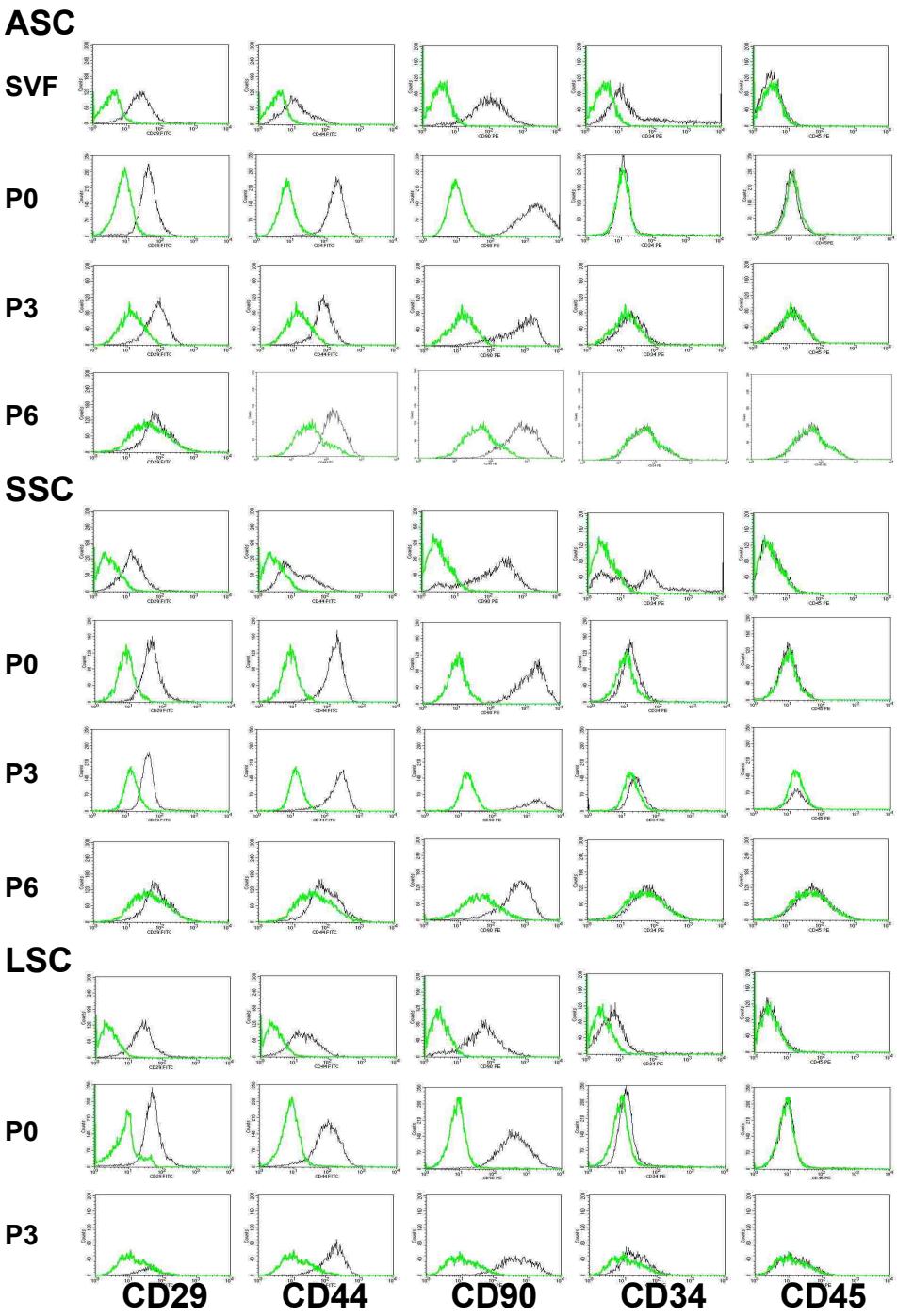

Figure 3 Representative immunophenotyping of SVF, P0, P3, and P6 ASC, SSC, and LSC

Columns are different passages and rows different surface makers. The black graphs represent stained cells and the green graphs autofluorescence.

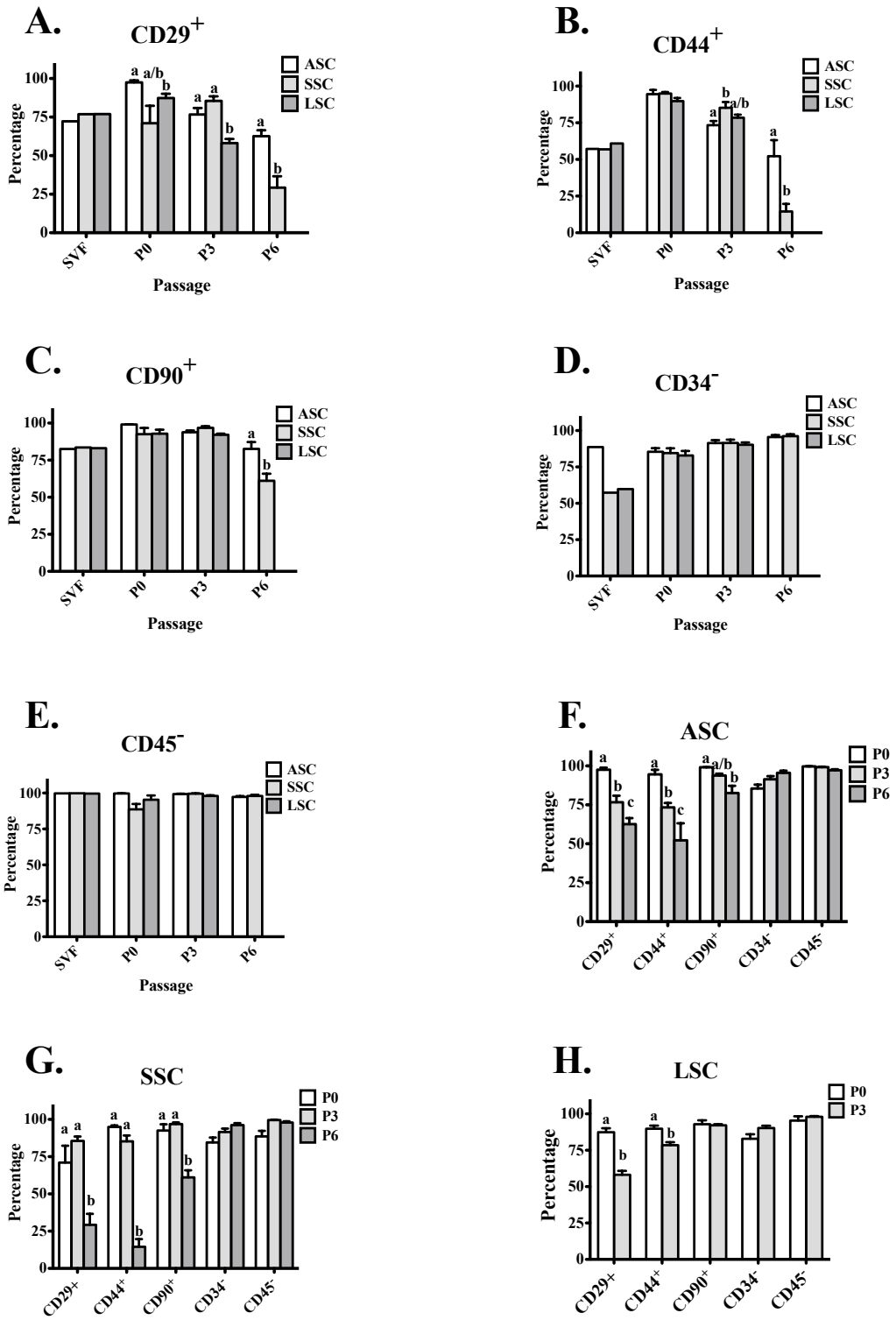

Figure 4 Cell percentages (mean ± SEM) of P0, 3, and 6 ASC, SSC, and LSC that were CD29+, CD44+, CD90+, CD34-, or CD45-

Columns with different letters within passages are significantly different from each other ($P < 0.05$).

2.4 Discussion

Stromal cell-mediated tissue regeneration is a promising approach for a wide range of medical applications. We have established the IFP as the optimum source of MSC in the canine stifle among those evaluated. Consistent with the hypothesis, the MSC population, *in vitro* expansion rates, and multipotentiality were highest in ASCs compared to SSCs and LSCs within individuals up to P6 based on cell doublings, CFU frequencies, MSC immunophenotypes, and target gene expression. As passages increased, cell doublings, CFU frequencies, MSC immunophenotypes, as well as MSC, adipogenic and osteogenic lineage-specific gene expression decreased in all three cell types, suggesting some reduction in MSC numbers and multipotentiality. Notably, the ASCs retained these characteristics the best through multiple cell passages. This information surrounding intra-articular MSCs may contribute to studies aimed at clinical translation of stromal cell technology.

Most stifle tissues are derived from interzonal mesenchyme, so MSCs derived from these tissues may share common features which are distinct from those residing elsewhere [17]. Orthotopic cell sources have advantages for intra-articular tissue regeneration based on *in vitro* differentiation studies, possibly a result of exposure to the local joint environment during development potentiating cell differentiation into specialized joint tissues [11, 21, 177]. Multipotent cell numbers, expansion capacity and multipotentiality vary among the different tissues that contain MSCs within the femorotibial joint such as IFP, synovium, synovial fluid, and CrCL [22, 169]. We sought to identify and establish the best MSC source for stifle-specific tissue regeneration by comparing some major intra-articular cell sources within individuals.

The ASC DT in this study was similar to previous reports for canine IFP and subcutaneous ASCs and human IFP ASCs [178, 179]. The DT for canine SSCs and

LSCs in this study were significantly lower than that those reported for human SSCs and LSCs [180]. In addition to species differences, the human LSCs were harvested from the anterior cruciate ligament (ACL) core minus synovium, collagenase digestion was not performed and a different culture medium was used. Hence, differences in results between the studies are not unexpected. In this study, decreasing cell doubling capacity with increasing passages in all cell types suggests that intra-articular MSCs from early passages may have the best expansion potential to meet therapeutic needs.

The ASC stromal, osteogenic, and adipogenic CFU frequencies in this study were higher than previously reported for dogs [174]. Differences may be because of the use of fresh versus revitalized cells. Indomethacin in the adipogenic medium in this study may have also contributed to higher CFU-Ad frequencies over the previous canine study (975.7±125.3) [181]. The higher adipogenic capacity of ASCs may also be due to a native preadipocyte population in P0 [182]. However, preadipocytes and multipotent cells are distinguished by the short preadipocyte lifespan in contrast to high expansion capacity and multipotentiality retained by MSCs through passages, so preadipocytes are unlikely to have affected later passages [111]. Canine IFP ASCs have been reported to have similar osteogenic capacity to bone marrow-derived stromal cells (BMSCs), which supports the superior osteogenesis of the ASCs compared SSCs and LSCs in this study [174]. Information surrounding direct comparisons of the chondrogenic potential of stifle joint tissues is limited, but rat SSCs reportedly have better chondrogenic potential than MSCs from subcutaneous fat [183]. Additionally, IFP ASCs had better chondrogenic potential than BMSCs and subcutaneous ASCs in elderly humans with osteoarthritis [184]. Though there was no difference in proteoglycan staining among intra-articular tissues evaluated in this

study, higher mRNA levels of Col2 and aggrecan mRNA in ASC pellets may indicate higher chondrogenic potential.

The identity of the MSC populations within each tissue was confirmed, in part, by the presence of common MSC cell surface markers detected with flow cytometry. The mRNA levels of embryonic stromal cell markers previously used to identify canine MSCs in adult tissue, Nanog and Sox2, also supported the MSC identity of cell populations isolated from all three intra-articular tissues in this study [24]. Cluster of differentiation (CD), also called cluster of determinants, are clusters of antigens that react with antibodies associated with various cell characteristics. They were originally used to identify different stages of lymphocyte maturation, but profiling of CD cell surface antigen expression with flow cytometry is now a standard mechanism by which MSC phenotypes are distinguished. The CD34+ cells within the SVF are consistent with human subcutaneous ASCs [185]. Type B synoviocytes (fibroblast-like) are also $CD34^+$ [186]. Since the LSCs were harvested from synovium around the ligament, it is reasonable that the SVF of LSCs as well as SSCs contained higher percentages of $CD34^+$ cells. Plastic adherence appeared to effectively select against $CD34^+$ cells with increasing passages.

The location, size, accessibility, and protective synovial capsule of the IFP make it a good potential MSC harvest option [174]. It may be feasible to isolate cells for reapplication prior to closure during standard surgical procedures. Additionally, cells may be expanded *in vitro* and banked for later application. The number of autologous MSC harvested from the synovium or CrCL in a diseased or injured stifle may be limited since synovium undergoes significant pathogenic changes in the presence of inflammation, and the CrCL is often partially or completely ruptured in injured stifles [187]. Despite this, it is feasible that synovium and CrCL may be

potential MSC sources for tissue-specific engineering since they may contain less primitive cells than the IFP. Further research is necessary to identify and confirm this possibility.

The IFP is encapsulated and separated from the joint by synovium [188]. Hence, MSCs niches within the IFP may therefore contain cells that receive less stimulation to induce differentiation and therefore remain more primitive compared to other intra-articular niches [179, 189]. Human IFP ASCs from osteoarthritic knees have comparable long-term cell expansion, multipotentiality, and MSC marker-expression as normal BMSCs [190]. This is distinct from intra-articular SSCs, BMSCs and cartilage-derived stromal cells, where cell morphology, proliferation, and multipotentiality are negatively affected by acute and chronic inflammation as well as the presence of OA [104, 191, 192]. The results of this study suggest that the IFP is the optimum tissue source for adult MSC isolation in the canine stifle compared to joint capsular or ACL synovium. The orthotopic advantages as well as the relative isolation of MSCs within the IFP in the face of injury or disease further supports the advantages of this tissue source. Study findings are limited to normal tissues, and additional studies are necessary to confirm them in abnormal joints with distinctions between those affected by injury versus degenerative changes. In conclusion, this side by side comparison of canine stifle joint tissue sources establishes the IFP as having the highest cell density and MSCs with the highest expansion capacity, multipotentiality, and MSC immunophenotype over multiple cell passages *in vitro*.

CHAPTER 3. ISOLATION AND CHARACTERIZATION OF FRESH AND REVITALIZED MULTIPOTENT CELLS FROM EXCISED FELINE ADIPOSE

3.1 Introduction

Adult multipotent stromal (stem) cells (MSCs) are gaining popularity in veterinary medicine due to their differentiation potential, immune privilege, and sustainability in culture [193]. The therapeutic effects of MSCs are thought to be, in part, due to their release of trophic and immunomodulatory factors [62, 194]. Of companion animal species, stromal cell therapy has been applied in dogs and horses, but comparably few MSC investigations have been performed with cat tissues [150, 195-197]. Most feline-specific MSC reports surround BMSCs, which are reported to have both neurogenic and cardiogenic capacities [25, 198-200]. Additionally, intra-renal injection of BMSCs and ASCs for chronic kidney disease has had promising results [151]. Feline inguinal ASCs have higher proliferative rates *in vitro* than BMSCs, one of the many attributes that make adipose an appealing source of MSCs [201].

In addition to those mentioned above, there are numerous pathological conditions in the cat that may benefit from ASC therapy. Potential targets include complications associated with diabetes mellitus, lymphoma, and retinal disease which affect between 0.2% and 2% cats in the United States [202-205]. There are reports of canine and human MSC therapies for these conditions at doses of 0.5 to 50 million MSCs/kg [202-205]. Prior to clinical application, heterogeneous MSC isolates should be thoroughly characterized to meet a minimum standard of care. At present, there are few tools to meet the standards of the International Society for Cell Therapy with feline MSCs [18]. Mechanisms to characterize feline MSCs are necessary for clinical translation of this novel treatment modality for feline companions.

Adipose-derived stromal cells can be isolated from both white adipose tissue (WAT) and brown adipose tissue (BAT). As a highly active metabolic tissue, WAT contains a large number of stromal vascular cells with great differentiation potential [206, 207]. Since epididymal adipose harvested during routine feline castration is one of the purest sources of WAT it is a promising tissue for ASC harvest [208]. According to the 2011-2012 National Pet Owners' Survey by the American Pet Products Association, 88% of approximately 86.4 million privately owned cats in the United States are spayed or neutered. ASCs harvested from tissue excised during neutering may be expanded *in vitro* and applied in the short term or cryopreserved for later application. Based on current information, therapeutic doses of MSCs range from 10^5 to 10^8 cells/kg. The differentiation potential and expansion rate of ASCs decreases with increasing passages in most species, and the cells tend to have the highest multipotentiality before P4 [174]. Based on results from other species, 0.5 ~ 2 x 10^6 nucleated cells can be expanded from one gram of inguinal or epididymal adipose tissue with a colony forming unit frequency of 1% to 10% [150, 209-211]. Cell doubling times for most species are approximately two days before P4 [174, 212]. Based on broad assumptions from the published literature in other species, approximately 2 ~ 3 g of feline epididymal adipose would be needed to yield 10^6 nucleated cells/g containing 10^4 ASCs to provide a dose of 10^7 ASCs within three cell passages. Our objective was to optimize ASC isolation and expansion so that therapeutic doses of ASCs can be harvested from individual cats based on the hypothesis that 10^7-10^8 ASCs are available within 3-4 cell passages to give an MSC treatment dose of 10^6-10^7 ASCs/kg from individual cat epididymal ASCs prior to and after cryopreservation.

3.2 Methods

3.2.1 Study Design

Epididymal tissue was collected during routine castration of 14 male domestic short hair cats (1.0 ± 0.2 years, 2.9 ± 0.3 Kg, mean ± SEM). The body conditioning score of the cats included in this study were around 4 – 6 on a scale of 1 – 9. Cell expansion rate, multipotentiality and progenitor cell surface markers were evaluated for both fresh and revitalized (cryopreserved for 1 month) cells from individual cats as follows: P0-5 cell doublings (CD) and doubling times (DT); P0, 1, 3 and 5 $CD29^{+}$, $CD44^{+}$, $CD90^{+}$, $CD34^{+}$, and $CD45^{+}$ cell percentages; P0, 1, 3 and 5 colony forming unit (CFU) -fibroblastic (F), adipogenic (Ad) and osteogenic (Ob) frequencies; P1 and 3 stromal and induced (adipogenic, osteogenic, and chondrogenic) cell MSC and lineage specific target gene mRNA levels. Fresh cells from each cat were further assessed: P0 chondrogenic pellet alcian blue (proteoglycan) staining; stromal vascular fraction (SVF), P0, 1 and 3 F-actin and Hoechst dye staining. The SVF CFU-F frequencies were also determined using pooled tissue from 10 other male domestic short hair cats to meet adequate cell numbers for seeding.

3.2.2 Materials

All reagents were purchased from Sigma Chemical Co. (St. Louis, MO) or Fisher Scientific (Dallas, TX) unless noted otherwise.

3.2.3 Isolation Method

Epididymal adipose was harvested, and tissue was processed within 4 hrs of harvest for each cat. Adipose tissue was isolated with sharp dissection, minced, and digested in 33 ml Type I collagenase per gram of adipose (Worthington, NJ).

The isolation method was first discovered using tissues from 5 cats. Tissues from the rest 9 cats were all digested with the best method. Tissues from each cat (n=5) were divided into three equal portions, and each portion was digested by one of three methods: 1) 0.3% type I collagenase in Kreb's Ringer buffer, 0.5 hr, 1000 rpm stirring (New); 2) 0.3% type I collagenase in Kreb's Ringer buffer, 1 hr, 1000 rpm stirring (Hour); and 3) 0.1% type I collagenase in DMEM, 0.5 hr, 60 rpm (Classic). The digestion solution was then filtered (100 μm, BD Falcon, Bedford, MA). The resulting pellet (260 g, 5 min) was resuspended in 5 ml red cell lysis buffer (0.16 mol/L NH_4Cl, 0.01 mol/L $KHCO_3$, 0.01% EDTA). The resulting SVF was seeded in a 10 mm cell culture dish (CellStar, Greiner, NC) in stromal medium (DMEM-Ham's F12, 10% fetal bovine serum (FBS), 1% antibiotic/antimycotic solution) and cultured under standard conditions (37°C, 5% CO_2). Medium was refreshed after overnight incubation and then every 2-3 days. When the first colony that contained > 20 cells was discovered, the number of colonies was counted. MSC density was calculated as colony number/adipose weight (g). The new method was selected to isolate ASCs for the remainder of the study based on the highest number of colonies/g epididymal adipose. For purposes of this study, primary cell isolates were considered the SVF and the first cell passage was P0. Cells were seeded at a density of 5 x 10^3 cells/cm^2 for P0 and all subsequent passages for all assays.

3.2.4 Cell Expansion

P0 cells were seeded in 12-well plates and counted after 2, 4, and 6 days of culture. Cell doublings and DT were determined with duplicate cultures and calculated with the formulae: $CD= \ln(N_f /N_i)/\ln(2)$ $DT= CT/CD$ (N_i: initial cell number; N_f: final cell number; CT=culture time) [172]. Day 2 and day 4 cell counts were used as the initial number to calculate expansion rates on days 4 and 6, respectively.

3.2.5 Trilineage Differentiation

Feline-specific induction media were developed in this study. Cells at P0 were first cultured in stromal medium to 80% confluence, and then transferred to adipogenic medium (α-MEM, 10% rabbit serum, 10% FBS, 10nM dexamethasone, 5μg/mL insulin, 50μM 5,8,11,14-eicosatetraynoic acid (ETYA) [Cayman, Ann Arbor, MI], 100μM indomethacin) for 10 days. Cells were fixed with 4% paraformaldehyde (PFA) and stained with Oil Red O. Confluent P0 cells were also cultured in osteogenic medium (DMEM, 10% FBS, 100 nM dexamethasone, 0.25 mM L-ascorbic acid) for 10 days and then in osteogenic medium supplemented with 10nM β-glycerophosphate for another 10 days to avoid delamination. Cells were fixed in 70% ethanol and stained with 2% alizarin red. For chondrogenesis, 5 x 10^5 cells were centrifuged (200 x g, 5 min) to form a pellet in a 15 ml tube (Corning, NY). The pellet was cultured in chondrogenic differentiation medium (Low glucose DMEM-Ham's F12, 1% FBS, 1% antibiotic/antimycotic solution, 50 μg/mL ascorbate phosphate, 100 nM dexamethasone, 40 μg/mL proline, 1 mM sodium pyruvate, 1% ITS, 10 ng/mL BMP-6, 10 ng/mL TGF- β1) for 21 days. Cell pellets were cultured in stromal medium for comparison. At the end of the culture period, pellets were formalin-fixed, paraffin-embedded, sectioned (5 μm) and stained with alcian blue.

3.2.6 Multipotentiality (SVF, P0, 3, 6)

Limiting-dilution assays to determine CFU-F, -Ad and -Ob frequencies were performed as previously reported with changes indicated [174]. Due to the low ASC density in the SVF, samples were pooled from 10 unrelated cats, and 8 replicates of 500, 250, 125, 63, 31, or 16 cells were seeded for CFU-F. For P0, 1, 3, and 5, 8 replicates of 5 x 10^3, 2.5 x 10^3, 1.25 x 10^3, 6.25 x 10^2, 3.12 x 10^2, or 1.56 x 10^2 cells/well were incubated in a 96-well plate. Cells were cultured in stromal media for

10 days. The CFU-F colonies were fixed with 4% PFA and stained with 0.1% toluidine blue. For CFU-Ad and -Ob, cells were cultured in lineage-specific induction media as described above, and the number of stained colonies in each well was counted. Wells were considered positive for fibroblast-like colonies, adipogenesis, or osteogenesis when there were ≥10 toluidine blue-stained colonies, ≥10 oil red O-stained colonies, or ≥1 alizarin red-stained colonies, respectively. The CFU frequencies were calculated as $F=e^{-x}$ (F: ratio of negative to total wells within a row, e: natural logarithm constant 2.71, x: CFU number per well). Based on Poisson's distribution, F = 0.37 occurs when the number of total cells plated (N) in a well contains a single CFU. The CFU frequency is reported as 100 / N %.

3.2.7 Immunophenotypes (P0, 1, 3, 6)

Cell aliquots (10^5 - 10^6) were resuspended in 200 ml PBS containing 5 µl of antibody. Cells were incubated with antibodies specific for feline antigens or validated for feline cross reactivity for 30 min at room temperature (Table 6). The cells were then washed with PBS and fixed with 4% PFA. For CD9, CD29, CD44, and CD90 samples, indirect immunofluorescence was done with goat anti-mouse IgG-FITC. For negative autofluorescence control, cells were not incubated with antibodies. Cellular fluorescence was evaluated by flow cytometry using a FACSCalibur flow cytometer and CellQuest Pro software (BD Biosciences). Cell percentages expressing each antigen were determined using population gated of fluorescence subtracting relative autofluorescence control.

3.2.8 Cell Morphology (SVF, P0, 1, 3)

Cells were cultured in stromal medium on glass coverslips for 7 days. Cells were washed with PBS, fixed in 4% PFA for 20 min, permeablized with 0.5% Triton-x100 for 20 min, and stained with Acti-stain™ 488 (1:150) (cytoskeleton, Denver, CO) and

Hoechst dye (1:2000) for 5min at RT. Samples were then viewed with a fluorescence microscope DM4500B (Leica, Buffalo Grove, IL).

Table 6 Antibodies for feline ASC Fluorescence-activated cell sorting (FACS) analysis

Antibody	Label	Target Species	Manufacturer	Cat No.	Marker Specification
CD9	N/A	Cat	Serotec	MCA1345	Myeloid
CD29	N/A	Human	BD Biosciences	610468	Cell adhesion, β1 integrin
CD44	N/A	Cat	VMRD	BAG40A	Hyaluronic acid receptor
CD90	N/A	Human	eBiosciences	14-0909-80	Thy-1, fibroblasts, MSC
CD105	PE	Human	eBiosciences	12-1057-41	Endoglin, mesenchymal, and erythroid progenitors
IgG	FITC	Mouse	Sigma-Aldrich	F9006	Goat anti-mouse IgG

3.2.9 Expression of marker genes (P1, 3)

Total RNA was extracted from cells using TRIzol reagent (Fisher) according to the manufacturer's instructions. Quantity was determined with a ND-100 spectrophotometer (NanoDrop Technologies, Wilmington, DE), and 1 μg of RNA was used for cDNA synthesis per 20 μl reaction using a QuantiTect Reverse Transcription Kit (Qiagen, Hilden, Germany). Feline-specific primers were used for all reactions (Table 7). qRT-PCR was performed in duplicate with a 20 μl total reaction using a QuantiTect SYBR Green PCR Kit (Qiagen), 0.3 μM for each forward and reverse primer in a 384 well PCR plate. PCR amplication was performed using Applied BioSystems 7900 Real-Time PCR System (SDS v2.4; Applied Biosystems, Carlsbad, CA) and stoped at 40 cycles according to the manufacturer's program. In the present study, the data are presented as the fold change in target gene expression in differentiated cells normalized to glyceraldehyde 3-phosphate dehydrogenase (GAPDH) and relative to the stromal cell control according to $2^{-\Delta\Delta Ct}$ [176].

Table 7 Feline-specific primer sequences

	Gene	Forward Primer	Reverse Primer
Housekeeping	GAPDH	GGTCATCCCAGAGCTGAATG	AGCTTGACAAAGTGGTCATTG
Adipogenic	PPAR-γ	GGGAGTTTCTAAAGAGCCTGAG	GTCCTCAATGGGCTTCACATTCAGC
	Leptin	CCATCTTGGACAAACTCAGGAC	GTTGAAGCTGTGCCAATCCG
Osteogenic	Col1	GACAAGGGTGAGACAGGCGAACAG	CTTCTCTTGAGGTGGCTGGGG C
	OPG	GTCTCATTCGAGAAGAACCC	CACAACCGCGTGTGCGAGTGC
Chondrogenic	Aggrecan	GCAGTACACATCATAGGTCTC	CATCGTGTTCCATTACAGAGC
	Col2	CACAGATTATGTCGTCGCAGAGGA C	CCAGACGCTGGTGCTGCTGACGC
MSC	Sox2	GGAGGTACATGCTGATCATG	CAGTACAACTCCATGACC
	Nanog	GATCTCCTCTGCAGAAGTGG	CTCCAGTGCCTGAGATTGATGG

PPAR-γ, peroxisome proliferator-activated receptor gamma; Col1, collagen type I; OPG, osteoprotegerin; Col2, collagen type II; Sox2, sex determining region Y-box 2; Nanog, homeobox protein nanog.

3.2.10 Statistical Analysis

All results are presented as mean ± SEM. Among passages, differences in CD, DT, CFU frequency, RNA levels and cell surface marker percentages were determined with one-way ANOVA and Tukey's post hoc tests ($P<0.05$) using SAS.

3.3 Results

3.3.1 Isolation Method

A mean of 0.2 ± 0.03g (wet weight) adipose was harvested from each cat. The Hour and Classic isolation methods yielded 3.8 and 1.6 colonies/g, respectively, which were not significantly different. The New isolation method had a higher yield of 126.3 ± 33.9 colonies/g with tissues from five cats (see A in Figure 5). Using tissues from 14 cats, the mean ASC yield was 76.3 ± 22.2 colonies/g of tissue, which was not

significantly different that the finding with five cats (see B in Figure 5). At 80% confluence, there were about 1 x 10^6 P0 cells per 10 cm dish for P0-2. With a consistent seeding density of 5 x 10^3 cells/cm^2, around 2 x 10^7 cells are available by P2, which is 7 x 10^6 cells/kg for the cats in this study.

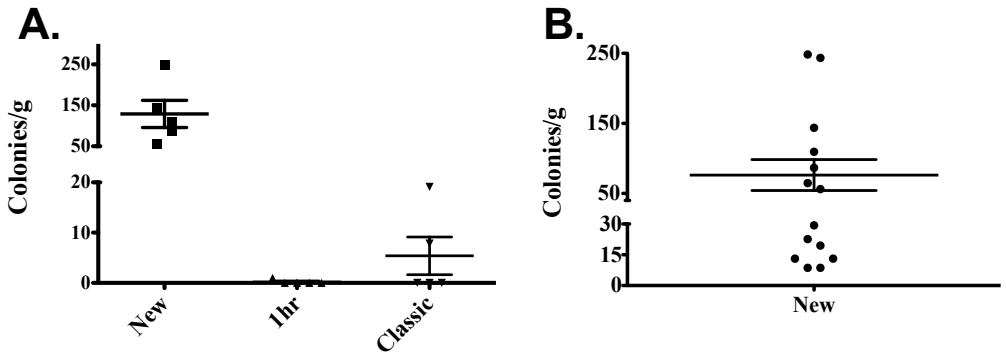

Figure 5 Feline epididymal adipose ASC isolation method

(A) Feline epididymal adipose ASC yields using three different digestion techniques (n=5). (B) ASC yield using the new digestion method (n=15).

3.3.2 Cell Morphology

Five days after seeding, adherent SVF cells showed a spindle-shaped morphology typical of ASCs (see A in Figure 6). Homogenous cultures and elongated shaped cells increased at P0 and 1 (see B,C in Figure 6), which became flattened and disorganized by P3 (see D in Figure 6).

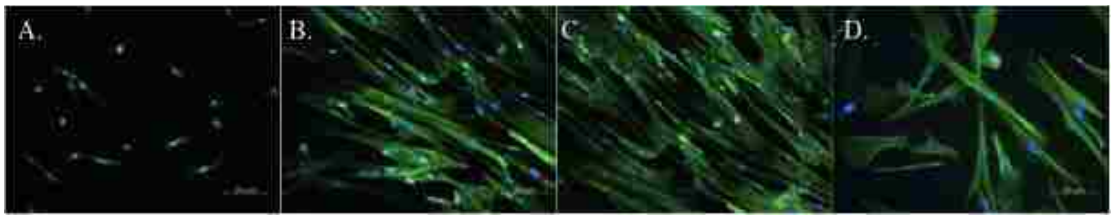

Figure 6 Feline ASC morphology

Cells of SVF (A), P0 (B), P1 (C) and P3 (D) were stained with FITC-F-actin (green) for the microfilaments and Hoechst dye (blue) for the nucleus (20x).

3.3.3 Cell Expansion

The overall CD for P0-5 fresh cells was 0.7 ± 0.1 CD/days, and the corresponding DT was 1.4 ± 0.2 days/CD. Generally, cell expansion rates decreased as passages increased. For fresh cells, P0-2 cells had significantly higher CD than P3-5 (Table 8), while P0-3 cells had significantly lower DT than P4 and 5 (Table 9). For revitalized cells, P1 and 2 cells had significantly higher CD than P3-5, and P1-3 cells had significantly lower DT than P4 and 5. Fresh cells at P4 and 5 had significantly higher CD and lower DT than revitalized cells.

Table 8 Fresh and revitalized feline ASC cell doublings (CDs/day) for P0-5 (mean ± SEM)

	P0	**P1**	**P2**	**P3**	**P4**	**P5**
Fresh	1.3 ± 0.1^{a}	1.1 ± 0.1^{b}	0.9 ± 0.1^{b}	0.5 ± 0.04^{c}	0.3 ± 0.02^{c}	$0.3\pm0.04^{*,c}$
Revitalized		1.1 ± 0.1^{a}	0.9 ± 0.1^{a}	0.5 ± 0.03^{b}	0.2 ± 0.02^{c}	0.1 ± 0.01^{c}

Values within columns with asterisks are significantly different from revitalized cells. Values with different lower-case letters within passages (columns) are significantly different ($p<0.05$).

Table 9 Fresh and revitalized feline ASC doubling times (days/CD) for P0-5 (mean ± SEM)

	P0	**P1**	**P2**	**P3**	**P4**	**P5**
Fresh	0.8 ± 0.2^{a}	0.9 ± 0.2^{a}	1.1 ± 0.2^{a}	2.0 ± 0.4^{a}	$3.3\pm0.6^{*,b}$	$3.3\pm1.2^{*,b}$
Revitalized		0.9 ± 0.1^{a}	1.1 ± 0.2^{a}	2.0 ± 0.4^{a}	5.0 ± 1.6^{b}	10.0 ± 1.2^{c}

Values within columns with asterisks are significantly different from revitalized cells. Values with different lower-case letters within passages (columns) are significantly different ($p<0.05$).

3.3.4 Trilineage Differentiation

After about four days of culture in adipogenic medium, cells became round, and, after 21 days, robust lipid droplets were apparent (see A in Figure 7). In osteogenic medium without β-glycerophosphate, cells assumed a compact, cuboidal appearance and expressed alkaline phosphatase (ALP) after 10 days of culture (see B in Figure 7). Following the addition of β-glycerophosphate, granular nodules formed that stained

with alizarin red (calcium deposition) after 21 days of culture (see C in Figure 7). Cells were apparent within lacunae in pellets cultured in chondrogenic induction medium after 21 days, and extra-cellular matrix stained with alcian blue (unsulfated proteoglycan) (see D in Figure 7). Pellets cultured in stromal medium did not show lacunae formation (see E in Figure 7).

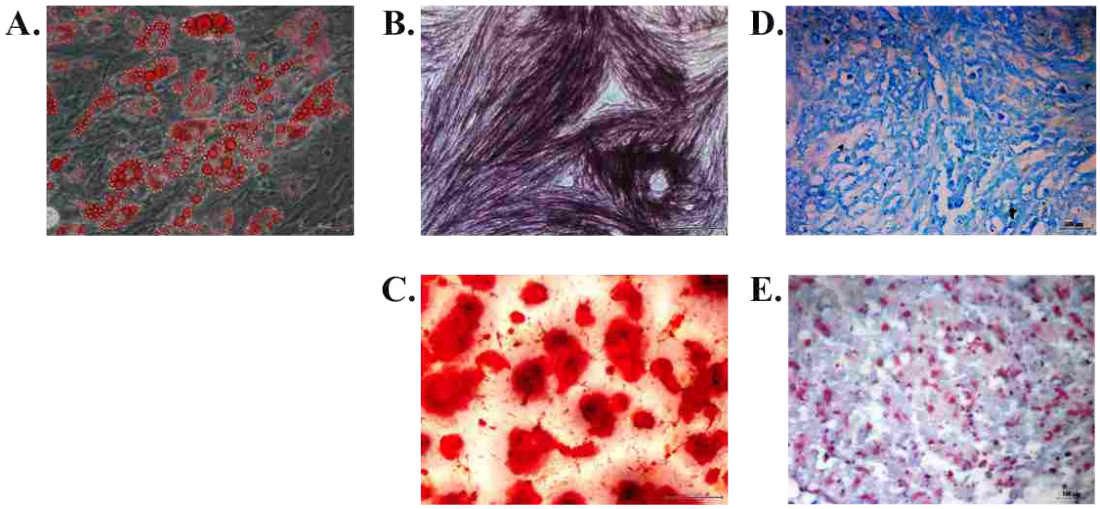

Figure 7 Feline ASC trilineage differentiation

(A) ASC adipogenesis. Lipid droplets were stained with oil red O after 10 days induction (40x). (B) Early stage osteogenesis. Alkaline phosphatase (ALP) was stained by 5-Bromo-4-chloro-3-indolyl phosphate/ nitro blue tetrazolium chloride after 10 days induction (10x). (C) Late stage osteogenesis. Extracellular matrix calcium was stained by alizarin red after 20 days induction (5x). (D) Early stage chondrogenesis. Cell pellet was stained with alcian blue after 20 days culture in induction or stromal medium (E) (64x).

3.3.5 Multipotentiality

The CFU frequency indicates the percentage of cells within a population that are capable of forming CFU-F, -Ad or -Ob colonies. Due to low expansion rates after P3, P5 revitalized cells were not included in CFU assays. The SVF CFU-F frequency was 1.6% (Table 10). Fresh cells at P0 and 1 had significantly higher CFU-F, -Ad, and -Ob frequencies than P3 and 5. Revitalized P1 cells had significantly higher CFU-F, -Ad, and -Ob frequencies than P3. Also, fresh P3 cells had significantly higher CFU-F and -Ob frequencies than revitalized cells.

Table 10 Colony forming unit (CFU) frequencies (mean ± SEM) for fresh and revitalized feline ASCs

CFU Frequencies (%, mean ± SEM)				
Passage	**Cell type**	**CFU-F (%)**	**CFU-Ad (%)**	**CFU-Ob (%)**
SVF	Fresh	1.6		
0	Fresh	2.2 ± 0.2^{a}	0.3 ± 0.02^{a}	0.7 ± 0.2^{a}
1	Fresh	2.0 ± 0.7^{a}	0.3 ± 0.08^{a}	0.6 ± 0.04^{a}
	Revitalized	1.9 ± 0.4^{a}	0.3 ± 0.03^{a}	0.5 ± 0.1^{a}
3	Fresh	$0.1\pm0.01^{*,b}$	0.03 ± 0.01^{b}	$0.1\pm0.01^{*,b}$
	Revitalized	0.04 ± 0.01^{b}	0.02 ± 0.01^{b}	0.03 ± 0.03^{b}
5	Fresh	0.02 ± 0.005^{c}	0.002 ± 0.002^{c}	0.01 ± 0.01^{c}

Values with asterisks are significantly different from revitalized cells within passage and CFU. Values with different lower-case letters within passages are significantly different.

3.3.6 Immunophenotypes

The majority of P0, 1, 3, and 5 cells were $CD9^{+}$, $CD29^{+}$, $CD44^{+}$, $CD90^{+}$, and $CD105^{+}$,

and there were no differences between new and classic isolation methods (Figure 8).

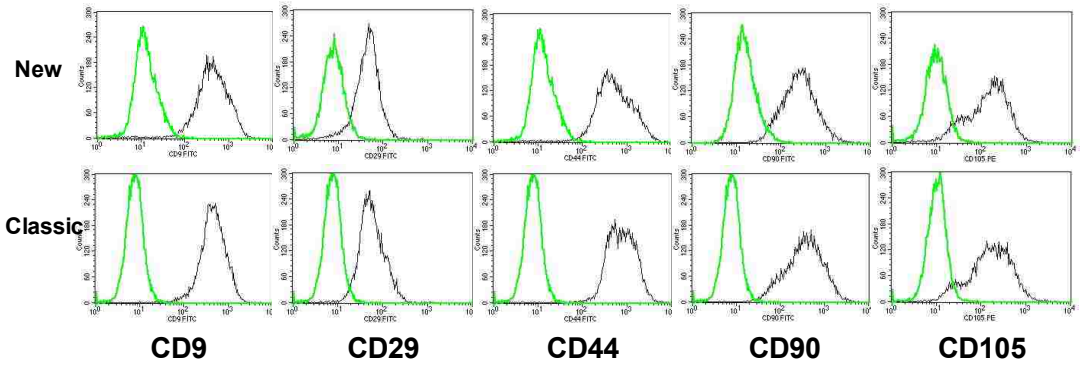

Figure 8 Representative immunophenotyping of P0 feline ASCs isolated using the new and classic methods

The black graphs represent stained cells and the green graphs autofluorescence.

Using the new method, P0 had significantly fewer CD105+ cells than P1, while P5 cells had significantly fewer CD9+ and CD105+ cells than P0 and 1 (See A in Figure 9). There were significantly more CD29+ cells at P1 and 3 than P5. Revitalized P3 cells had significantly more CD9+ and CD105+ cells than P1 (See B in Figure 9).

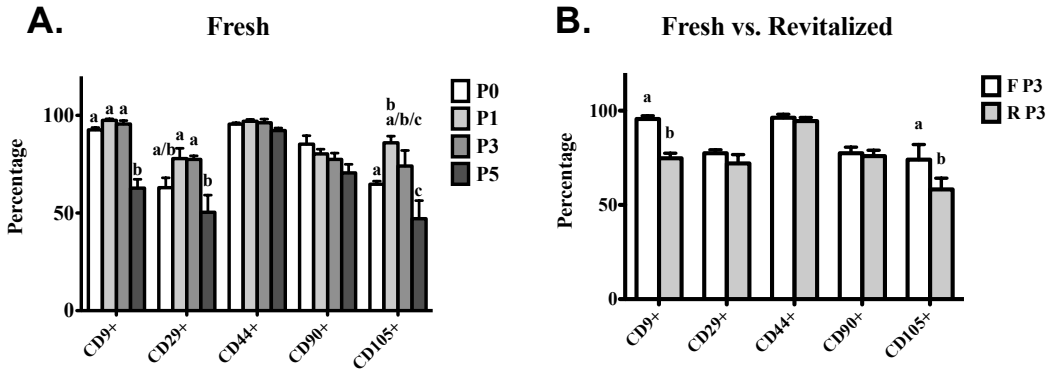

Figure 9 Cell percentages (mean ± SEM) of P0, 1, 3, and 5 fresh (F) and revitalized (R) ASCs positive for CD9, CD29, CD44, CD90, or CD105

Columns with different letters within markers are significantly different from each other ($P < 0.05$).

3.3.7 Expression of marker genes

Compared to P3 cells, induced P1 cells had significantly higher mRNA levels of peroxisome proliferator-activated receptor gamma (PPAR-γ) and leptin following adipogenic induction for both fresh and revitalized populations (See A,B in Figure 10). Both fresh and revitalized P1 cells following osteogenic induction also had significantly higher mRNA levels of osteoprotegerin (OPG) and collagen 1α1 (Col1α1) (See C,D in Figure 10). Both fresh and revitalized P1 cells after adipogenic or osteogenic induction had significantly higher levels of Sox2 than P3 (See E in Figure 10). Revitalized adipogenic P1 cells had significantly higher levels of Nanog than P3 (See Fin Figure 10). Also, fresh adipogenic P3 cells had significantly higher Nanog levels than revitalized cells. Additionally, both fresh and revitalized P1 cells had significantly higher Nanog levels than P3.

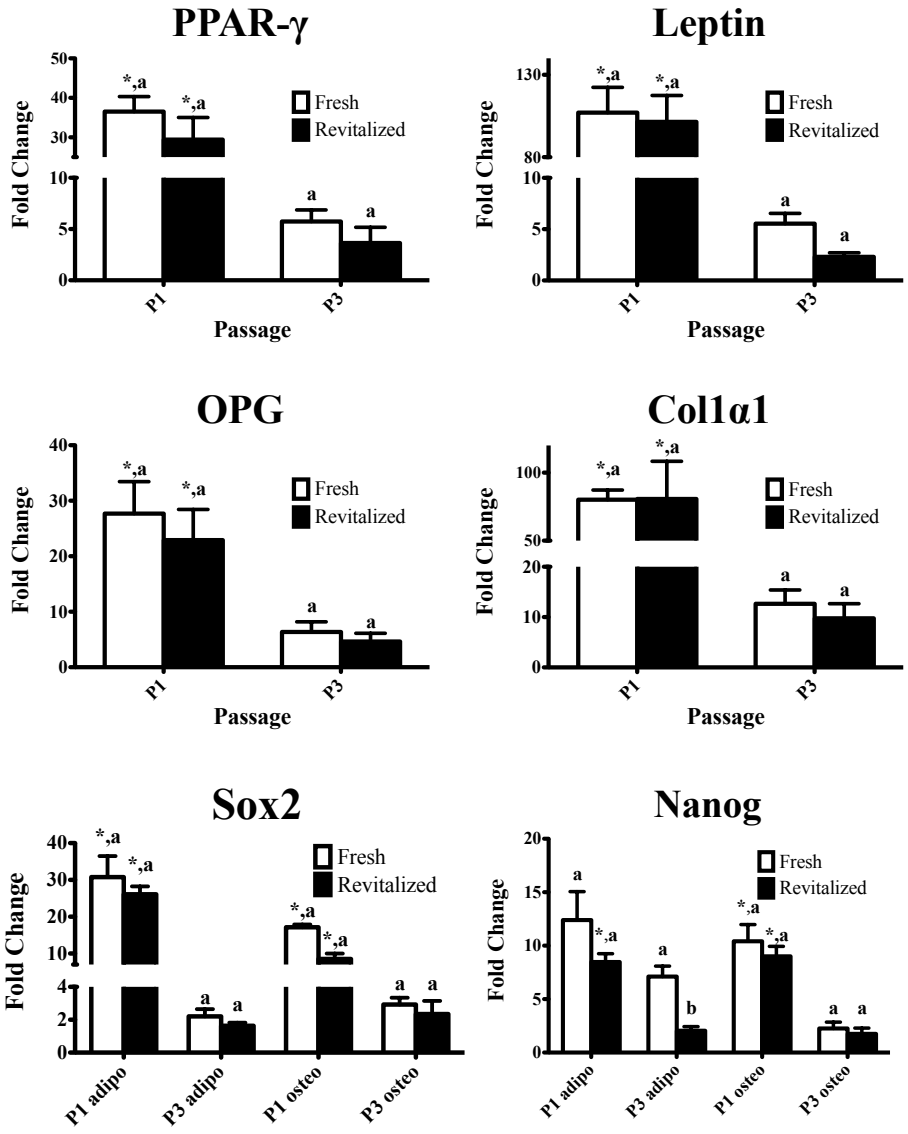

Figure 10 Fold change (mean ± SEM, n=5) of adipogenic and osteogenic target gene mRNA levels in feline ASCs

ASCs following adipogenic or osteogenic induction were compared to parallel cultures maintained in stromal medium Columns with different letters within markers are significantly different from each other ($P < 0.05$). Columns with asterisks are significantly different from revitalized cells.

3.4 Discussion

Stromal cell therapies may be an option for numerous feline pathologies. An efficient method to isolate ASC from feline epididymal adipose was developed in this study. Consistent with the hypothesis, a therapeutic dose of ASC was available within three cell passages (P2) of fresh or cryopreserved cells that retained their MSC properties.

Decreasing cell expansion, multipotentiality and MSC immunophenotype with increasing passages suggests that early passages of fresh or revitalized feline epididymal ASCs from have the greatest potential for therapeutic benefit. Hence, ASCs can be harvested from tissue that is routinely discarded and preserved for later administration, obviating the need for additional surgery or potential risks of allogenous cells. Further, the techniques to identify MSC surface marker expression in this study benefit efforts to isolate homogenous ASC populations for characterization and expansion.

There are several advantages to using epididymal adipose tissue for ASC isolation. It is a deposit of pure WAT in contrast to subcutaneous adipose tissue, a combination of BAT and WAT [207, 208]. White adipose tissue contains a higher ASC density compared to BAT [207]. Further, most cats are castrated as young animals. Numerous studies support the higher density and greater multipotentiality of ASC harvested from young versus older donors [213-215]. Cell banking for later administration is a feasible approach to address the consequences of aging in feline companions. While the results of this study are currently limited to toms, it is logical to extend this work to adipose tissue removed during routine spay procedures on queens.

Despite promising early results from clinical application in a number of species including cats (Table 11), standard protocols for ASC isolation, expansion and clinical application are lacking. Cell isolates are by nature heterogeneous and contain adipocyte precursors, mature endothelial cells, haematopoietic cell populations and tissue-specific progenitor cells [111]. Further, isolation procedures are generally customized for different adipose tissue harvest sites [216]. Significant variability among isolates can translate to unpredictable post-implantation behaviour [217].

Table 11 Therapeutic applications of MSCs

Trial	**Species**	**Source**	**Treatment**	**Results**
Chronic kidney disease [151]	Feline	1 ~ 4 x 10^6 ASCs 10^5 BMSCs	Intrarenal	2 of 4 cats with mild increase in glomerular filtration rate and decrease in serum creatinine concentration
Chronic kidney disease	Feline	1.47 x 10^6 ASC SVF/kg	Intrarenal	Creatinine improved 3.8%, BUN improved 19.6%
Type I diabetes [218]	Canine	5 x 10^7 BMSCs	Intrahepatical	Average blood glucose levels significantly increased
Lymphoma [219-221]	Canine	4 x 10^6 hematopoietic stem cells	Intravenous	Normal levels of serum thymidine kinase and the absence of peripheral blood clonal T-cell receptor gene rearrangements
Segmental bone defects [158]	Canine	125,000 BMSCs/cm^2	Ceramic carrier	Enhanced bone formation
Meniscus defects[48]	Caprine	10^7 BMSCs	Intraarticular	Enhanced tissue formation and reduced osteoarthritis
Chronic ischaemic cardiomyopathy [222]	Swine	2 ~ 20 x 10^7 BMSCs	Epicardially	Improved ventricular function and reduced size of infarct scar
Type I diabetes [217, 223-225]	Human	0.5 ~ 3 x 10^6 ASCs/kg	Intraportal or intra-arterial	Improvement of biological marker and no adverse effects
Type I diabetes [226, 227]	Human	3 x 10^6 BMSCs/kg	Intravenously	Induced prolonged insulin independence
Type II diabetes [228-230]	Human	3 ~ 4 x 10^8 BMSC SVF/kg	Intrapancreatical	Improved metabolic control and reduce insulin requirements
Retinal disease [231]	Human	10^7 BMSCs	Intravitreally	No detectable structural or functional toxicity

Though inherent individual variability among animals cannot be avoided, standardized isolation and characterization techniques for specific adipose deposits may significantly enhance the predictability of ASC behaviour and efficacy following administration. The efficient, repeatable ASC isolation technique from feline epididymal tissue established in this investigation is an option toward this goal. Further, selection of ASC by surface marker expression may likely increase consistency in *in vitro* and *in vivo* behaviour [99, 232].

The amount of adipose tissue available from excised castration tissue is about a tenth of that typically harvested from other adipose depots [233]. Despite this, a "dose" of cells was available within three cell passages in this study, using plastic affinity to select for ASCs [234]. Inconsistent cell expansion can contribute to differences among cell isolates since extensively expanded cells are technically "older" than those that have been expanded as much [235]. While SVF colony numbers were relatively low in this study, they were not significantly different among animals. Further, cell seeding density was identical for all cell passages. Given the age at which most of the cells will likely be isolated, they could be applied for congenital conditions, chronic illness or later for age related problems. Thus, the expansion time necessary for a characterized epididymal ASC isolate is unlikely to restrict use.

Kreb's ringer buffer contains 4-5 fold fewer nutrients than DMEM. It was used for collagenase digestion since DMEM components like high glucose and sulfhydryl and chelator-containing amino acids inhibit collagenase activity [236-239]. Mechanical agitation and lengthened digestion times were applied to promote tissue dissociation and facilitate collagenase activity, both of which can decrease cell viability [240, 241]. Study findings including cell phenotype, morphology, CD and DT and CFU frequencies were similar to those reported for cats and other species,

confirming that the vigorous digestion did not inhibit subsequent cell function [25, 151, 172, 174, 193, 210, 234, 242]. The significant increase in CD105+ cell percentages from P0 to P1 is consistent with ASC selection by plastic adherence [243, 244]. Decreased CD9+ and CD105+ cell percentages in late cell passages parallel the observed reductions in multipotentiality based on CFU-Ad and -Ob frequencies and tissue specific mRNA levels.

Differentiation media used in this study were optimized for feline ASC based on existing knowledge from other species [25, 151, 174]. Adipogenesis induction medium contained ETYA and indomethacin which promote lipid droplet formation by PPAR-γ activation, and rabbit serum, a component of canine and equine ASC adipogenic medium [25, 163, 181, 226]. Beta-glycerophosphate was added to osteogenic medium after 10 days of culture to avoid colony delamination [245]. For chondrogenesis, bone morphogenetic protein-6 was added to enhance proteoglycan synthesis as reported for equine MSC [163, 246, 247]. The induction media used in this study may be valuable for future feline ASC studies, especially in the area of *in vitro* tissue generation.

Results from the present study demonstrate that tissue excised from routine castration is a reliable source of feline ASCs. The New method of adipose tissue digestion results in a therapeutic dose of functional ASCs for potential autologous administration. Cell cryopreservation is a mechanism to maintain potent ASCs for later application that will reduce cell expansion time and avoid tissue harvest from sick or injured patients. Use of MSC surface antigens and major histocompatibility markers to isolate homogenous ASC populations is a natural extension of the work reported here that may enhance cell efficacy and reduce the potential for rejection or antigenic stimulation [53]. Prior to implementation of ASC administration as a

standard of care, standardized isolation and administration protocols as well as safety and efficacy, should be established with preclinical investigations and randomized, controlled clinical trials in accordance with established guidelines.

CHAPTER 4. *IN VITRO* CANINE CRANIAL CRUCIATE LIGAMENT REGENERATION USING ADULT INFRAPATELLAR ADIPOSE-DERIVED MULTIPOTENT STROMAL CELLS, COLLAGEN SCAFFOLD AND PDS SUTURES

4.1 Introduction

4.1.1 Cranial Cruciate Ligament Disease (CrCL)

The CrCL connects the lateral condyle of the femur and the anterior intercondylar area of the tibia. Rupture of the CrCL is one of the most common causes of hindlimb lameness in dogs. Sometimes, acute CrCL injury can occur due to trauma, when the dog jumps, slips, make a sudden turn or steps into a hole and the relative forces stressing the ligament exceed its breaking strength. However, only 20% of canine CrCL deficiencies are due to trauma. The majority of CrCLs rupture due to progressive and irreversible degeneration within the ligament itself [248, 249]. These non-traumatic ruptures are called spontaneous CrCL rupture. Both partial and complete CrCL rupture accelerates development of osteoarthritis (OA), a highly prevalent and progressive degenerative joint disorder which leads to pain, stiffness and decreased range of movement in both animals and humans. Age, genetic, conformational, environmental, immune-mediated, and inflammatory factors can contribute to development of OA [250-252].

Genetics exert a direct impact on the structural properties of the CrCL. Labrador Retrievers, Rottweilers, and Newfoundlands have a higher risk for non-traumatic CrCL deficiency, while Greyhounds have a relatively lower predisposition [253, 254]. A survey from 574 Newfoundlands showed 22% prevalence of CrCL deficiency and 51% penetrance in the recessive mode of inheritance [255]. A subsequent showed that four microsatellite markers from 4 respective chromosomes associated with CrCL disease were found in a subset of 90 Newfoundlands. Nonetheless, only 27% of CrCL deficient dogs were the result of genetic influence.

Another report showed no significant differences between the gene expression profiles of dogs with high risk of CrCL rupture and dogs relatively resistant to the rupture [256]. But protease and extracellular matrix genes (aggrecan, caspase 8, collagen 1A2, collagen 3A1, collagen 5A1, cathepsin B, cathepsin D, insulin-like growth factor 1, lumican, MMP-2, MMP-9, cyclooxygenase 2, tissue inhibitor of metalloprotease 1, and tenascin C) had higher expression in ruptured CrCLs compared to intact CrCLs, suggesting involvement in ligament rupture.

Conformational factors include both pelvic limb and stifle abnormalities. Genu varum (bow leggedness) is one of the most common conditions associated with CrCL degeneration [254]. It often appears as a poor coxofemoral conformation (dysplasia), femoral angulation, tibia internal rotation, proximal angulation and medial patellar luxation [251, 257]. Narrowed intercondylar notch (ICN) in dogs leads to impingement from the medial aspect of the lateral femoral condyle, or at the level of the intercondylar roof of the fossa [258]. Another theory is based on a biomechanical model developed by Slocum surrounding the tibial plateau angle [259]. Ground reaction forces propagate along the tibia while a shear force is generated by the compression of the femur against a caudally oriented tibial plateau slope. This theory is also the principle for the tibial plateau leveling osteotomy (TPLO). Patellar tendons also contribute to joint reaction forces [260]. The patellar tendon determines the alignment of the force generated by quadriceps contraction [261]. The TPLO is a fairly complex procedure with some potentially unrecognized pitfalls where iatrogenic errors can result in a change in limb angulation and rotation [262]

In CrCL disease, both humoral and cell-mediated immune responses are recognized. The structure is covered by a synovial membrane and hence protected from immune detection. However, once exposed, the CrCL can release antigens into

the synovial fluid (SF) that stimulate autoantigenicity [263-265]. Also, COLI released by injured CrCL was absorbed by macrophages, which became activated and presented collagen as the antigen to native T cells and B cells for antibody production. These antibodies were further released into synovial fluid, generating immune complexes. Or the collagen was phagocytositized by macrophages which began CrCL proteolytic degradation [266]. Need concluding statement

A number of biochemical factors have been discovered to induce the joint inflammation, both pro-inflammatory and anti-inflammatory. Different cytokines affect the inflammation process at different stages of the immune response. The imbalance between the pro-inflammatory and anti-inflammatory factors after CrCL injury may cause OA occurrence, and induce the upregulation of immunoregulatory factors, such as cytokine inhibitors and growth factors [267]. Cytokines such as IL-1β, IL-1rα, IL-6, IL-8, IL-10 and TNF-α are reported to be involved in CrCL injury [268-270]. It has also been confirmed that SF in joints with ruptured CrCLs contains collagen [271], glycosaminoglycan [272], proteoglycan, and fibronectin [273]. These particles may initiate and promote OA.

4.1.2 CrCL Pathogenesis

Ligament pathogenesis is a complicated series of events, including changes in ligament cells and extracellular matrix at molecular, biochemical, microstructural and macrostructural levels [274]. They share many degradative molecules with the initiation and progression of OA. Matrix metalloproteinases (MMP) are reported to be involved in both ligament pathogenesis and initiation of OA in CrCL disease, as well as collagenases [275], gelatinases [276], cathepsins [277]and other degradative enzymes. Recently, MMP expression in stifles with normal and partially disrupted canine CrCLs was compared [278]. The intact ligaments produced substantially more

MMP-2 and MMP-3 in response to explant ligament media *in vitro* compared to partially disrupted ligaments after 6 days of culture. This study confirmed the capacity of intact CrCLs to secret degradative enzymes when exposed to an abnormal environment. Because MMP-3 is able to cleave and activate other MMPs, it is possible that MMP-3 plays an essential role in both CrCL pathogenesis and initiation of OA. Interestingly, additional research showed that MMP-3 levels in synovial fluid were increased in older hounds compared to younger beagles with normal CrCLs [277]. Therefore, the level of MMP-3 expression can be used as a target to detect the occurence and condition of CrCL disease.

4.1.3 Cranial Cruciate Ligament Repair

Tissue repair requires coordination of a series of cellular and molecular events. Initially, local or undifferentiated cells start tissue repair by migrating into the injured area and proliferating [279]. Concurrently, physiological angiogenesis provides sufficient nutrients and oxygen to support cell survival. Cells going through proliferation and differentiation produce new extracellular matrix (ECM) and to restore the structure and the function of the damaged area [280]. The challenge of tissue repair is creating a well-organized ECM to direct progenitor cells while maintaining tissue structure and strength [281].

Generally, cells in ligaments are renewed at a relatively slower rate than most soft tissues, so ligaments heal more slowly than other tissues [282]. For extra-articular ligaments like the medial collateral ligament (MCL), spontaneous healing occurs in 4 phases. Phase I occurs within the first 72 hours with bleeding and hemostasis. The hematoma helps to bridge the torn ends. Then, in phase II, inflammatory cells, including monocytes, leukocytes, and macrophages aggregate, while fibroblasts slowly induce granulation tissue formation, and synthesize type III

collagen, and type I collagen to a lesser extent. Cells proliferate and matrix deposition forms a vascular neo-ligament in phase III, followed by the organization of collagenous tissue arrangement and synthesis of higher proportion of type I collagen and long-term remodeling in phase IV [283].

In the case of CrCL repair, when the thin synovial sheath of the CrCL is ruptured, blood dissipates into the synovial fluid, making it difficult to form a localized hematoma with cytokines, growth factors, and reparative cells at the injury site [284, 285]. Also, because the torn components retract, there is a high residual strain in the intact CrCL [286]. Additionally, compared with cells derived from other ligaments, CrCL fibroblasts have lower mobility, proliferation and metabolic activities, and matrix production tendencies, poorer adhesive strength, and higher MMP expression [287-291]. The CrCL therefore has limited healing capabilities compared to other ligaments.

A wide range of growth factors and cytokines have been reported to directly interact with transmembrane receptors to regulate cell functions during tissue repair [292]. Mechanisms are, in general, only partially described. Platelet-derived growth factor (PDGF) acts as a mitogen to help connective tissue cells grow, change shape and motility and reorganize actin filaments. Transforming growth factor-beta (TGF-β) is strongly related to morphogenicity and collagen synthesis. Type I insulin-like growth factor (IGF-I) is fully involved in cell survival, growth and metabolism. Finally, vascular endothelial growth factor (VEGF) and hepatocyte growth factor induce endothelial cell proliferation and migration, and angiogenesis [293-296].

Multiple growth factors were found to contribute to CrCL repair. Myostatin, also referred to as growth and differentiation factor 8 (GDF-8), is a member of the TGF-β1 superfamily of GDFs that is highly expressed in skeletal muscle [297, 298].

First, myostatin and its receptor, the type IIB activin receptor (ActRIIB), were found to increase cell proliferation and the expression of type I collagen in primary fibroblasts in the leg tendons of mice [298]. Myostatin binds theActRIIB and type I co-receptor (Alk4/5) to regulate the expression of downstream target genes such as myogenic differentiation protein (MyoD) and myogenic factor-5 (Myf-5) via a TGF-β signaling pathway [299]. With myostatin treatment, mouse tendon cells increase fibroblast proliferation and type I collagen expression [300]. Similarly, with myostatin treatment, proliferation, extracellular matrix synthesis and the expression of tenascin C (TNC), type 1 collagen and transforming growth factor-β1 increases in CrCLs of myostatin-deficient mice. Additionally, compared to injured MCLs, there was limited expression of PDGF and TGF-β1 in injured CrCLs in rabbit CrCL and MCL injury models [301]. Lower expression in the CrCLs was attributed to reduced vascular supply. The PDGF was localized intracellularly in tenocytes and epitenocytes, reaching maximum levels 4 days after injury. TGF-β1 was found in ECM on post-injury days one and two, and decreased with time, but intracellular expression was increased in epitenocytes throughout the tendon and endotenocytes at the injury site and reached the maximum on post-injury day seven. bFGF mainly expressed in ECM of the tendon, but rarely in tenocytes, and reached the maximum on day 28 after injury. These growth factors may be used for further analysis to study CrCL injury and repair.

4.1.4 Cranial Cruciate Ligament Regeneration

Traditional ACL repairs use biological based grafts that have good initial mechanical strength and promote cell and tissue growth. However, they have a number of disadvantages. Autografts from patellar hamstring or quadricep tendons are limited, and may cause donor site morbidity, increased recovery time and pain [121]. The

material strength of allografts and xenografts is compromised during harvest and processing [127, 128]. Concerns also include disease transmission, infection and immune rejection [123, 124]. Tissue engineering provides a promising alternative to auto- and allografts.

Adult MSCs do not express MHC II proteins, so they have immune privilege and can be transplanted into allogeneic hosts [302]. Also, they grow faster and secrete more COLI than ligament fibroblasts, and rabbit iliac crest BMSCs are reported to be a superior choice for CrCL regeneration compared to fibroblasts from the CrCL and MCL [118]. Those cells were detectable for at least 6 weeks after implantation. Additionally, orthotopic MSCs have greater commitment to tissue-specific lineages than those from heterotopic sources [167]. Intra-articular stromal cells showed better expansion capacity and potential for joint tissue regeneration than cells from other sources [177]. Species, cell passage and cryopreservation effects are also considerations for cell selection. In our previous study, canine infrapatellar (IFP) adipose-derived stromal cells (ASCs) up to P3 had higher proliferation rates, differentiation potential, MSC surface marker expression and lineage-specific gene expression than other intra-articular MSC sources.

As a required component in tissue regeneration engineering, a biological scaffold that is tailored to stem cells is central to their application for CrCL regeneration. Scaffolds can be designed to stimulate and direct tissue formation in order to replace parts or whole tissue structures. Scaffolds with appropriate pore size and microporosity (high interconnectivity between pores) can improve scaffold cell attachment, viability and tissue ingrowth [303]. The ideal pore diameter is around 200 μm for soft tissue [124].

Scaffold material selection is important for biocompatible scaffolds. The ideal replacement should possess similar physical and mechanical properties, degradability and structural integrity as the original tissue. For human ACL, the scaffold should withstand up to 3% physiologic strains during normal knee motion [304]. Additionally, the material needs to resist degradation by intra-articular inflammatory metabolites and proteolytic enzymes, such as plasmin [305], MMP [306] and glycosides [307].

Synthetic polymers are used for biocompatible scaffolds. Many are biodegradable materials like poly glycolic acid (PGA), poly lactic acid (PLA), or their copolymers, polyurethane urea (PUU), poly desaminotyrosyl-tyrosine ethyl carbonate (poly (DTE carbonate)), polydioxanone (PDS) and poly caprolactone (PCL) [308, 309]. The mechanical properties can be controlled by altering polymer concentrations, molecular weighst, crystallinity, structure and ratios. For example, braided PLLA scaffold provides specific pore size, well-integrated pores, resistance to wear and rupture, and mechanical properties comparable to the human ACL [310]. Also, the dense connective tissue infiltrates and bonds to the braided filaments 12 weeks afater implantation in adult New Zealand white rabbits [311, 312].

Since the major component of the ACL is type I collagen (COLI), it is popular in ACL tissue engineering studies [313, 314]. Type I Collagen is FDA-approved and biocompatible, and it can be formulated as a flexible gel, sponge or fiber [315]. It supports MSC attachment, proliferation and migration [316]. However, it has low biomechanical strength and relatively high degradation rates, and the use of COLI alone was found ineffective in improving CrCL healing in minipigs [317, 318]. This indicates that COLI should be combined with other materials with stronger mechanical properties.

Silk is another non-cytotoxic natural polymer with good biocompatibility, relatively slow degradability and excellent mechanical properties [319]. It can be used to create a structure similar to the ACL, and both human MSCs and fibroblasts attach, proliferate and form ECM on silk scaffolds [320, 321]. Composite scaffolds of nanofibrous PLGA and silk coated with bFGF support rabbit MSC attachment, proliferation and ligamentocyte differentiation [322, 323].

Different reagents have been applied to promote CrCL healing and formation. Some factors included in growth medium include TGF and epidermal growth factor (EGF), TGF and insulin (applied sequentially), insulin-like growth factor (IGF-I), bFGF, VEGF, platelet-derived growth factor (PDGF), and growth and differentiation factor (GDF). Platelets are activated COLI and secrete growth factors such as PDGF, TGF-b and VEGF[324]. Cytokine mixtures have been shown to improve cell proliferation but also suppress inflammation in humans [325]. A combination of primary suture repair and plate-concentrate resulted in greater stiffness, load at yield, and maximum tensile load after 4 weeks, and improved mechanical properties were observed as far as 14 weeks in a porcine model of CrCL wound repair [326, 327].

Previously, we identified the IFP to be the optimal MSC source for canine intra-articular tissue engineering [233]. These MSCs maintain their potency after cryopreservation up to passage (P) 3 [328]. Use of MSCs from healthy donors may have advantages of generating neo-tissue as well as immunoregulatory effects, since the number and differentiation potential of MSCs influences by disease and age [51, 104, 167]. The objective of this study is to generate viable canine neoligament tissues from adult canine IFP ASCs on COLI CrCL templates under dynamic perfusion bioreactor culture conditions *in vitro*. We hypothesized that canine IFP ASC attachment, proliferation, ligament differentiation and collagen deposition on COLI

CrCL templates will be higher with ligamentogenesis medium compared to stromal medium under identical perfusion bioreactor culture conditions.

4.2 Material and Methods

4.2.1 Study Design

Tissue harvest procedures were approved by the Institutional Animal Care and Use Committee (protocol #10-004). The ASCs from 6 mixed breed female dogs were isolated from IFP immediately after tissue harvest. Cryopreserved cell passage (P0) ASCs were revitalized and expanded to P3. Canine CrCL templates were constructed from #2 PDS II and bovine corium COLI (Avitene^{TM} Ultrafoam^{TM} Collagen Sponge, Davol Inc., subsidiary of C.R. Bard, Inc. Warwick, RI, USA). Cells (6×10^6 cells/scaffold) were seeded onto the templates using custom perfusion bioreactor chambers. Constructs were cultured in stromal or ligament-specific induction medium up to 21 days with dynamic perfusion in the same chambers (2 constructs/cell isolate/medium, 24 total). Loading efficiency was evaluated 2 hours after cell seeding (n=3). Samples (6 mm diameter) were collected 1 (upper), 2 (middle) and 3 (lower) cm from the top of the template using a biopsy punch immediately after loading and 7, 14 and 21 days of culture (Table 1). Samples were evaluated for cell proliferation (alamar blue), viability (calcein-ethidium bromide viability stain) and collagen deposition (sirus red stain). Procollagen was quantified in the medium (enzyme linked immunosorbant assay), and extracellular matrix (ECM) and cell ultra-structure was observed (scanning electron microscopy) at the same time points. Ligamentogenesis target gene expression (quantitative real-time PCR) was evaluated in ligament tissue at each time point as well.

Table 12 Sample Collection and Outcome Assessments

Outcome	Assay	Collection Time Points (Days of Culture	Sample size	Location of samples	# of Cell Isolates	Samples / Cell Isolate
Cell Proliferation	Alamar Blue (AB)	7, 14, 21	0.06cm^3	1, 2 and 3 cm from the top of the template	5	2
Cell Viability	CLSM	7, 14, 21	0.06cm^3	1, 2 and 3 cm away from the top of the template	3	1
Ultra-structure	Scannine Electron Microscopy (SEM)	7, 14, 21	0.06cm^3	Random	1	1
Micro-structure	Light Microscopy (LM)	7, 14, 21	0.06cm^3	Random	1	1
Collagen Deposition	Sirus Red (SR)	7, 14, 21	0.06cm^3	Random	6	2
Procollagen Synthesis	ELISA	7, 14, 21	200ul	Culture Medium	4	2
Ligamentogenesis Gene Expression	Quantitative real-time PCR (qRT-PCR)	7, 14, 21	1.2 cm^3	Upper half or lower half	4	1

4.2.2 Cell Harvest, Expansion and Preservation

The IFP adipose tissue was collected aseptically from normal stifles of six mixed breed female dogs (23.1 ± 0.9 kg, 3.3 ± 0.4 years, mean ± SEM). Adipose tissue was minced and digested at 37°C in an equal volume of Dulbecco's Modified Eagle Medium (DMEM) with 1% bovine serum albumin (BSA) and 0.1% type I collagenase (Worthington Biochemical, Lakewood, NJ). After washing with 1% BSA and centrifuging (260 g, 5 min), the resulting stromal vascular fraction (SVF) pellet was seeded at 5 x 10^3 cells/cm^2 in stromal medium (DMEM-Ham's F12, 10% fetal bovine serum (FBS), 1% antibiotic/antimycotic solution) followed by culture under standard conditions (37°C, 5% CO_2). For purposes of this study, the initial cell isolate is considered the stromal vascular fraction and the first cell passage is considered P0. Cell seeding density was 5 x 10^3 cells/cm^2 and cell passages were performed at 80% confluence. Passage 0 cells were detached with 0.25% trypsin, and cell aliquots (1 x

10^6 cells/ml) in cryopreservation medium (80% fetal bovine serum (FBS), 10% DMEM, 10% dimethylsulfoxide) were maintained in liquid nitrogen for a minimum of 30 days.

4.2.3 Immunophenotype – flow cytometry

Following thawing (37°C, 1 min), P0 cells were cultured in stromal medium and expanded to P3. Cell aliquots (P3, $5x10^3$ cells/dog, n=6) were combined in 200 ml PBS and incubated with 5 µg of unlabeled CD29 (α-human, catalog #610468, BD Biosciences, San Jose, CA, USA), PE-CD34 (α-dog, catalog #559369, BD Biosciences), FITC-CD44 (α-dog, catalogue # 115440, eBiosciences, San Diego, CA, USA), FITC-CD45 (α-dog, catalog #125451, eBiosciences) or CD90-PE (α-dog, catalog #125900, eBioscience,) antibodies for 30 min at room temperature. For CD29, cells were washed with phosphate buffered saline (PBS). Indirect immunofluorescence was performed by incubation with goat Ig-FITC (α-mouse, catalogue #F9006, Sigma Aldrich, Saint Louis, MI, USA) for 30 min at room temperature. Following incubation, cells were washed with PBS and fixed with 2% paraformaldehyde. Surface antigen expression was determined based on comparisons with negative controls illustrated on 10,000 even histogram plots using a fluorescence-activated cell sorting flow cytometer (FACSCalibur, BD Biosciences) and software (CellQuest Pro, BD Biosciences).

4.2.4 Perfusion bioreactor system

Following revitalization and culture expansion as described above, P3 cells were detached with trypsin, rinsed with PBS, and resuspended in stromal medium. Cells suspended in stromal medium were loaded onto templates with a perfusion bioreactor system (Figure 11). Each system was composed of two custom-made bioreactors connected to a 10 ml disposable vessel used as the medium reservoir

(Synthecon,Houston, TX) on their lowermost ends and to a peristaltic pump (Ismatec 404b, Glattbrugg, Switzerland) on their uppermost ends with 4.8 mm inner diameter flexible tubing (Tygon, Compagnie de Saint-Gobain, Courbevoie, France). The vessel provided oxygenation via a flat, silicone rubber gas transfer membrane. The bioreactors were made of polyvinyl chloride. One bioreactor in each system had a three-way stopcock at its lowermost end and a 0.22 μm syringe filter (Millipore, Billerica, MA, USA) between tubing attached to the bioreactor and tubing attached to the pump. Both bioreactors were 50 mm in length and had a 20 mm inner diameter (See A-C in Figure 12). Both ends were made with female screw locks. Within each chamber was a 45 mm long structure composed of two circular ends connected by 5 mm wide pieces (See D in Figure 12). Across the midpoint of each circular end, a 15 mm piece extended. The pieces on each end were offset 90 degrees to each other. The ends of the template were tied to the bisecting pieces such that the figure 8 configuration of the scaffold was maintained and the ends of the template were offset by about 45 degrees to replicate the CrCL structure. Each template was pre-soaked in 70% ethanol for 30 sec, UV sterilized for 15 min, hydrated with 10 μg/ml fibronectin in PBS for 30 minutes, and then tied to the frame as described above. The frame was inserted into the chamber and the ends of the chambers were sealed by parafilm.

4.2.3 PLLA: PEG scaffold construction and cell loading

A native canine CrCL was fixed in 1% PFA for 7 days and scanned with NextEngine® Desktop 3D Scanner and ScanStudio^{TM} software (NextEngine, Santa Monica, CA). The 3D prototype was printed using acrylonitrile butadiene styrene (ABS) and casted into a polydimethyl siloxane (PDMS) mold. The scan was modified with two cylinders (0.2 mm in length) on each end using Rhino® (McNeel North,

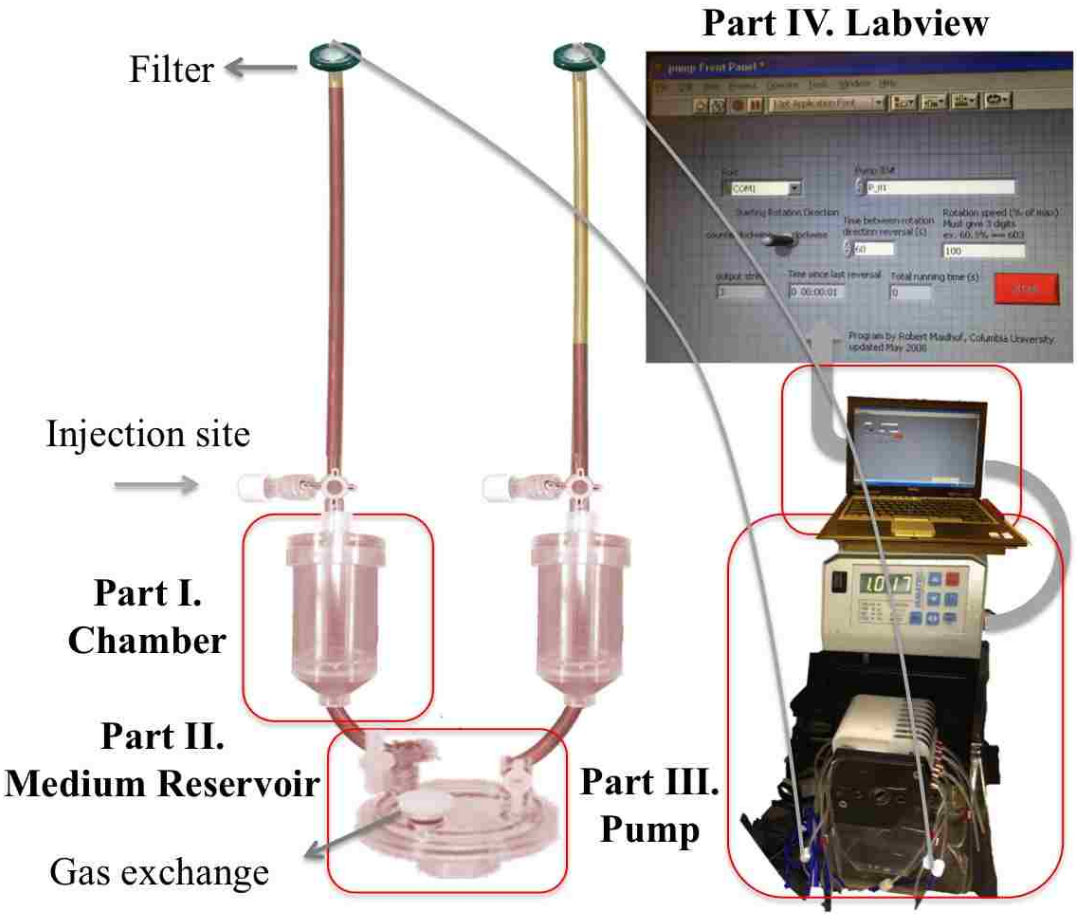

Figure 11 Perfusion bioreactor system

The original perfusion system was modified with two custom-made chambers (Part I) and medium reservoir with gas exchange export (Part II) (C). The system was connected to a peristaltic pump (Part III) and an external computer (Part IV). The flow direction and rate were controlled by Labview program.

America, Seattle, WA) and autoCAD were made by SolidWorks® (SolidWorks Waltham, WA). The PLLA (7%, wt) were dissolved in 1,4-dioxane, heated at 60°C, stirred for 2.5 hrs, cooled to RT, mixed with PEG (7%, wt) in a ratio of 6:4, and injected into the mold. The scaffold was unidirectionally freeze dried at -88°C at a rate of 1.6 ml/hr for 48 hrs, and divided into 6 parts with similar sizes [329].

All parts were gas sterilized with ethylene oxide before being assembled. The system was first loaded with medium through the stopcocks towards the chambers at both sides, and then followed by ASC suspensions (3 x 10^6 cells/scaffold) using the

original perfusion bioreactor at a fluid flow rate of 1 ml/min for 2 hrs in an incubator. Flow direction was reversed after medium reached the filter so that scaffolds remained immersed during the loading process. Scaffolds without cells were treated identically.

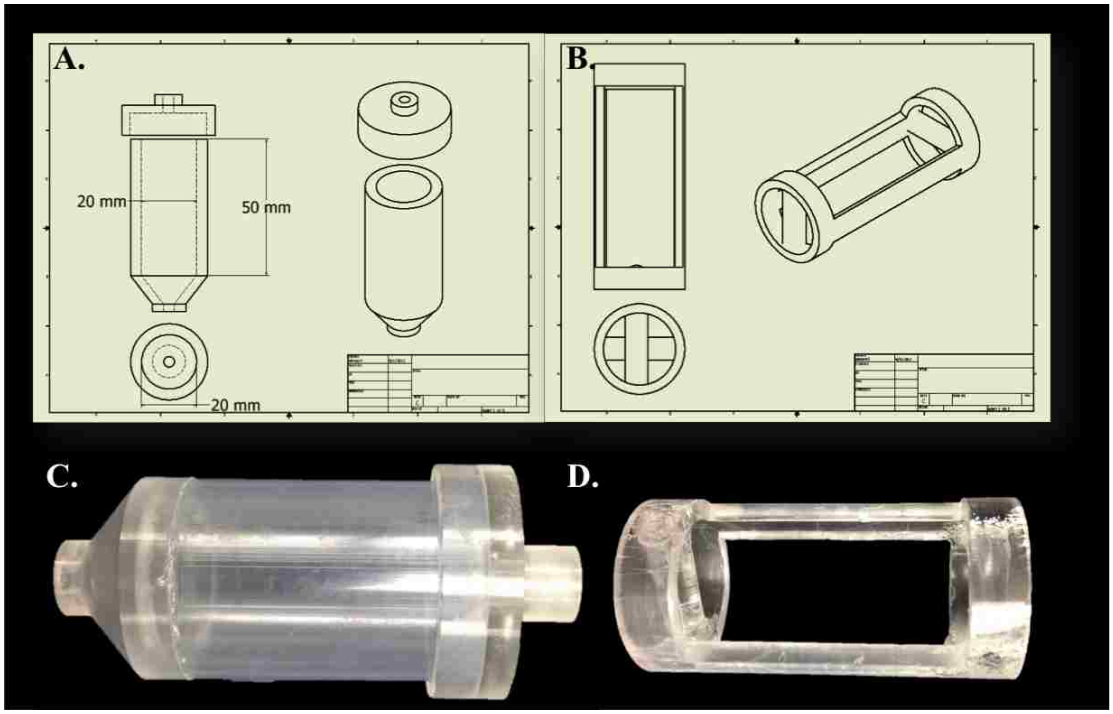

Figure 12 Custom-designed chamber

The chamber was 50 mm in length and had a 20 mm inner diameter and was adapted to the system with luer locks and a stopcock (A, C). The inner apparatus that could be inserted into the chamber was used to hold the scaffold with a 45 degree twist of both ends (B,D).

After loading, constructs were transferred into a 6 well plate and cultured in 4 types of media (10% PRP, 1% PRP, 0.1% PRP and stromal control) for up to 21 days. Scaffolds without cells were cultured as a negative control. The leftover media in the bioreactor was collected and tubings were trypsinized. Cell loading efficiency was calculated as (initial cell number – cells in the medium)/ initial cell number x 100%.

4.2.3 Template construction and 3D culture

The CrCL template frame was constructed using a 70 cm section of #2 PDS II in 4, 2 cm long figure-8 shapes (See A in Figure 13). The center of the figure-8 was secured

with two loops of suture wrapped around the structure and tied with a square knot. A 5 x 4 x 0.3 cm sheet of COLI moistened slightly with PBS was wrapped around the frame, overlapping about 3 mm. COLI The sponge was then saturated with medium causing it to shrink 30% and fit tightly to the frame. The COL sheet was secured to the PDS frame with a Chinese finger trap of #2-0 Vicryl (See B in Figure 13). Each template was pre-soaked in 70% ethanol for 30 sec, UV sterilized for 15 min, hydrated with 10 μg/ml fibronectin in PBS for 30 minutes, and then tied to the frame as described above. The frame was inserted into the chamber and the ends of the chambers were sealed by parafilm.

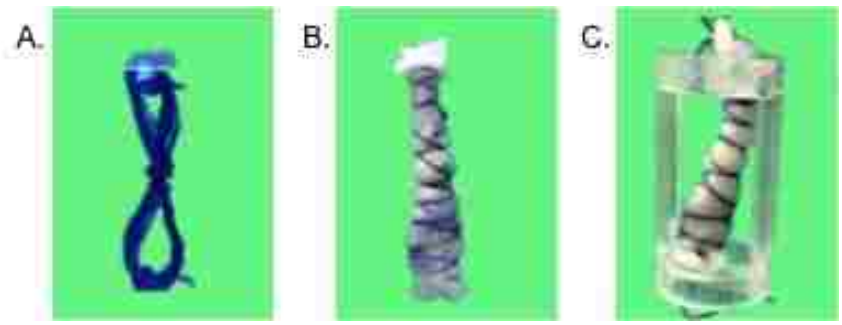

Figure 13 Template construction

The PDS*II #2-0 was used to configure the shape of major bands of the CrCL (A). The template was wrapped by collagen I scaffold and wrapped within a Chinese finger trap of #2-0 Vicryl (B). The template was secured in the inner apparatus (C).

Fluid flow direction and rate were controlled by LabVIEW (v8.5, National Instruments Corporation, Austin, TX, USA). Systems were primed with 48 ml ligament induction medium or stromal medium through the lowermost stopcock followed by addition of MSC suspensions (1 ml, 6 x 10^6 cells/template, 2.5 x 10^6 cells/cm^3) through the stopcock on the top of each bioreactor. Perfusion was performed (37ºC, 5% CO_2) at a fluid flow rate of 1 ml/min up to 21 days. Flow direction was reversed after medium reached the top of a bioreactor so that scaffolds remained immersed. The medium was refreshed every 7 days through the medium reservoir.

4.2.4 Cell viability and toxicity

For zinc medium, 3 replicates of 1.28 x 10^4, 6.4 x 10^3, 3.2 x 10^3, 1.6 x 10^3, 8 x 10^2, 4 x 10^2, 2 x 10^2, or 50 cells/well were incubated in a 96-well plate overnight in 4 types of zinc medium (0, 5, 10 or 20 μM $ZnCl_2$). The toxicity of the medium was determined using alamarBlue reagent (Invitrogen, Carlsbad, CA). Cells were rinsed with PBS, and incubated with 10% alamarBlue™ for 4 hrs. The fluorescence was measured using an excitation wavelength of 530 nm and an emission wavelength of 590 nm using a fluorescence microplate reader (Biotek, Winooski, VT).

The viability of cells on COLI scaffold was also evaluated using alamarBlue™. Samples immediately and 7 days after loading from both Zinc and stromal control groups were collected using a biopsy punch (6mm) from the top, medium and bottom area of the construct in duplicates. Samples were further incubated with 10% alamarBlue for 4 hrs, aliquots (100 μL) were placed in a 96-well plate, and fluorescence was measured. For growth factor medium, samples were similarly collected from four time points, immediately after loading, 7, 14 and 21 days of culture. Cell numbers were determined on a standard curve generated from known cell numbers.

4.2.5 Cell Viability – Confocal Laser Scanning Microscopy

Samples were rinsed with PBS and incubated in darkness for 30 min at room temperature with 5 μM calcein and 2 μM ethidium bromide (EB) (Sigma Chemical Co., St. Louis, MO) in 200 μL PBS such that live cells fluoresced green while non-viable cells fluoresced red. A total of 20 consecutive photomicrographs (20x) of the entire sample cross-section along the thinnest side (2 mm) were generated every 100 μm using a spectral confocal laser scanning microscope digital imaging system (Leica TCS SP2, Leica Microsystems, Buffalo Grove, IL, USA).

4.2.6 Ultra Structure – Scanning Electron Microscopy

Samples were fixed (2% PFA and 1.25% glutaraldehyde in 0.1 M sodium cacodylate (CAC) buffer, pH 7.4) for 1hr at room temperature and transferred to buffer (3% glutaraldehyde in 0.1 M CAC buffer, pH 7.4) for 30 min. Samples were rinsed with washing buffer (5% sucrose, 0.1 M CAC buffer, pH 7.4), post-fixative buffer (1% osmium tetroxide in 0.1 M CAC buffer, pH 7.4) and water, serially dehydrated, critical point dried, and sputter coated with gold. They were observed with a scanning electron microscope at 15 kVP (Quanta 200, FEI Company, Hillsboro, OR).

4.2.7 Collagen deposition – Sirius Red

Constructs were digested with 500 µl of pepsin solution (0.25 mg/ml), and stained with Sirius red collagen detection kit (Chondrex, Redmond, WA) according to the manufacturer's instructions. Absorbance was read at 540 nm using a microplate reader (Biotek, Winooski, VT). Values were normalized to scaffold only. The collagen in each sample was extrapolated from a standard curve provided with the kit.

4.2.8 Procollagen Synthesis – Procollagen I N-terminal Peptide (PINP) Enzyme Linked Immunosorbant Assay (ELISA)

Concentration of procollagen I N-terminal peptide (PINP) was measured in medium when medium was changed every 7 days. Media were collected from each chamber and the reservoir. Samples were stored at -80°C, thawed on ice and thoroughly mixed before using. PINP levels were measured using the canine PINP ELISA kit (Biotang, Framingham, MA) according to manufacturer's instructions. Absorbance at a wavelength of 450 nm was measured. Concentrations were determined from a standard curve provided with the kit. Concentrations in the results reflected the PINP release in the time period since the prior media changed.

4.2.9 Target Gene Expression - qRT-PCR (quantitative reverse transcription-polymerase chain reaction) mRNA levels

Constructs were rinsed with PBS, and homogenized (TissueLyser II, Qiagen, Valencia, California, USA) in TRIzol reagent (Sigma). Total RNA was extracted by phenol-chloroform extraction according to TRIzol reagent's instructions. Quantity was determined with a ND-100 spectrophotometer (NanoDrop Technologies, Wilmington, DE), and only samples with an A260/A280 ratio higher than 1.7 were used. mRNA was reverse transcribed into cDNA using a QuantiTect Reverse Transcription Kit (Qiagen, Hilden, Germany). Canine-specific primers against collagen I (col1), collagen III (col3), biglycan (BGN), decorin (DCN), tenascin-c (TCN), fibronectin (FN) and tenomodulin (TNMD) were designed using Primer3 and annotation databases available at the University of California, Santa Cruz (UCSC) Genome Browser database (http://genome.ucsc.edu/) (Table 14). qRT-PCR was performed in duplicate using a QuantiTect SYBR Green PCR Kit (Qiagen) in a 384 well PCR plate. PCR amplification was performed using Applied BioSystems 7900 Real-Time PCR System (SDS v2.4; Applied Biosystems, Carlsbad, CA). In the present study, the data was normalized to GAPDH, and presented as the fold change in target gene expression relative to the stromal control according to $2^{-\Delta\Delta Ct}$ [176].

4.2.10 Statistical analysis

Values are presented as mean ± SEM. Two-way ANOVA models were applied to determine effects of culture time and induction medium on cell metabolic activities, collagen deposition and procollagen synthesis with Tukey's post-hoc tests. One-way ANOVA was used to analyze mRNA expression levels. Significance was considered at $P<0.05$.

Table 13 Canine-specific primer sequences for ligament differentiation

	Forward Primer	**Reverse Primer**
GAPDH	TGGCAAAGTGGATATTGTCG	AGATGGACTTCCCGTTGATG
Col1	CTATGACCGAGACGTATGGA	GTTTCTTGGTCGGTAGGTGAC
Col3	CAGAGATCCCATTTGGAG	CATTTCTCCCAGGAATACC
BGN	CCACAACCAGATCCGCATGAT	AGAAGTCGTTGACGCCCAC
DCN	CTCTAGCCAACACTCCTCAT	GGCAGAAGTCATTAGATCCG
TNC	CCACAATGGCAGATCCTTC	CCTTCCAGTGGAACCAGTTA
FN	GGTTTGTACCTGTTACGGAG	CAGATCATGGAGTCCTTAGG
TNMD	CCAGCAGAAAAGCCTATTG	GACCACCCACTGCTCGTTT

4.3 Results

4.3.1 PLLA: PEG scaffold construction

A CrCL structure mold was successfully printed (Figure 14A). However, during polymer injection, the mold split and polymers leaked during freezing. Further modifications were made with two columns by both sides, one for injecting materials and the other for air ventilation (See B-D in Figure 14). The outside structure of PLLA: PEG scaffold was similar to the native CrCL, and the inside pores were 44 x 22 μm^2 (See A, B in Figure 14).

4.3.2 Loading Efficiency

The loading efficiency for the PLLA: PEG scaffold in stromal medium was 83% (Figure 15). With fibronection coating, collagen scaffold had significantly higher loading efficiency than non-coated groups. No significant changes were shown using different loading medium with PLLA: PEG or collagen scaffold.

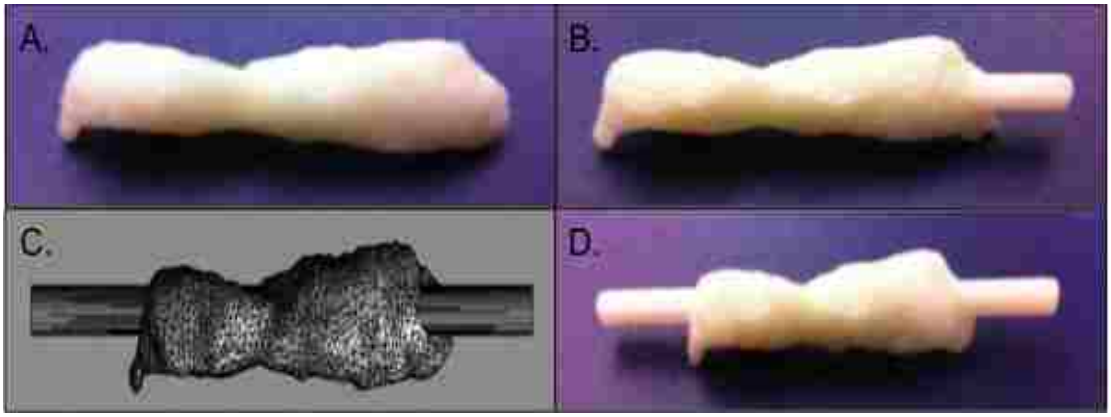

Figure 14 PLLA: PEG scaffold

The 3D prototype was printed using acrylonitrile butadiene styrene (ABS) (A), and modified with columns (B,D). Rhinoceros 4.0 prototype C (C).

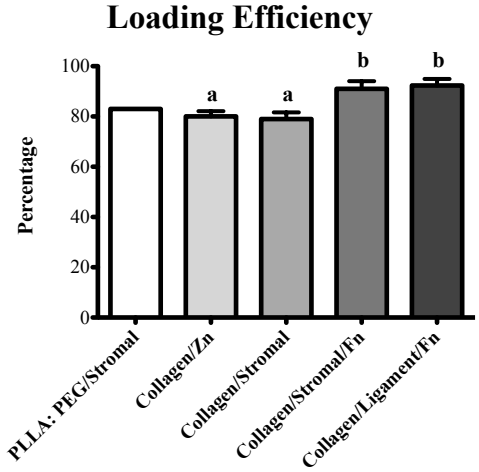

Figure 15 Loading efficiency (mean ± SEM, n=3)

PLLA: PEG and collagen scaffolds were loaded in stromal medium or ligament induction medium for 2 hrs with or without coating with fibronection (Fn). Needs more description. What is shown here?

4.3.3 SEM Images of PLLA: PEG Scaffold Cultured in PRP and stromal media

The construct cultured with 10% PRP was fully covered with platelets after 21 days of culture (See C in Figure 16). Cells were also evident in scaffolds cultured in other media, 1% PRP (See D in Figure 16), 0.1% PRP (See E in Figure 16) and stromal medium (See F in Figure 16). However, the scaffold failed to maintain the structure during 3D culture. Different types of scaffold were used in later studies.

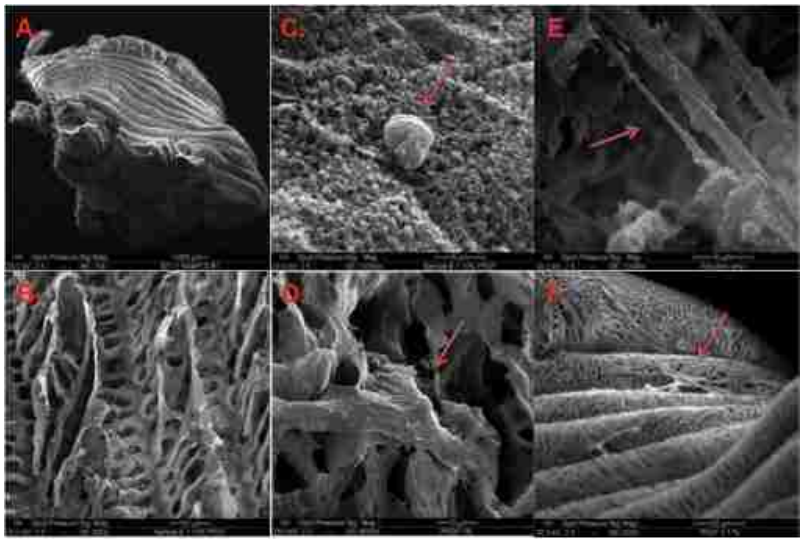

Figure 16 Scanning electron photomicrograph of PLLA: PEG scaffold

The outside was similar to native CrCL (A), and the inside was porous (B). The scaffold was covered with platelets (red arrows) following culture in 10% PRP medium (C). The IFP ASCs (red arrows) were attached to the surface of the scaffold in 1% PRP medium (D), 0.1% PRP medium (E) and stromal medium (F).

4.3.4 Cytotoxicity of $ZnCl_2$ Medium

After 4 hrs incubation, monolayer cells did not show significant toxicity effects with up to 20 μM $ZnCl_2$ (See A in Figure 17). No significant differences were found in metabolic activities of biopsy samples from different locations. Therefore, data were combined for further analysis. There was no significant change of cell metabolic activities between zinc and stromal medium immediately after loading (See B in Figure 17). However, medium became acidic with a pH of 4.2 after 7 days of culture, and the majority of cells were dead (See C,D in Figure 17). Additonally, scaffolds had significantly lower metabolic activities after 7 days culture in medium with zinc than 2hr after loading (See B in Figure 17). In contrast, after 7 days of culture in stromal medium, cells on the collagen scaffold had significantly higher metabolic activities. Based on these results, zinc was not used in induction medium.

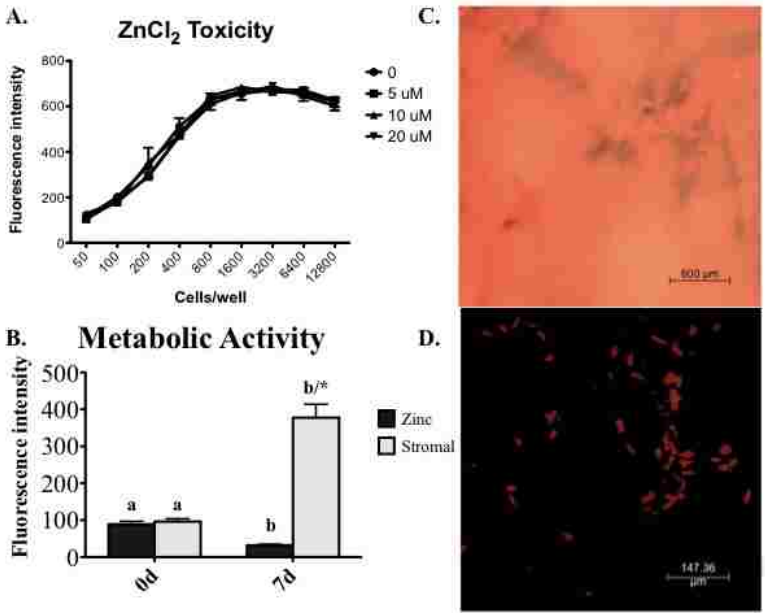

Figure 17 Cytotoxicity of $ZnCl_2$

Cells were cultured in stromal medium with different concentrations of $ZnCl_2$ overnight and then stained with Alamar Blue for 4hr (A). Cells were loaded onto the collagen scaffold, and metabolic activity (mean ± SEM, n=3) was measured immediately after loading and 7 days (B). Construct was stained with calcein (green) and ethidium bromise (red) and observed with fluorescent and (5x) (C) and confocal laser microscopy (20x) (D). Columns with different letters are significantly different from stromal control ($P < 0.05$). Columns with asterisks are significantly different from 0d.

4.3.5 Growth Factor Medium

When collagen scaffolds were coated with Fn, the metabolic activity was significantly higher than non-coated controls (See A in Figure 18). There were more cells apparent with viability staining and confocal laser microscopy (See B in Figure 18). Based on these results, COLI scaffolds were first incubated with Fn for 30 min before loading. Additionally, no significant differences were found among biopsy samples from different locations of the construct (1, 2, 3 cm from the top of the template), so data were combined.

No significant differences were found in cell metabolic activity between growth factor and stromal medium up to 21 days (See A in Figure 19). There was significantly higher cell activity after 7 days of bioreactor culture for both groups, and

cells were larger (See B in Figure 19). After 21 days of culture, more cells were apparent in confocal laser and scanning electron images (Figures 20, 21), and constructs had significantly higher activity than 7 and 14 days (See A in Figure 19).

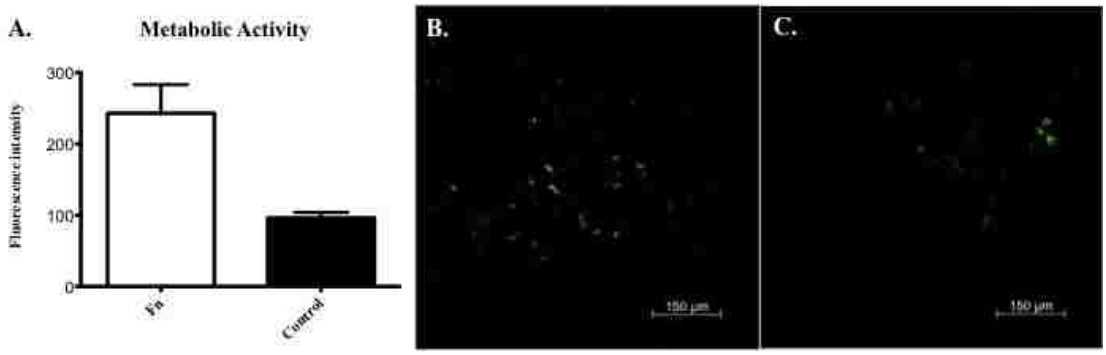

Figure 18 Metabolic activity (mean ± SEM, n=6) of construct with Fn coating for cell loading

Collagen scaffolds were soaked in Fn solution for 30 min before loading. After 2 hrs, metabolic activity was measured for both Fn and control group. Samples were stained with calcein (green) and EB (red), and observed by confocal microscope.

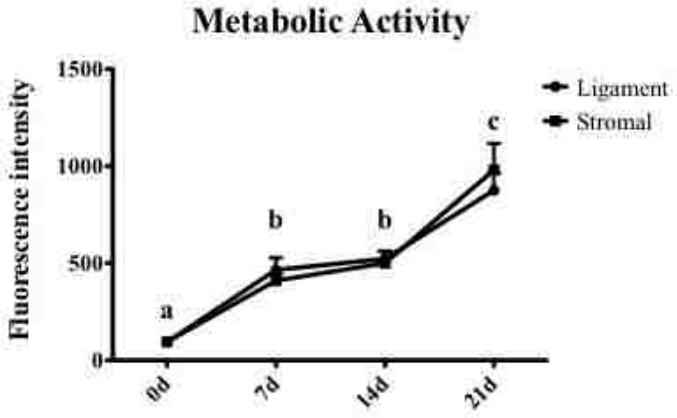

Figure 19 Metabolic activity (mean ± SEM, n=5) of canine ASC–COLI constructs

Canine ASC-COLI constructs were cultured in a perfusion bioreactor up to 21 days. Metabolic activity was measured after 0, 7, 14 and 21 days of culture in ligamentogenesis or stromal medium.

4.3.6 Collagen Deposition

Since Sirius red stains the collagen, staining was normalized to scaffold only (cultured for the same period of time). Constructs in ligamentogenesis medium had higher collagen than those cultured in stromal medium after 21 days of culture (Figure 22). There was a slight increase in collagen content between 7 and 14 days in stromal

group, and collagen content was significantly greater in both groups after 21 days of culture compared to 7 days.

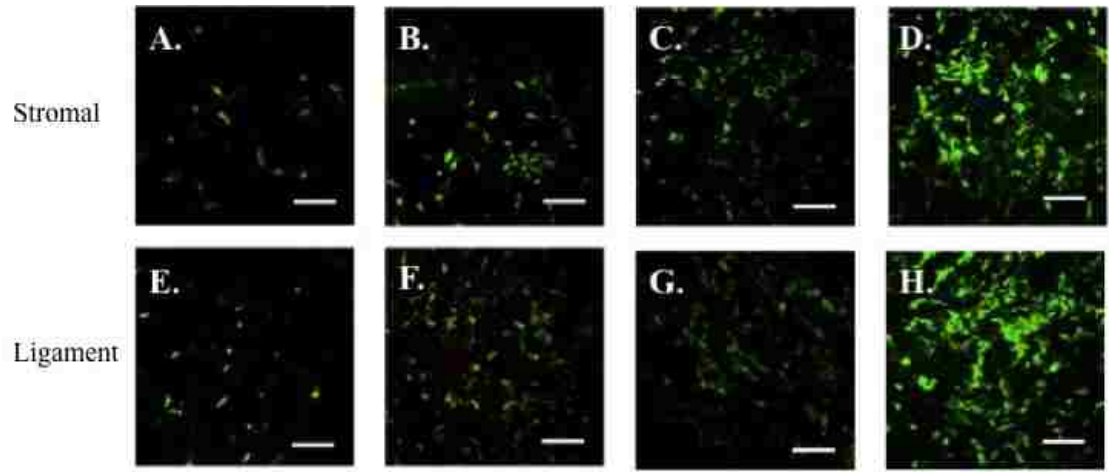

Figure 20 Confocal images of canine ASC-COLI constructs

Constructs were cultured in stromal (A-D) or ligamentogenesis (E-H) medium up to 21 days. Samples were collected after 7 (B,E), 14 (C,F) and 21 (D,G) days of culture. Samples were stained with calcein (green, viable) and ethidium bromide (red, nonviable), and observed with confocal laser scanning microscopy. Scale bar: 150 μm.

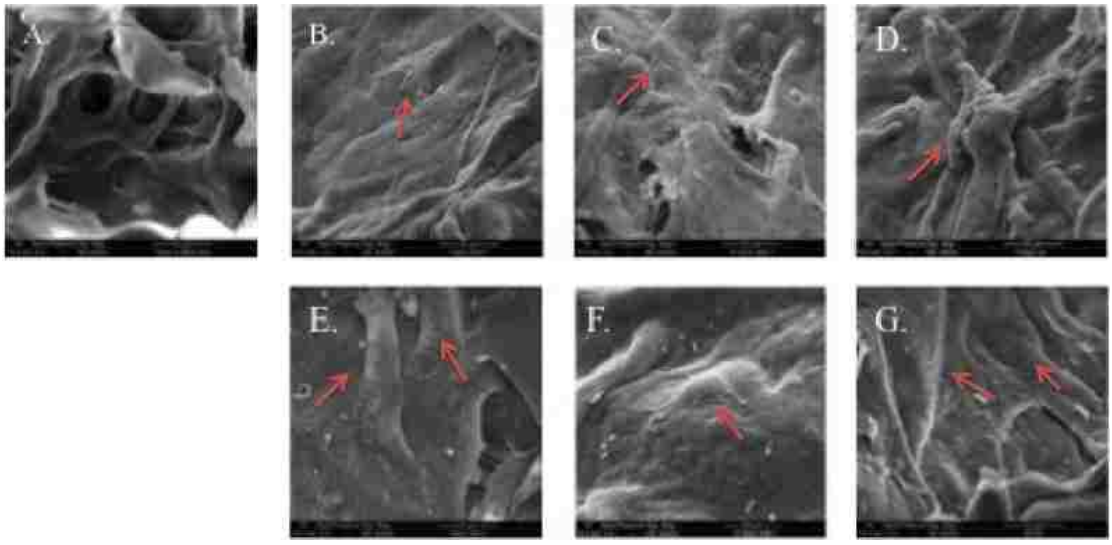

Figure 21 SEM images of canine ASC-COLI constructs

The ASCs (red arrows) – COLI constructs were cultured in ligamentogenesis (B-D) or stromal (E-G) medium up to 21 days. Samples were collected after 7 (B,E), 14 (C,F) and 21 (D,G) days of culture. Collagen scaffold is shown for comparison (A).

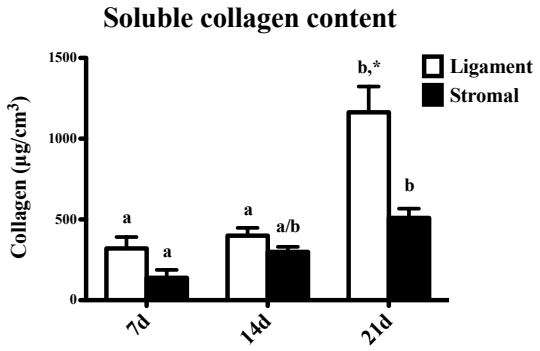

Figure 22 Total collagen content (mean ± SEM, n=6) of canine ASC-COLI constructs cultured in stromal or ligamentogenesis medium for 7, 14 or 21 days.

Scaffold was digested with pepsin and total collagen deposition was measured, normalized to scaffold only, and determined on a standard curve. Columns with different letters are significantly different from other time points within treatment cohorts ($P < 0.05$). Columns with asterisks are significantly different from stromal control within time points.

4.3.7 Pro-collagen Synthesis

The medium PINP levels were significantly higher in medium surrounding constructs cultured in ligamentogenesis medium versus those in stromal medium after 7 and 21days of culture (Figure 23). Within cohorts, levels were significantly higher in the ligamentogenesis medium group after 21 versus 7 and 14 days of culture, and in the stromal medium group after 21 and 14 days versus 7 and 14 days of culture.

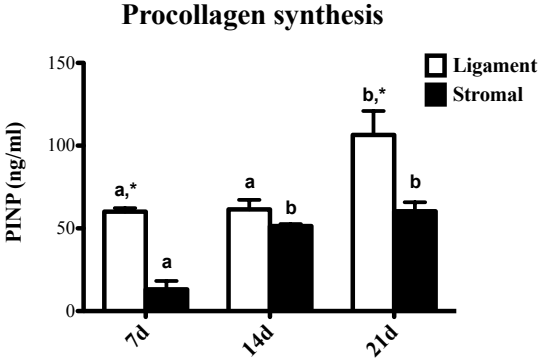

Figure 23 Pro-collagen synthesis (mean ± SEM, n=4) of canine ASC/ColI scaffold construct

Medium was collected at day 7, 14 and 21 after loading. Concentration of PINP was measured using an ELISA kit. Columns with different letters are significantly different from other time points within treatment cohorts ($P < 0.05$). Columns with asterisks are significantly different from stromal control within time poitns.

4.3.8 Ligamentogenesis Target Gene Expression

In general, constructs cultured in ligamentogenesis medium had higher mRNA levels of COLI, COLIII, TNMD, FN TNC, BGN and DCN than those cultured in stromal medium (Figure 25). Additionally, mRNA levels of the genes were highest after 21 days of induction, followed by 14 and 7 days. The col1, TNC and TNMD expression was significantly higher at day 21 compared to day 7.

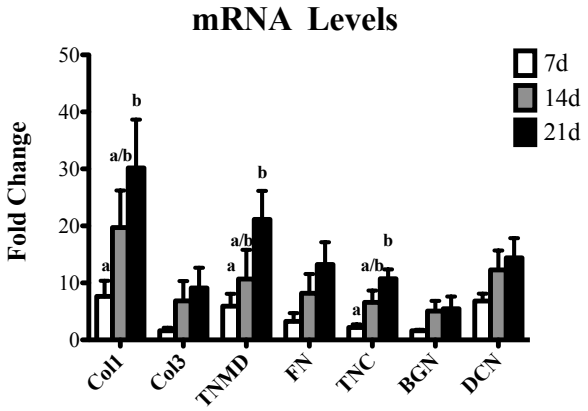

Figure 24 Fold change (mean ± SEM, n=4) of ligament target gene mRNA levels in canine ASC/ColI scaffold constructs

Fold change of mRNA levels in the constructs cultured in ligament induction medium relative to those in stromal medium for 7, 14 or 21 days. Columns with different letters are significantly different from each other ($P < 0.05$).

4.4 Discussion

The ideal regenerated tissue will have cell proliferation, protein synthesis, deposition of ECX and mechanical properties similar to the native tissue. Consistent with the hypothesis, the collagen type I porous scaffold with PDS II suture supported IFP ASC attachment, proliferation, ligament differentiation and collagen deposition when cultured in ligamentogenosous induction medium.

The IFP was used as the MSC source in this study. Different cell sources have been used in ligament tissue engineering such as MSCs and fibroblasts [330-333]. Previous work in the laboratory confirmed that, up to P3, MSCs from the IFP have higher *in vitro* expansion, multipotentiality and progenitor immunophenotypes

compared to those from joint capsular and CrCL synovium [233]. Other studies have shown that rabbit BMSCs from iliac crest have higher proliferation and collagen excretion than ACL and MCL fibroblasts [118]. Since orthotopic MSCs generally have higher potential for tissue-specific cell differentiation than heterotopic cells, IFP ASCs may be an optimal cell source for ACL tissue regeneration [167]. To optimize cell attachment, the scaffold was coated with fibronection [140]. A relatively low cell seeding density was used since the ACL is relatively hypocellular compared to other tissues [334].

The scaffold material selection is also critical to provide similar physical and mechanical properties, degradability, and structural integrity similar to the original CrCL. The ideal pore diameter for soft tissue formation is around 200 – 250 μm [124]. Both PLLA and PGA are biocompatible materials approved by the FDA for clinical applications [308, 309]. Both have been applied for ligament engineering with promising short-term. However, in this study, these materials failed to maintain their structure during long-time dynamic culture. Previous studies have also shown poor tissue integration, poor abrasion resistance and fatigue on long-term impact [335, 336]. Further modifications in relative ratios and construct structure may help resolve some of the problems observed [308].

Type I collagen is the major component of the CrCL. The scaffold used in this study is commercially available and has been applied in orthopedic tissue regeneration [316]. It possesses interconnected pores with an average diameter of 190 μm [337]. However, collagen alone is not durable enough for long-term application [317, 318]. Compared to other absorbable sutures, PDS II has relatively higher tensile strength and failure load [338]. Therefore, a PDS suture was used to constructs the scaffold frame to mimic the orientation of the major bands of the native CrCL and to

confer mechanical strength and durability to the scaffold. The template was also constructed with implantation in mind. Since the structure must be secured to the tibia and femur within bone tunnels, the construct has elongated suture ends covered with COLI and ASCs to secure the graft and facilitate integration into bone.

Perfusion bioreactors have been shown to improve the efficiency of 3D tissue engineering [334]. The custom-made chamber allowed homogenous cell distribution and maintenance of the scaffold with a 45-degree turn at the midpoint. Different fluid flow rates have been applied in perfusion bioreactors. Very-low flow rates (0.01 ml/min) have been used to achieve low shear stress and high cell viability [144, 339]. In contrast, high flow rates result in lower cell viability [334]. To provide optimal distribution of cells, nutrients, oxygen and removal of wastes for orthopedic applications, a fluid flow range from 0.2 to 1 ml/min has been suggested [334]. According to Haagen-Poisseuille equation, $\tau = 32\mu Q/\pi d^3$ (τ: shear stress; Q: flow rate; d: diameter; μ: kinetic viscosity), shear stress is directly proportional to flow rate and inversely proportional to vessel diameter [340]. Considering the relatively large volume of the system, this study used the flow rate at 1 ml/min.

Though the exact cocktail to differentiate MSCs into ligament fibroblasts still has yet to determined, several chemicals and growth factors have been identified. Platelet-rich plasma has been widely applied for *in vivo* intraarticular CrCL repair and regeneration [341]. However, high concentrations (10%) of PRP interfered with ASC attachment to scaffold in this study based on the size of particles (3μm) in SEM images. Zinc promotes ligamentous healing, and has been reported to stimulate MSC proliferation and DNA synthesis [342]. However, in this study, it significantly induced pH reduction and cell death at low concentrations. The results are consistent to what have been found in acidithiobacillus caldus cells [343]. Growth factors like

βFGF, TGFβ, PDGF, VEGF and IGF are reported to induce ligamentogenesis [344-346]. A combination of βFGF and TGFβ were previously reported to induce significantly higher COLI deposition and tissue strength through matrix synthesis in human BMSCs than other formulations *in vitro* [345]. Previous studies also found that TGFβ and PDGF cultured with rabbit BMSCs were in high concentrations during the initial phases of CrCL healing, and were crucial for neo-tissue formation and restoration of function both *in vitro* and *in vivo* [346, 347]. Lower serum was applied in the induction medium since it achieved significant increase of COLI mRNA levels compared to the stromal medium *in vitro* [345]. The medium described in this study appeared to generate significant higher ligamentogenesis based on target gene expression, collagen deposition and pro-collagen synthesis. The medium may prove useful to generate viable grafts in vitro.

The mRNA data from this study suggests that constructs cultured in induction medium had increased ligament target gene expression. Although there is no single specific gene for ligamentogenesis, col I, col III, TNMD, TNC, BGN, DCN and FN are all expressed in normal and healing CrCL [348-352]. Early stage markers, TNMD and TNC, are necessary for cell proliferation and collagen fibril maturation [353, 354]. Collagen II and proteoglycans like BGN and DCN regulate assembly of collagen fibrils at later stages of ligament development or repair [355-357]. Additionally, the upregulation of TNC suggests ligament being mechanically stimulated, indicating successful mechanical stimulation provided in the perfusion bioreactor [358]. The significant increase of col I, TNMD and TNC with no change in col III, BGN and DCN in this study is more consistent with a pattern of early stage ligament development rather than repair.

Regenerated tissues with MSCs have advantages over traditional therapies. The MSCs from healthy and young donors may have advantages of generating neo-tissue as well as immunoregulatory effects, since the number and differentiation potential of MSCs are interfered by diseased or aged conditions [51, 104, 167]. The MSCs would not only differentiate into tissue-specific lineages, but also attract bioactive factors to accelerate healing process without stimulating the host immune response. This study designed a specific perfusion bioreactor system to regenerate a viable canine CrCL graft with the native structure. Further MSC sorting with MSC and immunogenic surface markers may generate a purer population that can be further applied to grow the CrCL. Longer *in vitro* culture time in the induction medium may also help ligamentogenesis and maturation of MSCs. Additional studies should include comparisons of CrCLs generated from ligamentogenesis or stromal medium in rodent models. Even though this *in vitro* study cannot reflect *in vivo* characteristics of the CrCL, it provides vital translational information of MSC in tissue engineering to achieve better efficiency and efficacy after implantation *in vivo*.

CHAPTER 5. CONCLUSIONS AND FURTHER STUDIES

This dissertation is focused on translational studies of adult multipotent stromal cells (MSCs). Overall, MSC-mediated therapies are in the early stage of development. Due to their apparent versatility, MSCs have been applied in over 100 human clinical trials to treat various diseases and conditions. Unfortunately, results have been inconsistent and, in some cases, less than favorable.. It is clear that controlled investigations are necessary in the field of adult MSCs. The International Society for Cellular Therapy position has minimal standards to define human MSCs. A standard definition of adult MSC in veterinary medicine is also needed. However, limited technical resources like species-specific antibodies make this goal challenging. Major contributions of the studies described in this dissertation are species specific techniques to isolate and characterize canine and feline MSCs.

An efficient adipose derived multipotent stromal cell (ASC) isolation technique was developed for the feline study. Using the technique, ASCs can be harvested from limited tissue to avoid the need for significant tissue harvest from one animal or to combine tissues from several animals. Use of tissues from one animal may also lower risk of rejection. Feline-specific induction medium was designed and tested to confirm feline MSC multi-potentiality and to be used in future feline tissue regeneration studies. Results of the study showed that feline ASCs are only suitable for treatment or tissue engineering up to 3 passages *in vitro*. Evaluation of the effects of cryopreservation showed that feline ASCs could be banked without losing their expansion and differentiation capabilities. The MSC surface markers that were validated in the study can be used to select MSCs from a heterogenous cell isolate.

The results from the canine intra-articular MSC study showed that adipose-derived MSCs (ASCs) have the most promise for intraarticular application. Tissues evaluated in the study are the three most popular MSC sources inside the stifle and the results will be of interest to both surgeons and scientists. Considering IFP tissue is often excised during stifle surgeries, it is a reasonable choice for cell isolation that will not require specific tissue harvest. It is also possible that ASCs from IFP tissues may be protected from intra-articular inflammation. The fact that ASCs maintain their properties after cryopreservation may make it possible to use allogeneic ASCs from normal stifle joints. The MSC phenotype was confirmed in this study and the techniques can be used for unrelated canine MSC studies to benefit research and clinical application.

The third part of this describes use of canine IFP ASCs, to regenerate cranial cruciate ligament (CrCL) neotissues. It is possible that the viable structures can be matured into grafts for clinical application or may serve as a template to promote CrCL generation *in vivo*. The scaffold template may support both approaches to CrCL repair. For the study, custom scaffold templates were designed, ligamentogenesis medium optimized for canine ACS ligament induction and a novel bioreactor seeding and culture system designed and applied to grow constructs up to 21 days. Progressive tissue maturation was confirmed at various time points during the culture period. Implantation of induced cells may have significant advantages over naïve MSCs. This work is highly novel and may benefit both canine and human patients that suffer from rupture of the major ligament in the stifle (knee) joint.

This dissertation provides critical information to translate MSC from the laboratory to clinical application. Further studies may include purification of feline MSCs with MSC and immunogenic surface markers, mechanical testing of CrCL

generated *in vitro*, further maturation of CrCL with longer culture time and MSC supplement *in vitro* and characterization and functional analysis of generated CrCL *in vivo*.

REFERENCES

1. Wilson, E., The Cell in Development and Inheritence1896, MacMillan, London.

2. Becker, A.J., C.E. Mc, and J.E. Till, Cytological demonstration of the clonal nature of spleen colonies derived from transplanted mouse marrow cells. Nature, 1963. 197: p. 452-4.

3. Siminovitch, L., E.A. McCulloch, and J.E. Till, The Distribution of Colony-Forming Cells among Spleen Colonies. J Cell Physiol, 1963. 62: p. 327-36.

4. Friedenstein, A.J., S. Piatetzky, II, and K.V. Petrakova, Osteogenesis in transplants of bone marrow cells. J Embryol Exp Morphol, 1966. 16(3): p. 381-90.

5. Urist, M.R., Bone: formation by autoinduction. Science, 1965. 150(698): p. 893-9.

6. Caplan, A.I., Review: mesenchymal stem cells: cell-based reconstructive therapy in orthopedics. Tissue Eng, 2005. 11(7-8): p. 1198-211.

7. Van de Putte, K.A. and M.R. Urist, Osteogenesis in the interior of intramuscular implants of decalcified bone matrix. Clin Orthop Relat Res, 1965. 43: p. 257-70.

8. Castro-Malaspina, H., et al., Characterization of human bone marrow fibroblast colony-forming cells (CFU-F) and their progeny. Blood, 1980. 56(2): p. 289-301.

9. Caplan, A.I. and S.P. Bruder, Mesenchymal stem cells: building blocks for molecular medicine in the 21st century. Trends in molecular medicine, 2001. 7(6): p. 259-64.

10. Caplan, A.I. and S. Koutroupas, The control of muscle and cartilage development in the chick limb: the role of differential vascularization. J Embryol Exp Morphol, 1973. 29(3): p. 571-83.

11. Caplan, A.I. and A.C. Stoolmiller, Control of chondrogenic expression in mesodermal cells of embryonic chick limb. Proc Natl Acad Sci U S A, 1973. 70(6): p. 1713-7.

12. Woodbury, D., et al., Adult rat and human bone marrow stromal cells differentiate into neurons. Journal of neuroscience research, 2000. 61(4): p. 364-70.

13. Safford, K.M., et al., Neurogenic differentiation of murine and human adipose-derived stromal cells. Biochemical and biophysical research communications, 2002. 294(2): p. 371-9.

14. Hofstetter, C.P., et al., Marrow stromal cells form guiding strands in the injured spinal cord and promote recovery. Proceedings of the National Academy of Sciences of the United States of America, 2002. 99(4): p. 2199-204.

15. Caplan, A.I., Mesenchymal stem cells. Journal of orthopaedic research : official publication of the Orthopaedic Research Society, 1991. 9(5): p. 641-50.

16. Horwitz, E.M., et al., Clarification of the nomenclature for MSC: The International Society for Cellular Therapy position statement. Cytotherapy, 2005. 7(5): p. 393-5.

17. Bianco, P., P.G. Robey, and P.J. Simmons, Mesenchymal stem cells: revisiting history, concepts, and assays. Cell Stem Cell, 2008. 2(4): p. 313-9.

18. Dominici, M., et al., Minimal criteria for defining multipotent mesenchymal stromal cells. The International Society for Cellular Therapy position statement. Cytotherapy, 2006. 8(4): p. 315-7.

19. Parker, A.M. and A.J. Katz, Adipose-derived stem cells for the regeneration of damaged tissues. Expert opinion on biological therapy, 2006. 6(6): p. 567-78.

20. De Schauwer, C., et al., In search for cross-reactivity to immunophenotype equine mesenchymal stromal cells by multicolor flow cytometry. Cytometry. Part A : the journal of the International Society for Analytical Cytology, 2012. 81(4): p. 312-23.

21. Pittenger, M.F., et al., Multilineage potential of adult human mesenchymal stem cells. Science, 1999. 284(5411): p. 143-7.

22. da Silva Meirelles, L., P.C. Chagastelles, and N.B. Nardi, Mesenchymal stem cells reside in virtually all post-natal organs and tissues. J Cell Sci, 2006. 119(Pt 11): p. 2204-13.

23. Jones, E.A., et al., Isolation and characterization of bone marrow multipotential mesenchymal progenitor cells. Arthritis and rheumatism, 2002. 46(12): p. 3349-60.

24. Neupane, M., et al., Isolation and characterization of canine adipose-derived mesenchymal stem cells. Tissue engineering. Part A, 2008. 14(6): p. 1007-15.

25. Martin, D.R., et al., Isolation and characterization of multipotential mesenchymal stem cells from feline bone marrow. Experimental hematology, 2002. 30(8): p. 879-86.

26. Baksh, D., R. Yao, and R.S. Tuan, Comparison of proliferative and multilineage differentiation potential of human mesenchymal stem cells derived from umbilical cord and bone marrow. Stem Cells, 2007. 25(6): p. 1384-92.

27. De Bari, C. and F. Dell'accio, Cell therapy: a challenge in modern medicine. Bio-medical materials and engineering, 2008. 18(1 Suppl): p. S11-7.

28. Phinney, D.G. and D.J. Prockop, Concise review: mesenchymal stem/multipotent stromal cells: the state of transdifferentiation and modes of tissue repair--current views. Stem Cells, 2007. 25(11): p. 2896-902.

29. De Bari, C. and F. Dell'accio, Mesenchymal stem cells in rheumatology: a regenerative approach to joint repair. Clinical science, 2007. 113(8): p. 339-48.

30. Scadden, D.T., The stem-cell niche as an entity of action. Nature, 2006. 441(7097): p. 1075-9.

31. Kobel, S. and M. Lutolf, High-throughput methods to define complex stem cell niches. Biotechniques, 2010. 48(4): p. ix-xxii.

32. Vats, A., et al., The stem cell in orthopaedic surgery. J Bone Joint Surg Br, 2004. 86(2): p. 159-64.

33. da Silva Meirelles, L., A.I. Caplan, and N.B. Nardi, In search of the in vivo identity of mesenchymal stem cells. Stem Cells, 2008. 26(9): p. 2287-99.

34. Fuchs, E., T. Tumbar, and G. Guasch, Socializing with the neighbors: stem cells and their niche. Cell, 2004. 116(6): p. 769-78.

35. Kurth, T.B., et al., Functional mesenchymal stem cell niches in adult mouse knee joint synovium in vivo. Arthritis and rheumatism, 2011. 63(5): p. 1289-300.

36. Wilson, A. and A. Trumpp, Bone-marrow haematopoietic-stem-cell niches. Nature reviews. Immunology, 2006. 6(2): p. 93-106.

37. Kuhn, N.Z. and R.S. Tuan, Regulation of stemness and stem cell niche of mesenchymal stem cells: implications in tumorigenesis and metastasis. Journal of cellular physiology, 2010. 222(2): p. 268-77.

38. Crisan, M., et al., A perivascular origin for mesenchymal stem cells in multiple human organs. Cell Stem Cell, 2008. 3(3): p. 301-13.

39. Diaz-Flores, L., et al., Pericytes. Morphofunction, interactions and pathology in a quiescent and activated mesenchymal cell niche. Histology and histopathology, 2009. 24(7): p. 909-69.

40. Brighton, C.T., et al., The pericyte as a possible osteoblast progenitor cell. Clinical orthopaedics and related research, 1992(275): p. 287-99.

41. Diaz-Flores, L., et al., Pericytes as a supplementary source of osteoblasts in periosteal osteogenesis. Clinical orthopaedics and related research, 1992(275): p. 280-6.

42. Caplan, A.I., Adult mesenchymal stem cells for tissue engineering versus regenerative medicine. Journal of cellular physiology, 2007. 213(2): p. 341-7.

43. Crisan, M., et al., Perivascular cells for regenerative medicine. Journal of cellular and molecular medicine, 2012.

44. Dowthwaite, G.P., et al., The surface of articular cartilage contains a progenitor cell population. Journal of cell science, 2004. 117(Pt 6): p. 889-97.

45. Mitsiadis, T.A., et al., Stem cell niches in mammals. Experimental cell research, 2007. 313(16): p. 3377-85.

46. Caplan, A.I. and J.E. Dennis, Mesenchymal stem cells as trophic mediators. Journal of cellular biochemistry, 2006. 98(5): p. 1076-84.

47. Li, Y., et al., Gliosis and brain remodeling after treatment of stroke in rats with marrow stromal cells. Glia, 2005. 49(3): p. 407-17.

48. Murphy, J.M., et al., Stem cell therapy in a caprine model of osteoarthritis. Arthritis and rheumatism, 2003. 48(12): p. 3464-74.

49. Laflamme, M.A. and C.E. Murry, Regenerating the heart. Nature biotechnology, 2005. 23(7): p. 845-56.

50. Chen, J., et al., Intravenous bone marrow stromal cell therapy reduces apoptosis and promotes endogenous cell proliferation after stroke in female rat. Journal of neuroscience research, 2003. 73(6): p. 778-86.

51. Djouad, F., et al., Immunosuppressive effect of mesenchymal stem cells favors tumor growth in allogeneic animals. Blood, 2003. 102(10): p. 3837-44.

52. Brooke, G., et al., Molecular trafficking mechanisms of multipotent mesenchymal stem cells derived from human bone marrow and placenta. Stem cells and development, 2008. 17(5): p. 929-40.

53. Abumaree, M., et al., Immunosuppressive properties of mesenchymal stem cells. Stem cell reviews, 2012. 8(2): p. 375-92.

54. Chan, W.K., et al., MHC expression kinetics and immunogenicity of mesenchymal stromal cells after short-term IFN-gamma challenge. Experimental hematology, 2008. 36(11): p. 1545-55.

55. Deuse, T., et al., Immunogenicity and immunomodulatory properties of umbilical cord lining mesenchymal stem cells. Cell transplantation, 2011. 20(5): p. 655-67.

56. Dickhut, A., et al., Mesenchymal stem cells obtained after bone marrow transplantation or peripheral blood stem cell transplantation originate from host tissue. Annals of hematology, 2005. 84(11): p. 722-7.

57. Le Blanc, K., et al., HLA expression and immunologic properties of differentiated and undifferentiated mesenchymal stem cells. Experimental hematology, 2003. 31(10): p. 890-6.

58. Nauta, A.J. and W.E. Fibbe, Immunomodulatory properties of mesenchymal stromal cells. Blood, 2007. 110(10): p. 3499-506.

59. Tse, W.T., et al., Suppression of allogeneic T-cell proliferation by human marrow stromal cells: implications in transplantation. Transplantation, 2003. 75(3): p. 389-97.

60. Schurgers, E., et al., Discrepancy between the in vitro and in vivo effects of murine mesenchymal stem cells on T-cell proliferation and collagen-induced arthritis. Arthritis research & therapy, 2010. 12(1): p. R31.

61. Selmani, Z., et al., Human leukocyte antigen-G5 secretion by human mesenchymal stem cells is required to suppress T lymphocyte and natural killer function and to induce CD4+CD25highFOXP3+ regulatory T cells. Stem Cells, 2008. 26(1): p. 212-22.

62. Volarevic, V., et al., Interleukin-1 receptor antagonist (IL-1Ra) and IL-1Ra producing mesenchymal stem cells as modulators of diabetogenesis. Autoimmunity, 2010. 43(4): p. 255-63.

63. Asari, S., et al., Mesenchymal stem cells suppress B-cell terminal differentiation. Experimental hematology, 2009. 37(5): p. 604-15.

64. Corcione, A., et al., Human mesenchymal stem cells modulate B-cell functions. Blood, 2006. 107(1): p. 367-72.

65. Aggarwal, S. and M.F. Pittenger, Human mesenchymal stem cells modulate allogeneic immune cell responses. Blood, 2005. 105(4): p. 1815-22.

66. Abdi, R., et al., Immunomodulation by mesenchymal stem cells: a potential therapeutic strategy for type 1 diabetes. Diabetes, 2008. 57(7): p. 1759-67.

67. Groh, M.E., et al., Human mesenchymal stem cells require monocyte-mediated activation to suppress alloreactive T cells. Experimental hematology, 2005. 33(8): p. 928-34.

68. Jiang, X.X., et al., Human mesenchymal stem cells inhibit differentiation and function of monocyte-derived dendritic cells. Blood, 2005. 105(10): p. 4120-6.

69. Li, C.D., et al., Isolation and Identification of a Multilineage Potential Mesenchymal Cell from Human Placenta. Placenta, 2005.

70. Tomic, S., et al., Immunomodulatory properties of mesenchymal stem cells derived from dental pulp and dental follicle are susceptible to activation by toll-like receptor agonists. Stem cells and development, 2011. 20(4): p. 695-708.

71. Munn, D.H., et al., Prevention of allogeneic fetal rejection by tryptophan catabolism. Science, 1998. 281(5380): p. 1191-3.

72. Morito, T., et al., Synovial fluid-derived mesenchymal stem cells increase after intra-articular ligament injury in humans. Rheumatology, 2008. 47(8): p. 1137-43.

73. Wang, C.H., et al., Late-outgrowth endothelial cells attenuate intimal hyperplasia contributed by mesenchymal stem cells after vascular injury. Arteriosclerosis, thrombosis, and vascular biology, 2008. 28(1): p. 54-60.

74. Karp, J.M. and G.S. Leng Teo, Mesenchymal stem cell homing: the devil is in the details. Cell Stem Cell, 2009. 4(3): p. 206-16.

75. Sackstein, R., The lymphocyte homing receptors: gatekeepers of the multistep paradigm. Current opinion in hematology, 2005. 12(6): p. 444-50.

76. Ruster, B., et al., Mesenchymal stem cells display coordinated rolling and adhesion behavior on endothelial cells. Blood, 2006. 108(12): p. 3938-44.

77. Katayama, Y., et al., PSGL-1 participates in E-selectin-mediated progenitor homing to bone marrow: evidence for cooperation between E-selectin ligands and alpha4 integrin. Blood, 2003. 102(6): p. 2060-7.

78. Hynes, R.O., Integrins: bidirectional, allosteric signaling machines. Cell, 2002. 110(6): p. 673-87.

79. Muller, W.A., Mechanisms of transendothelial migration of leukocytes. Circulation research, 2009. 105(3): p. 223-30.

80. Sorokin, L., The impact of the extracellular matrix on inflammation. Nature reviews. Immunology, 2010. 10(10): p. 712-23.

81. Kocher, A.A., et al., Myocardial homing and neovascularization by human bone marrow angioblasts is regulated by IL-8/Gro CXC chemokines. Journal of molecular and cellular cardiology, 2006. 40(4): p. 455-64.

82. Grunewald, M., et al., VEGF-induced adult neovascularization: recruitment, retention, and role of accessory cells. Cell, 2006. 124(1): p. 175-89.

83. Chavakis, E., et al., Role of beta2-integrins for homing and neovascularization capacity of endothelial progenitor cells. The Journal of experimental medicine, 2005. 201(1): p. 63-72.

84. Jin, H., et al., A homing mechanism for bone marrow-derived progenitor cell recruitment to the neovasculature. The Journal of clinical investigation, 2006. 116(3): p. 652-62.

85. Ip, J.E., et al., Mesenchymal stem cells use integrin beta1 not CXC chemokine receptor 4 for myocardial migration and engraftment. Molecular biology of the cell, 2007. 18(8): p. 2873-82.

86. Oh, I.Y., et al., Involvement of E-selectin in recruitment of endothelial progenitor cells and angiogenesis in ischemic muscle. Blood, 2007. 110(12): p. 3891-9.

87. Nishiwaki, Y., et al., Endothelial E-selectin potentiates neovascularization via endothelial progenitor cell-dependent and -independent mechanisms. Arteriosclerosis, thrombosis, and vascular biology, 2007. 27(3): p. 512-8.

88. Vajkoczy, P., et al., Multistep nature of microvascular recruitment of ex vivo-expanded embryonic endothelial progenitor cells during tumor angiogenesis. The Journal of experimental medicine, 2003. 197(12): p. 1755-65.

89. Rombouts, W.J. and R.E. Ploemacher, Primary murine MSC show highly efficient homing to the bone marrow but lose homing ability following culture. Leukemia : official journal of the Leukemia Society of America, Leukemia Research Fund, U.K, 2003. 17(1): p. 160-70.

90. De Becker, A., et al., Migration of culture-expanded human mesenchymal stem cells through bone marrow endothelium is regulated by matrix metalloproteinase-2 and tissue inhibitor of metalloproteinase-3. Haematologica, 2007. 92(4): p. 440-9.

91. Annabi, B., et al., Hypoxia promotes murine bone-marrow-derived stromal cell migration and tube formation. Stem Cells, 2003. 21(3): p. 337-47.

92. Rosova, I., et al., Hypoxic preconditioning results in increased motility and improved therapeutic potential of human mesenchymal stem cells. Stem Cells, 2008. 26(8): p. 2173-82.

93. Trounson, A., et al., Clinical trials for stem cell therapies. BMC medicine, 2011. 9: p. 52.

94. Phinney, D.G., et al., Donor variation in the growth properties and osteogenic potential of human marrow stromal cells. Journal of cellular biochemistry, 1999. 75(3): p. 424-36.

95. Mendez-Ferrer, S., et al., Mesenchymal and haematopoietic stem cells form a unique bone marrow niche. Nature, 2010. 466(7308): p. 829-34.

96. Charbord, P., et al., Human bone marrow mesenchymal stem cells: a systematic reappraisal via the genostem experience. Stem cell reviews, 2011. 7(1): p. 32-42.

97. Banfi, A., et al., Proliferation kinetics and differentiation potential of ex vivo expanded human bone marrow stromal cells: Implications for their use in cell therapy. Experimental hematology, 2000. 28(6): p. 707-15.

98. Battula, V.L., et al., Isolation of functionally distinct mesenchymal stem cell subsets using antibodies against CD56, CD271, and mesenchymal stem cell antigen-1. Haematologica, 2009. 94(2): p. 173-84.

99. Levi, B., et al., CD105 protein depletion enhances human adipose-derived stromal cell osteogenesis through reduction of transforming growth factor beta1 (TGF-beta1) signaling. The Journal of biological chemistry, 2011. 286(45): p. 39497-509.

100. Mesenchymal Stem Cells Derived from Rat Epicardial Versus Epididymal Adipose Tissue. Eslaminejad, Mohamadreza Baghaban; Mardpour, Soura; Ebrahimi, Marzieh Iran J Basic Med Sci.;Jan/Feb2011, Vol. 14 Issue 1, p25

101. Vinardell, T., et al., A comparison of the functionality and in vivo phenotypic stability of cartilaginous tissues engineered from different stem cell sources. Tissue engineering. Part A, 2012. 18(11-12): p. 1161-70.

102. Vieira, N.M., et al., Human multipotent mesenchymal stromal cells from distinct sources show different in vivo potential to differentiate into muscle cells when injected in dystrophic mice. Stem cell reviews, 2010. 6(4): p. 560-6.

103. Pires de Carvalho, P., et al., Comparison of infrapatellar and subcutaneous adipose tissue stromal vascular fraction and stromal/stem cells in osteoarthritic subjects. Journal of tissue engineering and regenerative medicine, 2012.

104. Murphy, J.M., et al., Reduced chondrogenic and adipogenic activity of mesenchymal stem cells from patients with advanced osteoarthritis. Arthritis and rheumatism, 2002. 46(3): p. 704-13.

105. Planat-Benard, V., et al., Plasticity of human adipose lineage cells toward endothelial cells: physiological and therapeutic perspectives. Circulation, 2004. 109(5): p. 656-63.

106. Sewter, C.P., et al., Regulation of tumour necrosis factor-alpha release from human adipose tissue in vitro. The Journal of endocrinology, 1999. 163(1): p. 33-8.

107. Krieger-Brauer, H.I. and H. Kather, Human fat cells possess a plasma membrane-bound H2O2-generating system that is activated by insulin via a mechanism bypassing the receptor kinase. The Journal of clinical investigation, 1992. 89(3): p. 1006-13.

108. Kazemi, M.R., et al., Adipocyte fatty acid-binding protein expression and lipid accumulation are increased during activation of murine macrophages by toll-like receptor agonists. Arteriosclerosis, thrombosis, and vascular biology, 2005. 25(6): p. 1220-4.

109. Cousin, B., et al., A role for preadipocytes as macrophage-like cells. The FASEB journal : official publication of the Federation of American Societies for Experimental Biology, 1999. 13(2): p. 305-12.

110. Saillan-Barreau, C., et al., Human adipose cells as candidates in defense and tissue remodeling phenomena. Biochemical and biophysical research communications, 2003. 309(3): p. 502-5.

111. Casteilla, L. and C. Dani, Adipose tissue-derived cells: from physiology to regenerative medicine. Diabetes & metabolism, 2006. 32(5 Pt 1): p. 393-401.

112. Dobson, D.E., et al., 1-Butyryl-glycerol: a novel angiogenesis factor secreted by differentiating adipocytes. Cell, 1990. 61(2): p. 223-30.

113. Claffey, K.P., W.O. Wilkison, and B.M. Spiegelman, Vascular endothelial growth factor. Regulation by cell differentiation and activated second messenger pathways. The Journal of biological chemistry, 1992. 267(23): p. 16317-22.

114. Bouloumie, A., et al., Leptin, the product of Ob gene, promotes angiogenesis. Circulation research, 1998. 83(10): p. 1059-66.

115. Sierra-Honigmann, M.R., et al., Biological action of leptin as an angiogenic factor. Science, 1998. 281(5383): p. 1683-6.

116. Lutolf, M.P., P.M. Gilbert, and H.M. Blau, Designing materials to direct stem-cell fate. Nature, 2009. 462(7272): p. 433-41.

117. Jung, Y., G. Bauer, and J.A. Nolta, Concise review: Induced pluripotent stem cell-derived mesenchymal stem cells: progress toward safe clinical products. Stem Cells, 2012. 30(1): p. 42-7.

118. Ge, Z., J.C. Goh, and E.H. Lee, Selection of cell source for ligament tissue engineering. Cell transplantation, 2005. 14(8): p. 573-83.

119. Clarke, D.L., et al., Generalized potential of adult neural stem cells. Science, 2000. 288(5471): p. 1660-3.

120. Hughes, G.C. and B.H. Annex, Angiogenic therapy for coronary artery and peripheral arterial disease. Expert review of cardiovascular therapy, 2005. 3(3): p. 521-35.

121. Cartmell, J.S. and M.G. Dunn, Development of cell-seeded patellar tendon allografts for anterior cruciate ligament reconstruction. Tissue engineering, 2004. 10(7-8): p. 1065-75.

122. O'Connell, P., Pancreatic islet xenotransplantation. Xenotransplantation, 2002. 9(6): p. 367-71.

123. Vunjak-Novakovic, G., et al., Tissue engineering of ligaments. Annual review of biomedical engineering, 2004. 6: p. 131-56.

124. Freeman, J.W., Tissue Engineering Options for Ligament Healing. Bone and Tissue Regeneration Insights, 2009. 2: p. 13-23.

125. Robert, L., Matrix biology: past, present and future. Pathologie-biologie, 2001. 49(4): p. 279-83.

126. Chan, B.P. and K.W. Leong, Scaffolding in tissue engineering: general approaches and tissue-specific considerations. European spine journal : official publication of the European Spine Society, the European Spinal Deformity Society, and the European Section of the Cervical Spine Research Society, 2008. 17 Suppl 4: p. 467-79.

127. Kuo, Y.R., et al., One-stage reconstruction of soft tissue and Achilles tendon defects using a composite free anterolateral thigh flap with vascularized fascia lata: clinical experience and functional assessment. Annals of plastic surgery, 2003. 50(2): p. 149-55.

128. Crossett, L.S., et al., Reconstruction of a ruptured patellar tendon with achilles tendon allograft following total knee arthroplasty. The Journal of bone and joint surgery. American volume, 2002. 84-A(8): p. 1354-61.

129. Guo, X., et al., In vitro generation of an osteochondral construct using injectable hydrogel composites encapsulating rabbit marrow mesenchymal stem cells. Biomaterials, 2009. 30(14): p. 2741-52.

130. Hemmrich, K., et al., Autologous in vivo adipose tissue engineering in hyaluronan-based gels--a pilot study. The Journal of surgical research, 2008. 144(1): p. 82-8.

131. Grohn, P., G. Klock, and U. Zimmermann, Collagen-coated Ba(2+)-alginate microcarriers for the culture of anchorage-dependent mammalian cells. Biotechniques, 1997. 22(5): p. 970-5.

132. Huaping Tan, K.G.M., Injectable, biodegradable hydrogels for tissue engineering applications. Materials, 2010. 3(3): p. 1746-1767.

133. Baba, S., et al., Effectiveness of scaffolds with pre-seeded mesenchymal stem cells in bone regeneration--assessment of osteogenic ability of scaffolds implanted under the periosteum of the cranial bone of rats. Dental materials journal, 2010. 29(6): p. 673-81.

134. Ohgushi, H., et al., Tissue engineered ceramic artificial joint--ex vivo osteogenic differentiation of patient mesenchymal cells on total ankle joints for treatment of osteoarthritis. Biomaterials, 2005. 26(22): p. 4654-61.

135. Solchaga, L.A., et al., Hyaluronan-based polymers in the treatment of osteochondral defects. Journal of orthopaedic research : official publication of the Orthopaedic Research Society, 2000. 18(5): p. 773-80.

136. Park, H., et al., Injectable biodegradable hydrogel composites for rabbit marrow mesenchymal stem cell and growth factor delivery for cartilage tissue engineering. Biomaterials, 2007. 28(21): p. 3217-27.

137. Bian, L., et al., Enhanced MSC chondrogenesis following delivery of TGF-beta3 from alginate microspheres within hyaluronic acid hydrogels in vitro and in vivo. Biomaterials, 2011. 32(27): p. 6425-34.

138. Martin, I., D. Wendt, and M. Heberer, The role of bioreactors in tissue engineering. Trends in biotechnology, 2004. 22(2): p. 80-6.

139. Goldstein, A.S., et al., Effect of convection on osteoblastic cell growth and function in biodegradable polymer foam scaffolds. Biomaterials, 2001. 22(11): p. 1279-88.

140. Grayson, W.L., et al., Effects of initial seeding density and fluid perfusion rate on formation of tissue-engineered bone. Tissue engineering. Part A, 2008. 14(11): p. 1809-20.

141. Grayson, W.L., et al., Engineering anatomically shaped human bone grafts. Proceedings of the National Academy of Sciences of the United States of America, 2010. 107(8): p. 3299-304.

142. Bilodeau, K. and D. Mantovani, Bioreactors for tissue engineering: focus on mechanical constraints. A comparative review. Tissue engineering, 2006. 12(8): p. 2367-83.

143. Yeatts, A.B. and J.P. Fisher, Bone tissue engineering bioreactors: dynamic culture and the influence of shear stress. Bone, 2011. 48(2): p. 171-81.

144. Bancroft, G.N., et al., Fluid flow increases mineralized matrix deposition in 3D perfusion culture of marrow stromal osteoblasts in a dose-dependent manner. Proceedings of the National Academy of Sciences of the United States of America, 2002. 99(20): p. 12600-5.

145. Gomes, M.E., et al., In vitro localization of bone growth factors in constructs of biodegradable scaffolds seeded with marrow stromal cells and cultured in a flow perfusion bioreactor. Tissue engineering, 2006. 12(1): p. 177-88.

146. Lu, H.H., et al., Anterior cruciate ligament regeneration using braided biodegradable scaffolds: in vitro optimization studies. Biomaterials, 2005. 26(23): p. 4805-16.

147. Herthel DJ. Suspensory desmitis therapies. Proc 12th ACVS Symp. 2002. pp. 165–167.

148. Weissman, I.L., Stem cells: units of development, units of regeneration, and units in evolution. Cell, 2000. 100(1): p. 157-68.

149. Schaffler, A. and C. Buchler, Concise review: adipose tissue-derived stromal cells--basic and clinical implications for novel cell-based therapies. Stem Cells, 2007. 25(4): p. 818-27.

150. Black, L.L., et al., Effect of adipose-derived mesenchymal stem and regenerative cells on lameness in dogs with chronic osteoarthritis of the coxofemoral joints: a randomized, double-blinded, multicenter, controlled trial. Veterinary therapeutics : research in applied veterinary medicine, 2007. 8(4): p. 272-84.

151. Quimby, J.M., et al., Evaluation of intrarenal mesenchymal stem cell injection for treatment of chronic kidney disease in cats: a pilot study. Journal of feline medicine and surgery, 2011. 13(6): p. 418-26.

152. Marshall, J.L. and S.E. Olsson, Instability of the knee. A long-term experimental study in dogs. The Journal of bone and joint surgery. American volume, 1971. 53(8): p. 1561-70.

153. Wilke, V.L., et al., Estimate of the annual economic impact of treatment of cranial cruciate ligament injury in dogs in the United States. Journal of the American Veterinary Medical Association, 2005. 227(10): p. 1604-7.

154. Harasen, G., Canine cranial cruciate ligament rupture in profile: 2002-2007. The Canadian veterinary journal. La revue veterinaire canadienne, 2008. 49(2): p. 193-4.

155. Jackson, J., et al., Pathologic changes in grossly normal menisci in dogs with rupture of the cranial cruciate ligament. Journal of the American Veterinary Medical Association, 2001. 218(8): p. 1281-4.

156. Buckwalter, J.A. and T.D. Brown, Joint injury, repair, and remodeling: roles in post-traumatic osteoarthritis. Clinical orthopaedics and related research, 2004(423): p. 7-16.

157. Schaefer, S.L., et al., Effect of rhBMP-2 on tibial plateau fractures in a canine model. Journal of orthopaedic research : official publication of the Orthopaedic Research Society, 2009. 27(4): p. 466-71.

158. Bruder, S.P., et al., The effect of implants loaded with autologous mesenchymal stem cells on the healing of canine segmental bone defects. The Journal of bone and joint surgery. American volume, 1998. 80(7): p. 985-96.

159. Institute of Medicine of the National Academies Report. Relieving Pain in America: A Blueprint for Transforming Prevention, Care, Education, and Research, 2011. The National Academies Press, Washington DC.

160. Griffith, C.J., et al., Anatomy and biomechanics of the posterolateral aspect of the canine knee. Journal of orthopaedic research : official publication of the Orthopaedic Research Society, 2007. 25(9): p. 1231-42.

161. Marshall, K.W. and A.D. Chan, Arthroscopic anterior cruciate ligament transection induces canine osteoarthritis. The Journal of rheumatology, 1996. 23(2): p. 338-43.

162. Visco, D.M., et al., Experimental osteoarthritis in dogs: a comparison of the Pond-Nuki and medial arthrotomy methods. Osteoarthritis and cartilage / OARS, Osteoarthritis Research Society, 1996. 4(1): p. 9-22.

163. Vieira, N.M., et al., Isolation, characterization, and differentiation potential of canine adipose-derived stem cells. Cell transplantation, 2010. 19(3): p. 279-89.

164. Hiyama, A., et al., Transplantation of mesenchymal stem cells in a canine disc degeneration model. Journal of orthopaedic research : official publication of the Orthopaedic Research Society, 2008. 26(5): p. 589-600.

165. Guercio, A., et al., Production of canine mesenchymal stem cells from adipose tissue and application in dogs with chronic osteoarthritis of the humeroredal joints. Cell biology international, 2011.

166. Van Eijk, F., et al., Tissue engineering of ligaments: a comparison of bone marrow stromal cells, anterior cruciate ligament, and skin fibroblasts as cell source. Tissue engineering, 2004. 10(5-6): p. 893-903.

167. Pollina, E.A. and A. Brunet, Epigenetic regulation of aging stem cells. Oncogene, 2011. 30(28): p. 3105-26.

168. Kurth, T.B., et al., Functional mesenchymal stem cell niches in the adult knee joint synovium in vivo. Arthritis and rheumatism, 2011.

169. Caplan, A.I. and S.P. Bruder, Mesenchymal stem cells: building blocks for molecular medicine in the 21st century. Trends Mol Med, 2001. 7(6): p. 259-64.

170. Cooper, J.A., Jr., et al., Evaluation of the anterior cruciate ligament, medial collateral ligament, achilles tendon and patellar tendon as cell sources for tissue-engineered ligament. Biomaterials, 2006. 27(13): p. 2747-54.

171. Hofstetter, C.P., et al., Marrow stromal cells form guiding strands in the injured spinal cord and promote recovery. Proc Natl Acad Sci U S A, 2002. 99(4): p. 2199-204.

172. Vidal, M.A., et al., Cell growth characteristics and differentiation frequency of adherent equine bone marrow-derived mesenchymal stromal cells: adipogenic and osteogenic capacity. Veterinary surgery : VS, 2006. 35(7): p. 601-10.

173. Rainaldi, G., et al., Reduction of proliferative heterogeneity of CHEF18 Chinese hamster cell line during the progression toward tumorigenicity. In vitro cellular & developmental biology : journal of the Tissue Culture Association, 1991. 27A(12): p. 949-52.

174. Spencer, N.D., et al., In vitro expansion and differentiation of fresh and revitalized adult canine bone marrow-derived and adipose tissue-derived stromal cells. Vet J, 2011.

175. Spencer, N.D., et al., In vitro expansion and differentiation of fresh and revitalized adult canine bone marrow-derived and adipose tissue-derived stromal cells. Veterinary journal, 2012. 191(2): p. 231-9.

176. Livak, K.J. and T.D. Schmittgen, Analysis of relative gene expression data using real-time quantitative PCR and the 2(-Delta Delta C(T)) Method. Methods, 2001. 25(4): p. 402-8.

177. Mochizuki, T., et al., Higher chondrogenic potential of fibrous synovium- and adipose synovium-derived cells compared with subcutaneous fat-derived cells: distinguishing properties of mesenchymal stem cells in humans. Arthritis and rheumatism, 2006. 54(3): p. 843-53.

178. Jones, E.A., et al., Isolation and characterization of bone marrow multipotential mesenchymal progenitor cells. Arthritis Rheum, 2002. 46(12): p. 3349-60.

179. Dragoo, J.L., et al., Tissue-engineered cartilage and bone using stem cells from human infrapatellar fat pads. The Journal of bone and joint surgery. British volume, 2003. 85(5): p. 740-7.

180. Cheng, M.T., et al., Isolation and characterization of multipotent stem cells from human cruciate ligaments. Cell proliferation, 2009. 42(4): p. 448-60.

181. Styner, M., et al., Indomethacin promotes adipogenesis of mesenchymal stem cells through a cyclooxygenase independent mechanism. Journal of cellular biochemistry, 2010. 111(4): p. 1042-50.

182. Gregoire, F.M., C.M. Smas, and H.S. Sul, Understanding adipocyte differentiation. Physiological reviews, 1998. 78(3): p. 783-809.

183. Yoshimura, H., et al., Comparison of rat mesenchymal stem cells derived from bone marrow, synovium, periosteum, adipose tissue, and muscle. Cell and tissue research, 2007. 327(3): p. 449-62.

184. Alegre-Aguaron, E., et al., Differences in surface marker expression and chondrogenic potential among various tissue-derived mesenchymal cells from elderly patients with osteoarthritis. Cells, tissues, organs, 2012. 196(3): p. 231-40.

185. Traktuev, D.O., et al., A population of multipotent CD34-positive adipose stromal cells share pericyte and mesenchymal surface markers, reside in a periendothelial location, and stabilize endothelial networks. Circ Res, 2008. 102(1): p. 77-85.

186. Hirohata, S., et al., Induction of type B synoviocyte-like cells from plasmacytoid dendritic cells of the bone marrow in rheumatoid arthritis and osteoarthritis. Clinical immunology, 2011. 140(3): p. 276-83.

187. Brandt, K.D., et al., Osteoarthritic changes in canine articular cartilage, subchondral bone, and synovium fifty-four months after transection of the anterior cruciate ligament. Arthritis and rheumatism, 1991. 34(12): p. 1560-70.

188. Baird, D.K., et al., Low-field magnetic resonance imaging of the canine stifle joint: normal anatomy. Veterinary radiology & ultrasound : the official journal of the American College of Veterinary Radiology and the International Veterinary Radiology Association, 1998. 39(2): p. 87-97.

189. Wickham, M.Q., et al., Multipotent stromal cells derived from the infrapatellar fat pad of the knee. Clinical orthopaedics and related research, 2003(412): p. 196-212.

190. English, A., et al., A comparative assessment of cartilage and joint fat pad as a potential source of cells for autologous therapy development in knee osteoarthritis. Rheumatology, 2007. 46(11): p. 1676-83.

191. Crop, M.J., et al., Inflammatory conditions affect gene expression and function of human adipose tissue-derived mesenchymal stem cells. Clinical and experimental immunology, 2010. 162(3): p. 474-86.

192. Jones, E., et al., Mesenchymal stem cells in rheumatoid synovium: enumeration and functional assessment in relation to synovial inflammation level. Annals of the rheumatic diseases, 2010. 69(2): p. 450-7.

193. Spencer, N.D., J.M. Gimble, and M.J. Lopez, Mesenchymal stromal cells: past, present, and future. Veterinary surgery : VS, 2011. 40(2): p. 129-39.

194. Zdravkovic, N., et al., Regulatory T cells and ST2 signaling control diabetes induction with multiple low doses of streptozotocin. Molecular immunology, 2009. 47(1): p. 28-36.

195. Frisbie, D.D., et al., Evaluation of adipose-derived stromal vascular fraction or bone marrow-derived mesenchymal stem cells for treatment of osteoarthritis. Journal of orthopaedic research : official publication of the Orthopaedic Research Society, 2009. 27(12): p. 1675-80.

196. Frisbie, D.D. and R.K. Smith, Clinical update on the use of mesenchymal stem cells in equine orthopaedics. Equine veterinary journal, 2010. 42(1): p. 86-9.

197. Serigano, K., et al., Effect of cell number on mesenchymal stem cell transplantation in a canine disc degeneration model. Journal of orthopaedic research : official publication of the Orthopaedic Research Society, 2010. 28(10): p. 1267-75.

198. Jin, G.Z., et al., Generation of neuronal-like cells from umbilical cord blood-derived mesenchymal stem cells of a RFP-transgenic cloned cat. The Journal of veterinary medical science / the Japanese Society of Veterinary Science, 2008. 70(7): p. 723-6.

199. Jin, G.Z., et al., Enhanced tyrosine hydroxylase expression in PC12 cells co-cultured with feline mesenchymal stem cells. Journal of veterinary science, 2007. 8(4): p. 377-82.

200. Kubo, H., et al., c-Kit+ bone marrow stem cells differentiate into functional cardiac myocytes. Clinical and translational science, 2009. 2(1): p. 26-32.

201. Webb, T.L., J.M. Quimby, and S.W. Dow, In vitro comparison of feline bone marrow-derived and adipose tissue-derived mesenchymal stem cells. Journal of feline medicine and surgery, 2012. 14(2): p. 165-8.

202. Panciera, D.L., et al., Epizootiologic patterns of diabetes mellitus in cats: 333 cases (1980-1986). Journal of the American Veterinary Medical Association, 1990. 197(11): p. 1504-8.

203. Djajadiningrat-Laanen, S.C., et al., Progressive retinal atrophy in Abyssinian and Somali cats in the Netherlands (1981-2001). Tijdschrift voor diergeneeskunde, 2002. 127(17): p. 508-14.

204. Essex M, F.D., The risk to humans from malignant diseases of their pets: An unsettled issue. . J Am Anim Hosp Assoc., 1976. 12: p. 386-90.

205. Baral, R., Rand, J. S., Catt, M. & Farrow, H. A. , Prevalence of feline diabetes mellitus in a feline private practice. (abs). J. Vet. Intern. Med. , 2003. 17: p. 433.

206. Federico, A., et al., Fat: a matter of disturbance for the immune system. World journal of gastroenterology : WJG, 2010. 16(38): p. 4762-72.

207. Prunet-Marcassus, B., et al., From heterogeneity to plasticity in adipose tissues: site-specific differences. Experimental cell research, 2006. 312(6): p. 727-36.

208. Loncar, D., B.A. Afzelius, and B. Cannon, Epididymal white adipose tissue after cold stress in rats. I. Nonmitochondrial changes. Journal of ultrastructure and molecular structure research, 1988. 101(2-3): p. 109-22.

209. Oedayrajsingh-Varma, M.J., et al., Adipose tissue-derived mesenchymal stem cell yield and growth characteristics are affected by the tissue-harvesting procedure. Cytotherapy, 2006. 8(2): p. 166-77.

210. Arrigoni, E., et al., Isolation, characterization and osteogenic differentiation of adipose-derived stem cells: from small to large animal models. Cell and tissue research, 2009. 338(3): p. 401-11.

211. Monaco, E., et al., Strategies for regeneration of the bone using porcine adult adipose-derived mesenchymal stem cells. Theriogenology, 2011. 75(8): p. 1381-99.

212. Gimble, J.M. and M.E. Nuttall, Adipose-derived stromal/stem cells (ASC) in regenerative medicine: pharmaceutical applications. Current pharmaceutical design, 2011. 17(4): p. 332-9.

213. de Girolamo, L., et al., Human adipose-derived stem cells isolated from young and elderly women: their differentiation potential and scaffold interaction during in vitro osteoblastic differentiation. Cytotherapy, 2009. 11(6): p. 793-803.

214. Chen, H.T., et al., Proliferation and differentiation potential of human adipose-derived mesenchymal stem cells isolated from elderly patients with osteoporotic fractures. Journal of cellular and molecular medicine, 2012. 16(3): p. 582-93.

215. Wu, W., L. Niklason, and D.M. Steinbacher, The effect of age on human adipose-derived stem cells. Plastic and reconstructive surgery, 2013. 131(1): p. 27-37.

216. Adipose/Fat Worthington Tissue Dissociation References. Available at: http://www.worthington-biochem.com/tissuedissociation/Adipose_Fat.html. Accessed 2013

217. Gir, P., et al., Human adipose stem cells: current clinical applications. Plastic and reconstructive surgery, 2012. 129(6): p. 1277-90.

218. Zhu, S., et al., Effects of intrahepatic bone-derived mesenchymal stem cells autotransplantation on the diabetic Beagle dogs. The Journal of surgical research, 2011. 168(2): p. 213-23.

219. Lupu, M., et al., Use of multigeneration-family molecular dog leukocyte antigen typing to select a hematopoietic cell transplant donor for a dog with T-cell lymphoma. Journal of the American Veterinary Medical Association, 2006. 228(5): p. 728-32.

220. Appelbaum, F.R., et al., Cure of malignant lymphoma in dogs with peripheral blood stem cell transplantation. Transplantation, 1986. 42(1): p. 19-22.

221. Sandmaier, B.M., et al., Allogeneic transplant of canine peripheral blood stem cells mobilized by recombinant canine hematopoietic growth factors. Blood, 1996. 87(8): p. 3508-13.

222. Shake, J.G., et al., Mesenchymal stem cell implantation in a swine myocardial infarct model: engraftment and functional effects. The Annals of thoracic surgery, 2002. 73(6): p. 1919-25; discussion 1926.

223. Trivedi, H.L., et al., Human adipose tissue-derived mesenchymal stem cells combined with hematopoietic stem cell transplantation synthesize insulin. Transplantation proceedings, 2008. 40(4): p. 1135-9.

224. Vanikar, A.V., et al., Cotransplantation of adipose tissue-derived insulin-secreting mesenchymal stem cells and hematopoietic stem cells: a novel therapy for insulin-dependent diabetes mellitus. Stem cells international, 2010. 2010: p. 582382.

225. Volarevic, V., et al., Concise review: Mesenchymal stem cell treatment of the complications of diabetes mellitus. Stem Cells, 2011. 29(1): p. 5-10.

226. Couri, C.E., et al., C-peptide levels and insulin independence following autologous nonmyeloablative hematopoietic stem cell transplantation in newly diagnosed type 1 diabetes mellitus. JAMA : the journal of the American Medical Association, 2009. 301(15): p. 1573-9.

227. Voltarelli, J.C., et al., Autologous nonmyeloablative hematopoietic stem cell transplantation in newly diagnosed type 1 diabetes mellitus. JAMA : the journal of the American Medical Association, 2007. 297(14): p. 1568-76.

228. Bhansali, A., et al., Efficacy of autologous bone marrow-derived stem cell transplantation in patients with type 2 diabetes mellitus. Stem cells and development, 2009. 18(10): p. 1407-16.

229. Estrada, E.J., et al., Combined treatment of intrapancreatic autologous bone marrow stem cells and hyperbaric oxygen in type 2 diabetes mellitus. Cell transplantation, 2008. 17(12): p. 1295-304.

230. Wang, L., et al., Autologous bone marrow stem cell transplantation for the treatment of type 2 diabetes mellitus. Chinese medical journal, 2011. 124(22): p. 3622-8.

231. Siqueira, R.C., et al., Intravitreal injection of autologous bone marrow-derived mononuclear cells for hereditary retinal dystrophy: a phase I trial. Retina, 2011. 31(6): p. 1207-14.

232. James, A.W., et al., Perivascular stem cells: a prospectively purified mesenchymal stem cell population for bone tissue engineering. Stem cells translational medicine, 2012. 1(6): p. 510-9.

233. Zhang, N., M.A. Dietrich, and M.J. Lopez, Canine Intra-Articular Multipotent Stromal Cells (MSC) From Adipose Tissue Have the Highest In Vitro Expansion Rates, Multipotentiality, and MSC Immunophenotypes. Veterinary surgery : VS, 2013.

234. Gimble, J.M., A.J. Katz, and B.A. Bunnell, Adipose-derived stem cells for regenerative medicine. Circulation research, 2007. 100(9): p. 1249-60.

235. Fossett, E. and W.S. Khan, Optimising human mesenchymal stem cell numbers for clinical application: a literature review. Stem cells international, 2012. 2012: p. 465259.

236. Ruan, H., et al., Standard isolation of primary adipose cells from mouse epididymal fat pads induces inflammatory mediators and down-regulates adipocyte genes. The Journal of biological chemistry, 2003. 278(48): p. 47585-93.

237. Langdon, S.P., Basic principles of cancer cell culture. Methods in molecular medicine, 2004. 88: p. 3-15.

238. Leehey, D.J., et al., Decreased degradative enzymes in mesangial cells cultured in high glucose media. Diabetes, 1995. 44(8): p. 929-35.

239. Seifter, S., et al., Studies on collagen. II. Properties of purified collagenase and its inhibition. The Journal of biological chemistry, 1959. 234(2): p. 285-93.

240. Thompson, A.C.S., The role of different adipocyte size populations in the mediation of obesity-related insulin resistance and inflammation, 2008, University of Arizona: Tucson, Arizona. p. 62 leaves.

241. Leandra Baptista, K.S., Carolina Pedrosa and Radovan Borojevic Advanced Techniques in Liposuction and Fat Transfer, N. Serdev, Editor 2011.

242. Zhang, N., M.A. Dietrich, and M.J. Lopez, Canine Intra-Articular Multipotent Stromal Cells (MSC) From Adipose Tissue Have the Highest In Vitro Expansion Rates, Multipotentiality, and MSC Immunophenotypes. Veterinary surgery : VS, 2013. 42(2): p. 137-46.

243. Varma, M.J., et al., Phenotypical and functional characterization of freshly isolated adipose tissue-derived stem cells. Stem cells and development, 2007. 16(1): p. 91-104.

244. Mitchell, J.B., et al., Immunophenotype of human adipose-derived cells: temporal changes in stromal-associated and stem cell-associated markers. Stem Cells, 2006. 24(2): p. 376-85.

245. Jaiswal, N., et al., Osteogenic differentiation of purified, culture-expanded human mesenchymal stem cells in vitro. Journal of cellular biochemistry, 1997. 64(2): p. 295-312.

246. Sekiya, I., D.C. Colter, and D.J. Prockop, BMP-6 enhances chondrogenesis in a subpopulation of human marrow stromal cells. Biochemical and biophysical research communications, 2001. 284(2): p. 411-8.

247. Vidal, M.A., et al., Comparison of chondrogenic potential in equine mesenchymal stromal cells derived from adipose tissue and bone marrow. Veterinary surgery : VS, 2008. 37(8): p. 713-24.

248. Pond, M.J. and J.R. Campbell, The canine stifle joint. I. Rupture of the anterior cruciate ligament. An assessment of conservative and surgical treatment. J Small Anim Pract, 1972. 13(1): p. 1-10.

249. Narama, I., et al., Morphogenesis of degenerative changes predisposing dogs to rupture of the cranial cruciate ligament. J Vet Med Sci, 1996. 58(11): p. 1091-7.

250. Vasseur, P.B., et al., Correlative biomechanical and histologic study of the cranial cruciate ligament in dogs. Am J Vet Res, 1985. 46(9): p. 1842-54.

251. Read, R.A. and G.M. Robins, Deformity of the proximal tibia in dogs. Vet Rec, 1982. 111(13): p. 295-8.

252. Slocum, B. and T.D. Slocum, Tibial plateau leveling osteotomy for repair of cranial cruciate ligament rupture in the canine. Vet Clin North Am Small Anim Pract, 1993. 23(4): p. 777-95.

253. Whitehair, J.G., P.B. Vasseur, and N.H. Willits, Epidemiology of cranial cruciate ligament rupture in dogs. J Am Vet Med Assoc, 1993. 203(7): p. 1016-9.

254. Duval, J.M., et al., Breed, sex, and body weight as risk factors for rupture of the cranial cruciate ligament in young dogs. J Am Vet Med Assoc, 1999. 215(6): p. 811-4.

255. Wilke, V.L., et al., Inheritance of rupture of the cranial cruciate ligament in Newfoundlands. J Am Vet Med Assoc, 2006. 228(1): p. 61-4.

256. Clements, D.N., et al., Gene expression profiling of normal and ruptured canine anterior cruciate ligaments. Osteoarthritis Cartilage, 2008. 16(2): p. 195-203.

257. Griffon, D.J., A review of the pathogenesis of canine cranial cruciate ligament disease as a basis for future preventive strategies. Vet Surg. 39(4): p. 399-409.

258. Aiken SW, Kass PH, Toomps JP: Intercondylar notch width in dogs with and without cranial cruciate ligament injuries. Vet Comp Orthop Trauma 1995;8:128-132.

259. Slocum, B. and T. Devine, Cranial tibial thrust: a primary force in the canine stifle. J Am Vet Med Assoc, 1983. 183(4): p. 456-9.

260. Nisell, R., G. Nemeth, and H. Ohlsen, Joint forces in extension of the knee. Analysis of a mechanical model. Acta Orthop Scand, 1986. 57(1): p. 41-6.

261. Kowaleski, M.P., et al., The effect of tibial plateau leveling osteotomy position on cranial tibial subluxation: an in vitro study. Vet Surg, 2005. 34(4): p. 332-6.

262. Wheeler, J.L., A.R. Cross, and W. Gingrich, In vitro effects of osteotomy angle and osteotomy reduction on tibial angulation and rotation during the tibial plateau-leveling osteotomy procedure. Vet Surg, 2003. 32(4): p. 371-7.

263. Alm, A. and B. Stromberg, Vascular anatomy of the patellar and cruciate ligaments. A microangiographic and histologic investigation in the dog. Acta Chir Scand Suppl, 1974. 445: p. 25-35.

264. Arnoczky, S.P., R.M. Rubin, and J.L. Marshall, Microvasculature of the cruciate ligaments and its response to injury. An experimental study in dogs. J Bone Joint Surg Am, 1979. 61(8): p. 1221-9.

265. Osborne, A.C., et al., Anti-collagen antibodies and immune complexes in equine joint diseases. Vet Immunol Immunopathol, 1995. 45(1-2): p. 19-30.

266. Doom, M., et al., Immunopathological mechanisms in dogs with rupture of the cranial cruciate ligament. Veterinary immunology and immunopathology, 2008. 125(1-2): p. 143-61.

267. Fernihough, J.K., et al., Changes in the local regulation of insulin-like growth factors I and II and insulin-like growth factor-binding proteins in osteoarthritis of the canine stifle joint secondary to cruciate ligament rupture. Veterinary surgery : VS, 2003. 32(4): p. 313-23.

268. Cameron, M.L., et al., Synovial fluid cytokine concentrations as possible prognostic indicators in the ACL-deficient knee. Knee surgery, sports traumatology, arthroscopy : official journal of the ESSKA, 1994. 2(1): p. 38-44.

269. Cameron, M., et al., The natural history of the anterior cruciate ligament-deficient knee. Changes in synovial fluid cytokine and keratan sulfate concentrations. The American journal of sports medicine, 1997. 25(6): p. 751-4.

270. Irie, K., E. Uchiyama, and H. Iwaso, Intraarticular inflammatory cytokines in acute anterior cruciate ligament injured knee. The Knee, 2003. 10(1): p. 93-6.

271. Chu, Q., et al., Elevation of a collagenase generated type II collagen neoepitope and proteoglycan epitopes in synovial fluid following induction of joint instability in the dog. Osteoarthritis Cartilage, 2002. 10(8): p. 662-9.

272. Arican, M., et al., Measurement of glycosaminoglycans and keratan sulphate in canine arthropathies. Res Vet Sci, 1994. 56(3): p. 290-7.

273. Innes, J.F., M. Sharif, and A.R. Barr, Relations between biochemical markers of osteoarthritis and other disease parameters in a population of dogs with naturally acquired osteoarthritis of the genual joint. Am J Vet Res, 1998. 59(12): p. 1530-6.

274. Hayashi, K., et al., Evaluation of a collagenase generated osteoarthritis biomarker in naturally occurring canine cruciate disease. Vet Surg, 2009. 38(1): p. 117-21.

275. Spindler, K.P., et al., Expression of collagen and matrix metalloproteinases in ruptured human anterior cruciate ligament: an in situ hybridization study. J Orthop Res, 1996. 14(6): p. 857-61.

276. Volk, S.W., et al., Gelatinase activity in synovial fluid and synovium obtained from healthy and osteoarthritic joints of dogs. Am J Vet Res, 2003. 64(10): p. 1225-33.

277. Muir, P., et al., Collagenolytic protease expression in cranial cruciate ligament and stifle synovial fluid in dogs with cranial cruciate ligament rupture. Vet Surg, 2005. 34(5): p. 482-90.

278. Breshears, L.A., et al., Detection and evaluation of matrix metalloproteinases involved in cruciate ligament disease in dogs using multiplex bead technology. Vet Surg. 39(3): p. 306-14.

279. Kajikawa, Y., et al., Platelet-rich plasma enhances the initial mobilization of circulation-derived cells for tendon healing. J Cell Physiol, 2008. 215(3): p. 837-45.

280. Hoffmann, A. and G. Gross, Tendon and ligament engineering in the adult organism: mesenchymal stem cells and gene-therapeutic approaches. Int Orthop, 2007. 31(6): p. 791-7.

281. Rehfeldt, F., et al., Cell responses to the mechanochemical microenvironment--implications for regenerative medicine and drug delivery. Adv Drug Deliv Rev, 2007. 59(13): p. 1329-39.

282. Amiel, D., et al., Tendons and ligaments: a morphological and biochemical comparison. J Orthop Res, 1984. 1(3): p. 257-65.

283. Frank, C., et al., Medial collateral ligament healing. A multidisciplinary assessment in rabbits. Am J Sports Med, 1983. 11(6): p. 379-89.

284. Murray, M.M., et al., Histological changes in the human anterior cruciate ligament after rupture. J Bone Joint Surg Am, 2000. 82-A(10): p. 1387-97.

285. Steadman, J.R., et al., A minimally invasive technique ("healing response") to treat proximal ACL injuries in skeletally immature athletes. J Knee Surg, 2006. 19(1): p. 8-13.

286. Boynton, M.D. and P.D. Fadale, The basic science of anterior cruciate ligament surgery. Orthop Rev, 1993. 22(6): p. 673-9.

287. Nagineni, C.N., et al., Characterization of the intrinsic properties of the anterior cruciate and medial collateral ligament cells: an in vitro cell culture study. J Orthop Res, 1992. 10(4): p. 465-75.

288. Bray, R.C., C.A. Leonard, and P.T. Salo, Vascular physiology and long-term healing of partial ligament tears. J Orthop Res, 2002. 20(5): p. 984-9.

289. McKean, J.M., A.H. Hsieh, and K.L. Sung, Epidermal growth factor differentially affects integrin-mediated adhesion and proliferation of ACL and MCL fibroblasts. Biorheology, 2004. 41(2): p. 139-52.

290. Sung, K.L., et al., Adhesion strength of human ligament fibroblasts. J Biomech Eng, 1994. 116(3): p. 237-42.

291. Zhou, D., et al., Differential MMP-2 activity of ligament cells under mechanical stretch injury: an in vitro study on human ACL and MCL fibroblasts. J Orthop Res, 2005. 23(4): p. 949-57.

292. Werner, S. and R. Grose, Regulation of wound healing by growth factors and cytokines. Physiol Rev, 2003. 83(3): p. 835-70.

293. Heldin, C.H. and B. Westermark, Mechanism of action and in vivo role of platelet-derived growth factor. Physiol Rev, 1999. 79(4): p. 1283-316.

294. Shi, Y. and J. Massague, Mechanisms of TGF-beta signaling from cell membrane to the nucleus. Cell, 2003. 113(6): p. 685-700.

295. Danielpour, D. and K. Song, Cross-talk between IGF-I and TGF-beta signaling pathways. Cytokine Growth Factor Rev, 2006. 17(1-2): p. 59-74.

296. Gerritsen, M.E., et al., Using gene expression profiling to identify the molecular basis of the synergistic actions of hepatocyte growth factor and vascular endothelial growth factor in human endothelial cells. Br J Pharmacol, 2003. 140(4): p. 595-610.

297. McPherron, A.C., A.M. Lawler, and S.J. Lee, Regulation of skeletal muscle mass in mice by a new TGF-beta superfamily member. Nature, 1997. 387(6628): p. 83-90.

298. Fulzele, S., et al., Role of myostatin (GDF-8) signaling in the human anterior cruciate ligament. J Orthop Res. 28(8): p. 1113-8.

299. Joulia-Ekaza, D. and G. Cabello, The myostatin gene: physiology and pharmacological relevance. Curr Opin Pharmacol, 2007. 7(3): p. 310-5.

300. Mendias, C.L., K.I. Bakhurin, and J.A. Faulkner, Tendons of myostatin-deficient mice are small, brittle, and hypocellular. Proc Natl Acad Sci U S A, 2008. 105(1): p. 388-93.

301. Lee, J., et al., Growth factor expression in healing rabbit medial collateral and anterior cruciate ligaments. Iowa Orthop J, 1998. 18: p. 19-25.

302. Le Blanc, K. and O. Ringden, Immunobiology of human mesenchymal stem cells and future use in hematopoietic stem cell transplantation. Biology of blood and marrow transplantation : journal of the American Society for Blood and Marrow Transplantation, 2005. 11(5): p. 321-34.

303. El-Ayoubi, R., et al., Design and dynamic culture of 3D-scaffolds for cartilage tissue engineering. J Biomater Appl. 25(5): p. 429-44.

304. Heijne, A., et al., Strain on the anterior cruciate ligament during closed kinetic chain exercises. Med Sci Sports Exerc, 2004. 36(6): p. 935-41.

305. Rosc, D., et al., Post-traumatic plasminogenesis in intraarticular exudate in the knee joint. Med Sci Monit, 2002. 8(5): p. CR371-8.

306. Fernandes, J.C., J. Martel-Pelletier, and J.P. Pelletier, The role of cytokines in osteoarthritis pathophysiology. Biorheology, 2002. 39(1-2): p. 237-46.

307. Shikhman, A.R., D.C. Brinson, and M. Lotz, Profile of glycosaminoglycan-degrading glycosidases and glycoside sulfatases secreted by human articular chondrocytes in homeostasis and inflammation. Arthritis Rheum, 2000. 43(6): p. 1307-14.

308. Laurencin, C.T. and J.W. Freeman, Ligament tissue engineering: an evolutionary materials science approach. Biomaterials, 2005. 26(36): p. 7530-6.

309. Bourke, S.L., J. Kohn, and M.G. Dunn, Preliminary development of a novel resorbable synthetic polymer fiber scaffold for anterior cruciate ligament reconstruction. Tissue engineering, 2004. 10(1-2): p. 43-52.

310. Freeman, J.W., M.D. Woods, and C.T. Laurencin, Tissue engineering of the anterior cruciate ligament using a braid-twist scaffold design. J Biomech, 2007. 40(9): p. 2029-36.

311. Cooper, J.A., Jr., et al., Biomimetic tissue-engineered anterior cruciate ligament replacement. Proceedings of the National Academy of Sciences of the United States of America, 2007. 104(9): p. 3049-54.

312. JA., C. Optimization and In vivo Evaluation of a Tissue-Engineered Anterior Cruciate Ligament Replacement. in Design. 2002. Drexel University, Philadelphia.

313. Murray, M.M., et al., Enhanced histologic repair in a central wound in the anterior cruciate ligament with a collagen-platelet-rich plasma scaffold. J Orthop Res, 2007. 25(8): p. 1007-17.

314. Murray, M.M., et al., The effect of thrombin on ACL fibroblast interactions with collagen hydrogels. J Orthop Res, 2006. 24(3): p. 508-15.

315. Lynn, A.K., I.V. Yannas, and W. Bonfield, Antigenicity and immunogenicity of collagen. Journal of biomedical materials research. Part B, Applied biomaterials, 2004. 71(2): p. 343-54.

316. Murphy, C.M., M.G. Haugh, and F.J. O'Brien, The effect of mean pore size on cell attachment, proliferation and migration in collagen-glycosaminoglycan scaffolds for bone tissue engineering. Biomaterials, 2010. 31(3): p. 461-6.

317. Schoeters, G., et al., Haemopoietic long-term bone marrow cultures from adult mice show osteogenic capacity in vitro on 3-dimensional collagen sponges. Cell Prolif, 1992. 25(6): p. 587-603.

318. Fleming, B.C., et al., Collagen scaffold supplementation does not improve the functional properties of the repaired anterior cruciate ligament. Journal of orthopaedic research : official publication of the Orthopaedic Research Society, 2010. 28(6): p. 703-9.

319. Fan, H., et al., Anterior cruciate ligament regeneration using mesenchymal stem cells and silk scaffold in large animal model. Biomaterials, 2009. 30(28): p. 4967-77.

320. Altman, G.H., et al., Silk matrix for tissue engineered anterior cruciate ligaments. Biomaterials, 2002. 23(20): p. 4131-41.

321. Chen, J., et al., Human bone marrow stromal cell and ligament fibroblast responses on RGD-modified silk fibers. Journal of biomedical materials research. Part A, 2003. 67(2): p. 559-70.

322. Sahoo, S., S.L. Toh, and J.C. Goh, A bFGF-releasing silk/PLGA-based biohybrid scaffold for ligament/tendon tissue engineering using mesenchymal progenitor cells. Biomaterials, 2010. 31(11): p. 2990-8.

323. Sahoo, S., et al., Bioactive nanofibers for fibroblastic differentiation of mesenchymal precursor cells for ligament/tendon tissue engineering applications. Differentiation; research in biological diversity, 2010. 79(2): p. 102-10.

324. Fufa, D., et al., Activation of platelet-rich plasma using soluble type I collagen. Journal of oral and maxillofacial surgery : official journal of the American Association of Oral and Maxillofacial Surgeons, 2008. 66(4): p. 684-90.

325. El-Sharkawy, H., et al., Platelet-rich plasma: growth factors and pro- and anti-inflammatory properties. Journal of periodontology, 2007. 78(4): p. 661-9.

326. Murray, M.M., et al., Collagen-platelet rich plasma hydrogel enhances primary repair of the porcine anterior cruciate ligament. Journal of orthopaedic research : official publication of the Orthopaedic Research Society, 2007. 25(1): p. 81-91.

327. Joshi, S., Mastrangelo, A., and Murray, M. Collagen-platelet composite enhances histologic healing of the ACL. . in 55th ORS, Las Vegas. 2009.

328. Spencer, N.D., et al., In vitro expansion and differentiation of fresh and revitalized adult canine bone marrow-derived and adipose tissue-derived stromal cells. Veterinary journal, 2011.

329. Kim, J.W., et al., Preparation of porous poly(L-lactic acid) honeycomb monolith structure by phase separation and unidirectional freezing. Langmuir : the ACS journal of surfaces and colloids, 2009. 25(9): p. 5304-12.

330. Hildebrand, K.A., F. Jia, and S.L. Woo, Response of donor and recipient cells after transplantation of cells to the ligament and tendon. Microscopy research and technique, 2002. 58(1): p. 34-8.

331. Jackson, D.W. and T.M. Simon, Donor cell survival and repopulation after intraarticular transplantation of tendon and ligament allografts. Microscopy research and technique, 2002. 58(1): p. 25-33.

332. Krampera, M., et al., Bone marrow mesenchymal stem cells inhibit the response of naive and memory antigen-specific T cells to their cognate peptide. Blood, 2003. 101(9): p. 3722-9.

333. Watanabe, N., et al., A method of tracking donor cells after simulated autologous transplantation: a study using synovial cells of transgenic rats. Cell and tissue research, 1999. 298(3): p. 519-25.

334. McCoy, R.J., C. Jungreuthmayer, and F.J. O'Brien, Influence of flow rate and scaffold pore size on cell behavior during mechanical stimulation in a flow perfusion bioreactor. Biotechnology and bioengineering, 2012. 109(6): p. 1583-94.

335. Silver, F.H., et al., Anterior cruciate ligament replacement: a review. Journal of long-term effects of medical implants, 1991. 1(2): p. 135-54.

336. Arnoczky, S.P., Anatomy of the anterior cruciate ligament. Clinical orthopaedics and related research, 1983(172): p. 19-25.

337. Shen, Y.H., M.S. Shoichet, and M. Radisic, Vascular endothelial growth factor immobilized in collagen scaffold promotes penetration and proliferation of endothelial cells. Acta biomaterialia, 2008. 4(3): p. 477-89.

338. Pietrzak, W.S. and B.L. Eppley, In vitro characteristics of a bioabsorbable suspension screw and suture system for endoscopic brow lift surgery. The Journal of craniofacial surgery, 2007. 18(2): p. 429-36.

339. Cartmell, S.H., et al., Effects of medium perfusion rate on cell-seeded three-dimensional bone constructs in vitro. Tissue engineering, 2003. 9(6): p. 1197-203.

340. Papaioannou, T.G. and C. Stefanadis, Vascular wall shear stress: basic principles and methods. Hellenic journal of cardiology : HJC = Hellenike kardiologike epitheorese, 2005. 46(1): p. 9-15.

341. Murray, M.M., et al., Enhanced histologic repair in a central wound in the anterior cruciate ligament with a collagen-platelet-rich plasma scaffold. Journal of orthopaedic research : official publication of the Orthopaedic Research Society, 2007. 25(8): p. 1007-17.

342. Ryu, J.M., et al., Zinc chloride stimulates DNA synthesis of mouse embryonic stem cells: involvement of PI3K/Akt, MAPKs, and mTOR. Journal of cellular physiology, 2009. 218(3): p. 558-67.

343. Aston, J.E., et al., Effects of cell condition, pH, and temperature on lead, zinc, and copper sorption to Acidithiobacillus caldus strain BC13. Journal of hazardous materials, 2010. 184(1-3): p. 34-41.

344. Goh, J.C., et al., Tissue-engineering approach to the repair and regeneration of tendons and ligaments. Tissue engineering, 2003. 9 Suppl 1: p. S31-44.

345. Moreau, J.E., et al., Growth factor induced fibroblast differentiation from human bone marrow stromal cells in vitro. Journal of orthopaedic research : official publication of the Orthopaedic Research Society, 2005. 23(1): p. 164-74.

346. Moreau, J.E., et al., Sequential growth factor application in bone marrow stromal cell ligament engineering. Tissue engineering, 2005. 11(11-12): p. 1887-97.

347. Lee, J., et al., Growth factor expression in healing rabbit medial collateral and anterior cruciate ligaments. The Iowa orthopaedic journal, 1998. 18: p. 19-25.

348. Shukunami, C., et al., Scleraxis positively regulates the expression of tenomodulin, a differentiation marker of tenocytes. Developmental biology, 2006. 298(1): p. 234-47.

349. Banos, C.C., A.H. Thomas, and C.K. Kuo, Collagen fibrillogenesis in tendon development: current models and regulation of fibril assembly. Birth defects research. Part C, Embryo today : reviews, 2008. 84(3): p. 228-44.

350. Riou, J.F., et al., Tenascin: a potential modulator of cell-extracellular matrix interactions during vertebrate embryogenesis. Biology of the cell / under the auspices of the European Cell Biology Organization, 1992. 75(1): p. 1-9.

351. Kapila, Y.L., S. Kapila, and P.W. Johnson, Fibronectin and fibronectin fragments modulate the expression of proteinases and proteinase inhibitors in human periodontal ligament cells. Matrix biology : journal of the International Society for Matrix Biology, 1996. 15(4): p. 251-61.

352. Kavanagh, E. and D.E. Ashhurst, Distribution of biglycan and decorin in collateral and cruciate ligaments and menisci of the rabbit knee joint. The journal of histochemistry and cytochemistry : official journal of the Histochemistry Society, 2001. 49(7): p. 877-85.

353. Docheva, D., et al., Tenomodulin is necessary for tenocyte proliferation and tendon maturation. Molecular and cellular biology, 2005. 25(2): p. 699-705.

354. H. Liu, H.F., E.J.W. Wong, S. Lok Toh, J.C.H Goh, Silk-based scaffold for ligament tissue engineering. 14th Nordic-Baltic Conference on Biomedical Engineering and Medical Physics2008.

355. Robinson, P.S., et al., Influence of decorin and biglycan on mechanical properties of multiple tendons in knockout mice. Journal of biomechanical engineering, 2005. 127(1): p. 181-5.

356. Zhang, G., et al., Decorin regulates assembly of collagen fibrils and acquisition of biomechanical properties during tendon development. Journal of cellular biochemistry, 2006. 98(6): p. 1436-49.

357. Liu, S.H., et al., Collagen in tendon, ligament, and bone healing. A current review. Clinical orthopaedics and related research, 1995(318): p. 265-78.

358. Chen, Y.J., et al., Effects of cyclic mechanical stretching on the mRNA expression of tendon/ligament-related and osteoblast-specific genes in human mesenchymal stem cells. Connective tissue research, 2008. 49(1): p. 7-14.

VITA

Nan Zhang was born in Linfen, Shanxi Province, China. She was accepted into Tianjin Medical School in the fall semester of 2003. After she received her bachelor's degree in Biomedical Engineering and Biotechnology in 2007, she came to the School of Veterinary Medicine at Louisiana State University in Baton Rouge to pursue her doctoral degree in the spring semester of 2008. She spent the first two years studying cancer gene therapy in the Department of Comparative Biomedical Sciences, and joined the Veterinary Clinical Sciences Department to study adult stem cells in the spring semester of 2010.